INVESTIGATION OF A HYDROGEN PRODUCTION PROCESS THROUGH ALUMINUM AND WATER CHEMICAL REACTION

By

Andre Bolt

A Thesis Submitted in Partial Fulfillment

of the Requirements for the degree of Master of Applied Science

in

Mechanical Engineering

Faculty of Engineering and Applied Science

Ontario Tech University

Oshawa, Ontario, Canada

December 2019

THESIS EXAMINATION INFORMATION

Submitted by: **Andre Bolt**

Master of Applied Science in **Mechanical Engineering**

Thesis title: Investigation of a Hydrogen Production Process Through Aluminum and Water Chemical Reaction

An oral defense of this thesis took place on December 5, 2019 in front of the following examining committee:

Examining Committee:

Chair of Examining Committee	Dr. Dipal Patel
Research Supervisor	Dr. Ibrahim Dincer
Research Co-supervisor	Dr. Martin Agelin- Chaab
Examining Committee Member	Dr. Ghaus Rizvi
Thesis Examiner	Dr. Sheldon Williamson

The above committee determined that the thesis is acceptable in form and content and that a satisfactory knowledge of the field covered by the thesis was demonstrated by the candidate during an oral examination. A signed copy of the Certificate of Approval is available from the School of Graduate and Postdoctoral Studies.

ABSTRACT

This thesis reported a novel hydrogen production experimental set up, which utilized the chemical reaction between aluminum and water to produce hydrogen. The constructed experimental setup had an aluminum powder spraying subsystem integrated within the overall setup. The effectiveness of this experimental set up was improved by using a fine size aluminum powder of 149 microns, and nitrogen gas as the medium to facilitate the spraying of the aluminum powder. In order to remove the oxide layer, this thesis study utilized sodium hydroxide as the reaction promoter. The various experimental conditions implemented during the testing process included changes in water temperature and system performance. The criteria used to evaluate system performance were the conversion efficiency, hydrogen production rate and the overall energy and exergy efficiencies. Although the tap water and additional sodium hydroxide displayed better results, seawater achieved a conversion efficiency of 58.8% which can be considered a viable option for future testing.

Keywords: Hydrogen production; aluminum; water; energy; exergy; efficiency.

ACKNOWLEDGEMENTS

I want to extend my utmost gratitude to my supervisors, Dr. Ibrahim Dincer and Dr. Martin Agelin-Chaab, for their close guidance, support, and constructive criticism, which has enabled me to complete this project. I would also like to thank them for this unique opportunity which they have given me, as it has helped me to further my education.

I would also like to extend my appreciation to my colleagues and friends within the clean energy research laboratory and in ACE 3030. My friends Maan, Ahmed, Khalid, Osamah, Harris, Aida, and Sherif, who have helped me through the experimental design/research process, and provided me with advice throughout the completion of this degree. In addition, I would like to exceptionally thank to Ghassan for his guidance and help in building the the experimental setup.

I want to thank those within my personal life, such as my parents David and Luwieth, and my two older siblings Patrice, and Tiffany, who have all helped in moulding me into the person I am today. It is their core values of determination and integrity, which has enabled me to complete this project. Also, I would like to thank my very close friends, Bismark, Branson, Daniel, Jules, and Samayet, for their tremendous support and positive encouragement, which gave me the added motivation to complete my work.

Lastly, I would like to thank NSERC for their financial contributions, which provided me with the necessary funding.

TABLE OF CONTENTS

LIST OF FIGURES

LIST OF TABLES

AUTHOR'S DECLARATION

I hereby declare that this thesis consists of original work of which I have authored. This is a true copy of the thesis, including any required final revisions, as accepted by my examiners.

I authorize the University of Ontario Institute of Technology to lend this thesis to other institutions or individuals for the purpose of scholarly research. I further authorize University of Ontario Institute of Technology to reproduce this thesis by photocopying or by other means, in total or in part, at the request of other institutions or individuals for the purpose of scholarly research. I understand that my thesis will be made electronically available to the public.

Andre Bolt

STATEMENT OF CONTRIBUTIONS

I hereby certify that I am the sole author of this thesis and that no part of this thesis has been published or submitted for publication. I have used standard referencing practices to acknowledge ideas, research techniques, or other materials that belong to others. Furthermore, I hereby certify that I am the sole source of the creative works and/or inventive knowledge described in this thesis.

NOMENCLATURE

e	Eulers number (kJ/kg)
Ea	Activation Energy (kJ)
$\dot{E}x$	exergy rate (kW)
f	degree of reaction (%)
G	Gibbs free energy (kJ/mol)
h	specific enthalpy (kJ/kg)
HHV	higher heating value (kJ/mol)
k	rate constant
LHV	lower heating value (kJ/mol)
m	mass (g and kg)
$\dot{m}$	mass flow rate (kg/s)
N	molar flow rate (mol)
r	radius (m)
s	specific entropy (kJ/kgK)
S_{gen}	entropy generation (kJ/K)
t	time (seconds)
T	temperature (^{o}C)
Q	work (J or kJ)
$\dot{Q}$	heat rate (W or kW)
V	volume (m^3, L, or mL)
W	weight (N)

Greek letters

η	efficiency
P	density (kg/m^3)
Δ	change
π	Pi number
Σ	Sum

Acronyms

α- Al_2O_3	Alpha Alumina
γ- Al_2O_3	Gamma Alumina
Al	Aluminum
$Al(OH)_4^-$	Aluminum Hydroxide
Ar	Argon
CaO	Calcium Oxide
CH_4	Methane
CO	Carbon Monoxide
CO_2	Carbon Dioxide
EES	Engineering Equation Solver
Ga	Gallium
H_2	Hydrogen Gas
H_2SO_4	Sulfuric Acid
He	Helium

Kr Krypton
Li Lithium
N_2 Nitrogen Gas
Na Sodium
NaOH Sodium Hydroxide
$Na_2Al_2O_4$ Sodium Aluminate (hydrated)
$Na_6Al_2O_6$ Sodium Aluminate
$NaAl(OH)_4$ Sodium Aluminate
Ne Neon
OH Hydroxide
U Uncertainty
QMD Quantum Molecular Dynamics

i

CHAPTER 1: INTRODUCTION

In recent history, people and organizations around the world are taking a more critical evaluation of how the environment is treated, from the vantage point of sustainability. The practice of sustainable development is achievable; however, several factors should be taken into consideration. Factors to be considered include; the ability to phase out fossil fuel as a source of energy, efficiency of energy production, and ability to reduce energy consumed [1]. Renewable sources of energy such as wind, solar, tidal, and others, are identified as a future alternative source of energy. However, the strategies used to conserve one energy source may not apply to another. Therefore, this can present a challenge when integrating multiple sources of renewable energy within a system. Furthermore, sustainable development through the use of renewable resources' is limited by its environment and environmental conditions [2].

1.1 Shift towards Renewable Energy in Canada

As climate change continues to become a growing concern within Canada, the Government of Canada has put in place a new initiative in order to mitigate potential issues that may arise as a result of climate change. Relative to 2005, the Canadian Government's objective is to eliminate 80% of greenhouse gas emissions by the year 2050. As recent as December 2017, the government of Canada has put forth a new plan in order to grow the economy, while lowering greenhouse gas emissions [3].

In order to achieve this goal, the Canadian Government has already started to implement renewable sources of power and invest in energy-efficient buildings. The implementation of renewable base and energy-efficient technology also can provide numerous benefits. The implementation of these technologies has caused growth within the technology industry, the creation of jobs, and has enabled Canada to meet climate change agreements.

The Canadian Government's timeline and milestones to reduce greenhouse gas emissions are displayed in Figure 1.1.

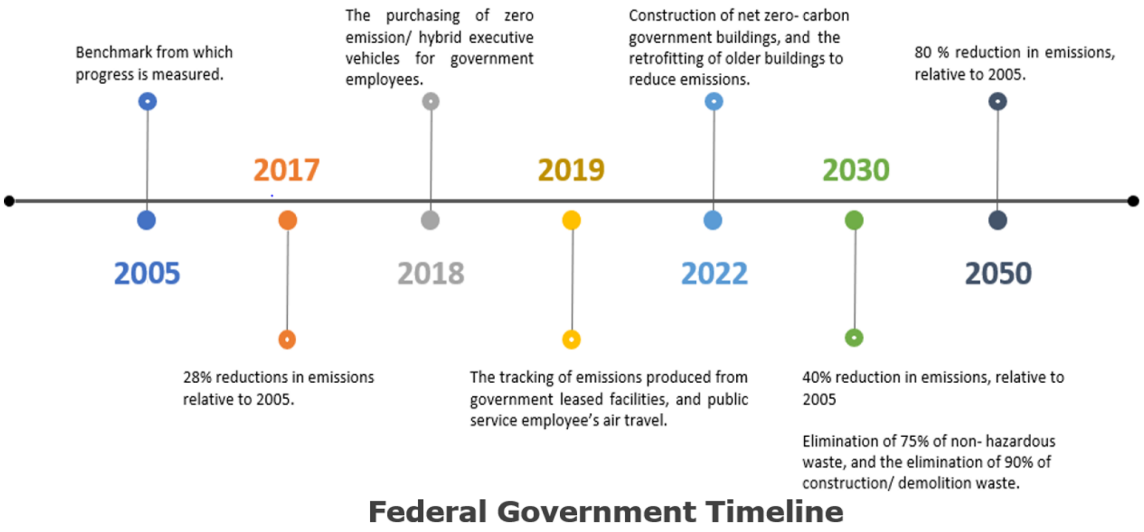

Fig. 1.1 Canada's Federal Government timeline for emission reductions

As recent as 2015, the total renewable energy capacity within Canada has a cumulative value of 109,554 MW. Presently, approximately 20% of Canada's total energy consumption was fulfilled by renewable energy resources [4]. The renewable energy resources which account for the 20% include hydropower, wind, biomass, solar and other sources. The distribution of renewable resources is shown in Figure 1.2.

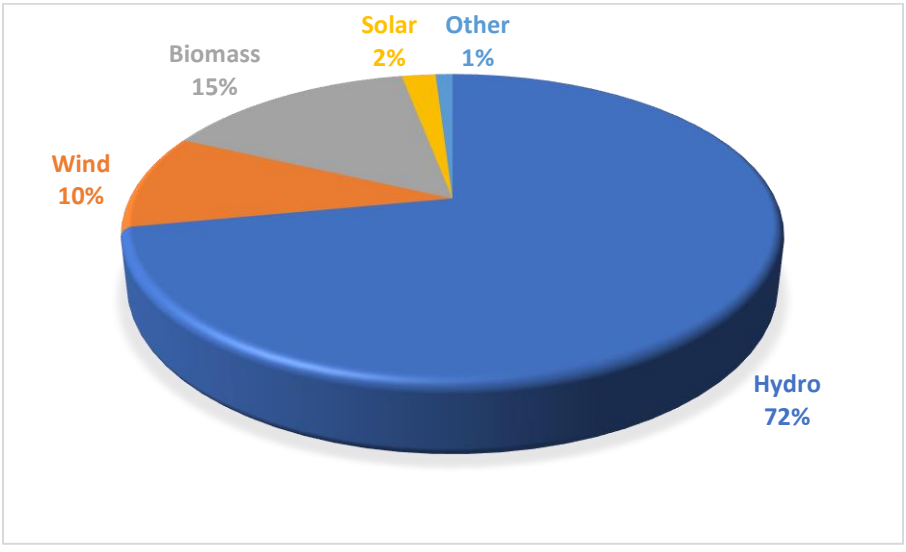

Fig. 1.2 Renewable energy distribution within Canada (data from [4])

Currently, in Canada, hydro is the primary renewable energy resource within Canada, with the wind, biomass, and solar energy following it in that order. However, hydrogen as an energy carrier has shown substantial benefits and, it is yet to be harnessed to its full capacity.

1.2 Potential applications of hydrogen

One of the most appealing aspects of hydrogen as a potential energy carrier is its diverse applications. Figure 1.3 depicts the three significant areas that hydrogen can be harnessed and its various sub-sections.

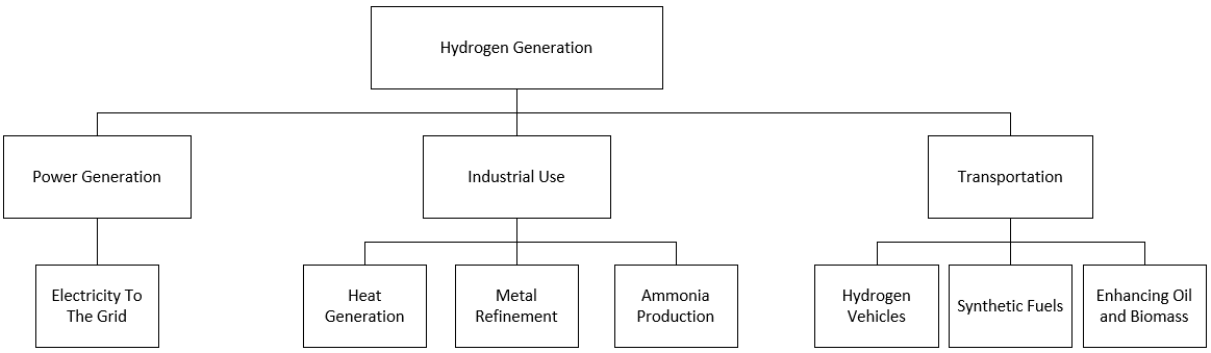

Fig. 1.3 Potential applications of hydrogen (data from [5])

Hydrogen is used for power generation, industrial use, and transportation. The power generation sector is straight forward as its primary focus is to provide energy to the grid. However, there is a large opportunity for growth in regards to transportation and industrial use.

1.3 Issues regarding hydrogen as a resource

There are significant issues regarding hydrogen as a potential energy carrier that cannot be overlooked. Some of these significant issues are listed below:

- production
- safety
- delivery
- storage
- cost

Hydrogen can be produced through a variety of methods, detailed within Section 1.6. However, one of the main issues facing hydrogen production is the identification of economically viable production techniques that do not compromise the environment. Currently, approximately 95% of the hydrogen produced today is a derivative of steam methane reforming [6]. By using methods such as steam methane reforming, this can be counter-productive, as the primary benefit of hydrogen is that it is considered to be a clean fuel. Therefore, those investigating hydrogen production strategies are directing their attention towards renewable methods of hydrogen production, such as water splitting, techniques. Presently, amongst the water splitting hydrogen production techniques, electrolysis is considered to be considerably more cost-effective, compared to techniques that harness aluminum and water's chemical reaction. Although aluminum is one of the cheapest and most abundant metals on earth, hydrogen's production cost using this technique is dictated by the cost of aluminum. For instance, if aluminum is priced at approximately $2.36/ kg, this would cause the production cost of hydrogen to be about $21/ kg. This far exceeds the United States DOE target cost of $2.00 to 3.00 [7]. Whereas in 2011 the hydrogen production cost using electrolysis was estimated to be approximately $4.20, and its target is $2.30 by the year 2020 [8]. However, it should be considered that the use of recycled aluminum can reduce the cost of hydrogen production.

Safety is also recognized as a significant issue regarding the implementation of hydrogen as an energy carrier. Hydrogen only needs to occupy 4% to 75% by volume within its environment to ignite as a result of only 0.02 mJ of energy. Furthermore, hydrogen is colourless and odourless, which makes it increasingly difficult to detect. Despite this, some consider hydrogen to be a safer alternative compared to gasoline, due to its low density, hydrogen molecules are buoyant. Therefore, rather than pooling underneath a vehicle in the event of a leak, it will rise instead.

After hydrogen is produced, it is in its natural gaseous state. After this, it must be stored so that it can be safely transported. In order to be stored, hydrogen must undergo a compression or liquefaction process. In order to compress hydrogen, a substantial amount of energy is required compared to other gases like methane. In order to calculate the amount of energy needed to compress hydrogen, it is treated as an adiabatic process, rather than an

isothermal [9]. However, according to the United States Department of Energy, the compression process to 350 and 700 bar from 20 bar, the energy requirement is 1.05 and 1.35 kWh/kg, respectively [10]. For vehicular applications, a higher compression pressure is required. If hydrogen undergoes a liquefication process, approximately 3.6 MJ/kg is required to decrease its temperature to 20 K. After this, the additional energy required to condense hydrogen to its liquid form at 101.325 kPa is 0.46 MJ/ kg [9].

Hydrogen can be delivered through a variety of methods, including ground transport through trucks, and oversea transport using ships. The major challenge associated with hydrogen transportation is in regards to the volume requirements of hydrogen. This is evident in the fact that hydrogen has a density of 70 kg/m^3 in its liquefied state, which is considerably small compared to other liquefied fuels such as natural gas. Furthermore, if hydrogen is being transported, it requires additional storage space for the specialized containers, container thermal insulation and other equipment. After everything is considered, the price for transporting hydrogen can be considerably high even if only 4200 lbs (2.1 tons) of hydrogen is being transported using a large truck.

Due to these various issues associated with hydrogen production, the challenge of those investigating hydrogen is to find cost-effective and efficient options to produce, deliver and store hydrogen. If a viable solution can be identified, this can serve as a tremendous benefit to the engineering sector and humanity.

1.4 Motivation

Presently, there is a growing interest in making a switch to renewable sources of energy. A prominent area in the field of renewable energy is harnessing hydrogen as a primary fuel source, and utilizing it as a method of energy storage. By countries continuing to use non-renewable resources, such as fossil fuel technology, to produce useful energy, it can cause irreparable damage to the environment through climate change. Also, fossil fuel technology can damage the health of those nearby power production facilities. This is a result of pollutants and other contaminants being produced during the combustion process, then entering nearby communities and ecosystems. Furthermore, the urgency of this matter is amplified through the rapid growth of the world's population and the continuous development of countries. As the population and industrialization of countries continue to

grow, it is predicted that the global energy demand will increase by 100% by the year 2050 [3].

A possible replacement to non- renewable resources, is the use of hydrogen as an energy carrier. Hydrogen can be generated through numerous production renewable techniques. By reacting to captured or generated hydrogen with oxygen, the reaction can be used to produce energy for fuel cells and heat engines. The stoichiometric reaction between hydrogen gas and oxygen is depicted within the following equation:

$$2H_2 + O_2 \rightarrow 2H_2O \quad (1.1)$$

As seen within the chemical reaction above, the molecule produced is H_2O. H_2O does not contribute to greenhouse gas emissions.

In addition to hydrogen not contributing to greenhouse gas emissions, the raw energy hydrogen carries per unit of mass should be taken into consideration. Figure 1.4. below serves as a visual representation and comparison of the amount of energy (MJ) hydrogen, hydrogen carries per unit of mass (kg).

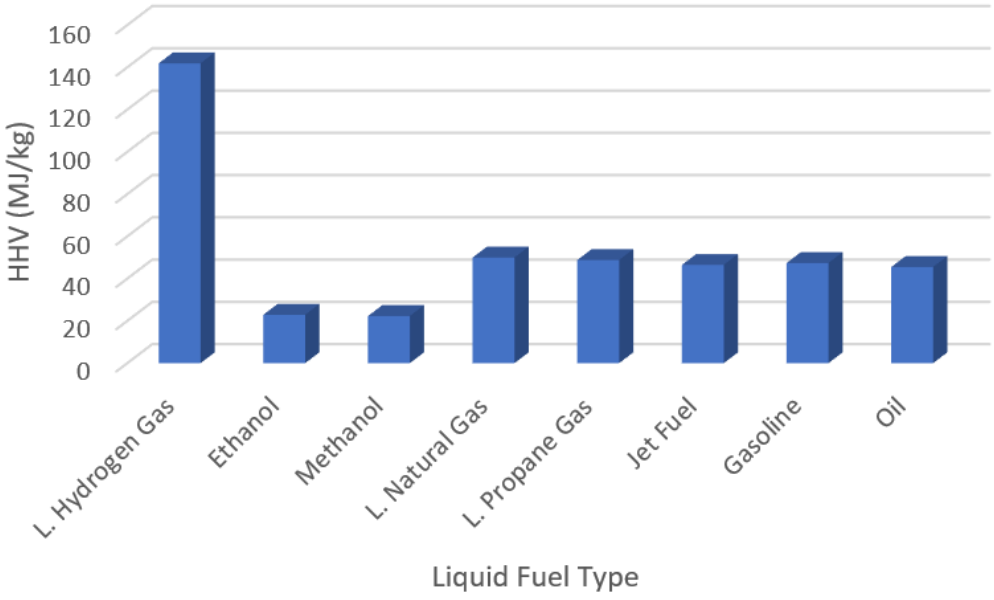

Fig. 1.4 Fuel energy per kg comparison (data from [12])

However, it should be noted that hydrogen carries the smallest amount of energy per unit volume, as seen in Figure 1.5, measuring volume in m^3.

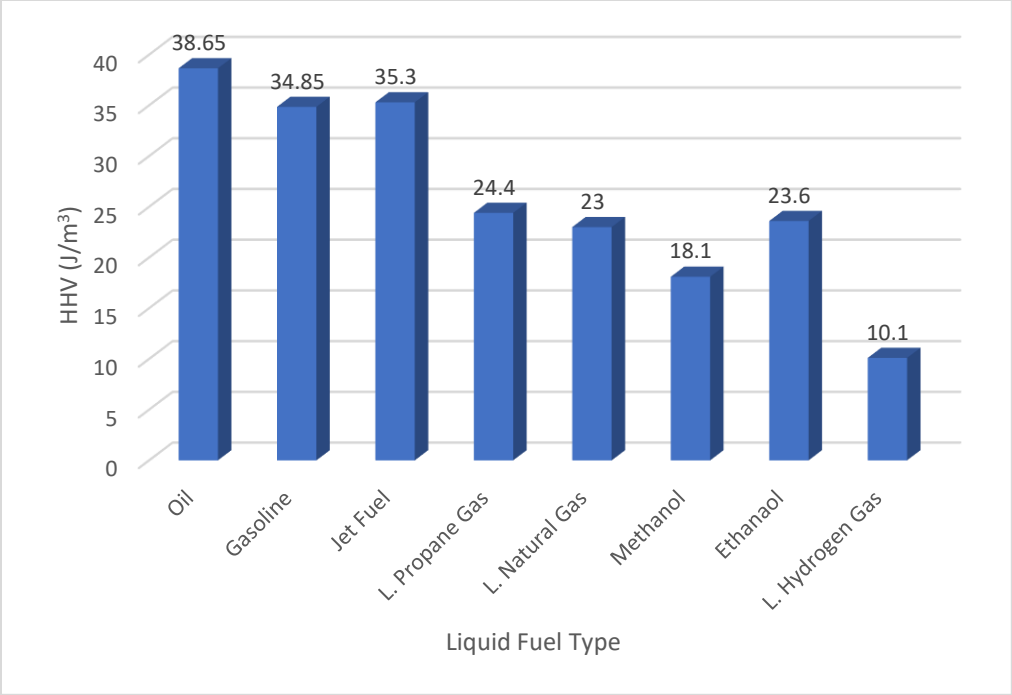

Fig. 1.5 Fuel energy per m^3 comparison (data from [12])

Based on Figure 1.4, hydrogen carries substantially more energy compared to other liquid fuels per kg. Therefore, if the energy can be produced, implemented, and harnessed effectively, hydrogen as a source of fuel has tremendous potential.

Furthermore, hydrogen molecules can be stored and collected within a pressurized vessel for use at a different time. Hydrogen's ability to be stored serves as a significant benefit over conventional electrical production systems, where electricity must be consumed at the same rate it is produced.

1.5 Hydrogen Production Overview

To produce hydrogen, there are numerous methods using fossil-fuel technology, as well as renewable resources. These techniques include hydrocarbon reforming, hydrocarbon pyrolysis, biomass, and water splitting. It should be noted that these four techniques can be divided into several categories, all of which have been summarized in Figures 1.6 and 1.7.

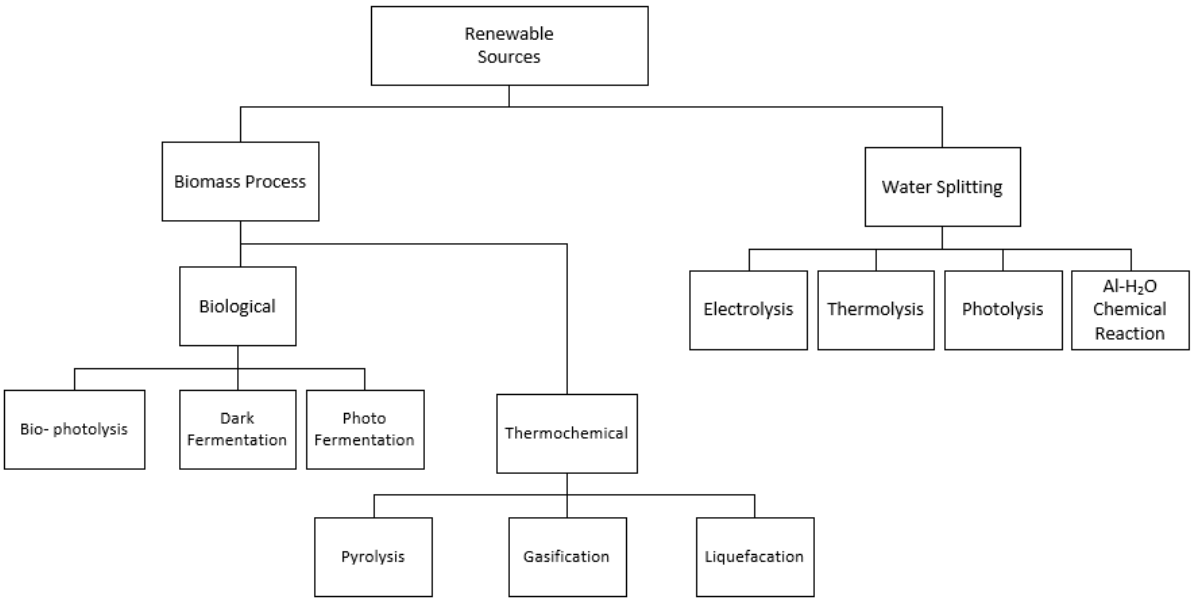

Fig. 1.6 Hydrogen production using renewable sources (adapted from [13]).

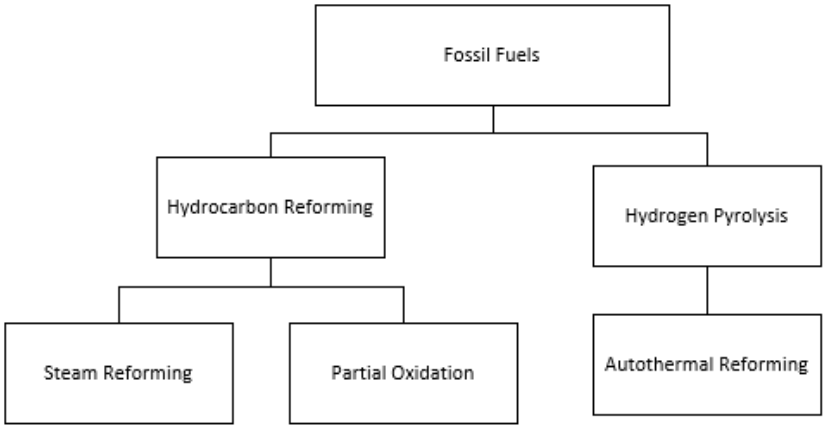

Fig. 1.7 Hydrogen production using fossil fuel technology (adapted from [13]).

1.5.1 Renewable Sources of Hydrogen Production

Presently, there are substantial benefits in using renewable energy sources to produced hydrogen gas. The largest of which being reductions in carbon and sulphur emissions [14]. By using renewable sources of energy to produce hydrogen gas, this coincides with the overall goal of moving towards clean energy. The use of renewable methods of hydrogen production should have a positive impact if life cycle assessment was conducted, and compared to hydrogen production strategies using non- renewable resources. Section 1.5.1 aims to identify the numerous methods of renewable hydrogen production.

1.5.1.1 Biophotolysis

In this process, blue and green alga extracts hydrogen molecules from water. For biophotolysis to take place, it must be done in the presence of light and anaerobic environment. Similar to dark fermentation and photo fermentation, this process utilizes bacteria; in this case, the bacteria used are cyanobacteria [15].

1.5.1.2 Dark Fermentation

Dark fermentation is considered to be a renewable method of hydrogen production, which utilizes biological waste. Currently, it was thought to have the most potential of all methods of hydrogen production, which are derived from biomass [16]. In dark fermentation, anaerobic bacteria grow within the darkness, where it ingests sugars such as glucose or cellulose. After consuming sugar, bacteria produces H_2, CO_2, and organic acid [17].

1.5.1.3 Photo Fermentation

Photo fermentation utilizes a different type of bacteria when compared to dark fermentation. Rather than using thermophiles and mesophiles as the bacteria which facilitate the process, it utilizes purple non-sulphur bacteria (PNSB). PNSB bacteria produce H_2 in the presence of sunlight, along with CO_2 [18].

1.5.1.4 Pyrolysis

Biomass produced from agriculture is dried to decrease the amount of water or moisture within the waste. After this, the biomass enters a pyrolysis reactor where heat is added, and the biomass is converted into char. The gas produced from the burning off biomass goes through a separator to extract larger particles. The condensing system within the pyrolysis reactor accepts vapours to be cooled into a bio-oil [19].

1.5.1.5 Gasification

Gasification utilizes organic base waste; therefore, biomass is commonly used as a fuel source. For gasification to take place, fuel is burned to produce a gas mixture. This gas produced from this process is known as syngas. Syngas contains an abundance of CO and H_2 molecules. Depending on the environment, the process is conducted within. This will dictate the energy content of the mixture. Typically, gasification is conducted in an environment containing O_2 or air [20].

1.5.1.6 Liquefaction

For hydrogen production to take place through liquefaction, the process consists of 3 main sections; compression, chilling, and expansion with throttling, in which air is the main working fluid [21].

1.5.1.7 Electrolysis

Electrolysis is a fairly common hydrogen production technique. In this method, the electrolyzer system consists of an anode and cathode, which is submerged within water. Between the anode and cathode, a polymer electrolyte member is placed to facilitate the flow of hydrogen ions [22]. To further understand this process, the anode and cathode utilize the following equations:

Anodic reaction:

$$2H_2O \rightarrow O_2 + 4H^+ + 4e^- \quad (1.2)$$

Cathodic reaction:

$$4H^+ + 4e^- \rightarrow 2H_2 \quad (1.3)$$

1.5.1.8 Thermolysis

Thermolysis is considered to be the decomposition of water molecules using thermal energy; it can be represented by the following chemical equations [23]:

$$H_2O = x_7(x_2\,H_2O + x_2OH + x_3H + x_4O + x_5H_2 + x_6O_2) \quad (1.4)$$

where the chemical equations can be balanced using the following equations:

Hydrogen Coefficient balance:

$$2x_1x_7 + x_2x_7 + x_3\,x_7 + 2x_5 = 2 \quad (1.5)$$

Oxygen Coefficient balance:

$$x_1x_7 + x_2x_7 + x_4x_7 + 2x_6x_7 = 1 \quad (1.6)$$

Mole fraction limit:

$$x_1 + x_2 + x_3 + x_4 + x_5 + x_6 = 1 \quad (1.7)$$

1.5.1.9 Photolysis

Photolysis is considered to be the decomposition of water molecules using ultraviolet or other forms of light. After light comes into contact with water molecules, they are split into hydrogen and oxygen atoms. To facilitate the reaction, the water within the process can be continuously stirred [24].

1.5.2 Non-Renewable Sources of Hydrogen Production

Although hydrogen production from non- renewable resources does not coincide with the goal of hydrogen being an ecologically friendly fuel or energy carrier, it should be noted that hydrogen production from non- renewable resources are considered to be highly effective. Section 1.2.2. identified the various hydrogen production strategies from non-renewable resources.

1.5.2.1 Steam Reforming

Steam reforming is a technique that utilizes natural gas as a fuel source within the furnace of the production facility. The waste heat produced from the burning of natural gas is used to generate steam. After this, steam and natural gas react to produce CO and H_2 if methane were used for instance. Lastly, the hydrogen can be extracted through the adsorptive separation process [25].

The chemical equation for the steam reforming process using methane is depicted below:

$$CH_4 + H_2O + thermal\ energy \rightarrow CO + 3H_2 \quad (1.8)$$

1.5.2.2 Partial Oxidation

In partial oxidation, the aims to produce hydrogen by reacting natural gas with a small amount of oxygen-derived from the air. For instance, the stoichiometric reaction of reacting $\frac{1}{2}$ mole of O_2 with CH_4 will give the following chemical reaction:

$$CH_4 + \frac{1}{2}\ O_2 \rightarrow\ CO + 2H_2 +\ thermal\ energy \quad (1.9)$$

Unlike steam reforming, the process is exothermic, not endothermic. Furthermore, the partial oxidation requires a smaller container for the reaction compared to steam reforming. While steam reforming is a slower process, it produces more moles of hydrogen compared to the amount of natural gas required to start the reaction [25].

1.5.2.3 Autothermal Reforming

Autothermal reforming also referred to as oxidative steam reforming. This process is an amalgamation of partial oxidation and steam reforming to produce H_2. Due to partial oxidation and steam reforming being an exothermic and endothermic process, respectively, additional energy input is not required. Typically, auto thermal reforming of methane is composed of 3 chemical reactions:

$$CH_4 + H_2O \rightarrow CO + 2H_2 \quad (1.10)$$

$$CO + H_2O \rightarrow CO_2 + H_2 \quad (1.11)$$

$$CH_4 + 2O_2 \rightarrow CO_2 + 2H_2O \quad (1.12)$$

A membrane reactor can be used to retrieve hydrogen for the process to take place more effectively [26].

1.5.3 Comparison Between Renewable and Non-Renewable Sources

Presently, hydrogen is primarily produced through non-renewable methods of production, listed in Section 1.2.2. These non- renewable methods utilize oil, coal, and natural gas due to its higher efficiency and low production cost [27]. However, the use of non-renewable resources to produce "clean" fuel is counterproductive. Therefore, the use of renewable resources to produce hydrogen should be investigated further to identify new and effective hydrogen production methods.

1.5.4 Implemented Production Strategy

Although hydrogen can be produced through a variety of methods, the idea of using water as a source of hydrogen production has great appeal, as water is a relatively abundant resource. This is evident in the fact that approximately 71% of the earth's surface is covered by water [28].

Also, aluminum is a relatively abundant metal, as it is currently ranked 3rd in abundance compared to other elements found in the earth's crust, accounting for 8.1%, and ranked behind oxygen at 46.6% and silicon at 27.7% [29]. Aluminum is considered relatively safe and benign metal for handling and testing when considering its metallurgic properties at standard temperature and pressure conditions. However, research is still being conducted

to identify if aluminum has toxic effects in regards to breast cancer and Alzheimer's disease [30]. Therefore, using water in conjunction with aluminum to produce hydrogen on a large scale can be economically and environmentally feasible, if implemented correctly.

1.6 Objectives

This thesis will focus on hydrogen generation using a chemical reaction between aluminum and water. By using the mole ratios within the aluminum water reaction, the amount of hydrogen produced can be projected. However, the production of hydrogen gas is not feasible at room temperature when using just these reactions. During the reaction between aluminum and water, a protective oxide layer forms on the exterior surface of the aluminum metal, which inhibits the reaction. The protective oxide layer, formed on the outer surface of the metal, is the most significant barrier to effectively produced hydrogen using this reaction. Therefore, in an attempt to mitigate this, strategies to have been implemented to remove or stop the formation of the oxide layer, so that the reaction can continue to take place.

This research project will aim to design and develop a novel and effective method to produce hydrogen from the chemical reaction between aluminum and water molecules. As previously described, the formation of the oxide layer on the outer surface of aluminum presents the most significant challenge in effectively producing hydrogen. This thesis study considers the size of the aluminum particles, water temperature, and composition used. The proposed experimental system contains basic distillation equipment, which allows water that was previously condensed from steam to be recycled back into the cycle.

This thesis study aims to accomplish the following sub-objectives:

- To construct a hydrogen production system which facilitates the reaction between aluminum and water, and collects freshwater at the end of the process to be recycled.
- To assess the performance of the above system using variations in water temperature conditions.

- To investigate the performance of the above system with variations in reactant mass and particle size.
- To evaluate the performance of the system using various water mediums (tap, sea, and distilled)/ water compositions.
- To compare different operating conditions efficiency and identify the ideal condition to produce hydrogen.

CHAPTER 2 : LITERATURE REVIEW

Before the commencement of this thesis project, an in-depth literature review was conducted, to identify the research completed in the past, as well as the current state of the industry. By completing this literature review, the work of various researchers can be considered during the experimental design process. After this, novel and practical studies were conducted.

Based on preliminary research, it was identified that the formation of the oxide layer is the most significant barrier; researchers and scientists must overcome to produce hydrogen effectively from an aluminum water reaction. Therefore, the topics explored within this literature review examined the reaction promoters typically used to reduce the formation of the oxide layer, and the different experimental conditions used in past. Each piece of literature reviewed within this section established a clear objective of the study, the methodology used, significant findings, and lastly, any gaps within the research conducted.

The topics explored within Chapter 2 first include aluminum and water reaction test parameters, which are often varied to identify changes within the system's behaviour. The investigated test parameters are as follows:

- variations in aluminum particle microstructure
- hydrogen production using variations in aluminum particle size and shape
- hydrogen production using various water mediums/ composition
- hydrogen production using various aluminum alloys
- hydrogen production using waste aluminum
- novel hydrogen production methods
- variations in water temperature

After this, the conventional methods utilized by scientists and engineers to mitigate the formation of the oxide layer were investigated within this chapter. The methods used to inhibit the formation of the oxide layer include the following, but not limited to:

- hydroxide promoters
- oxide promoters
- salt promoters

- combine oxide and salt promoters
- aluminum pretreatment
- molten aluminum alloys

2.1 Variations in Aluminum Particle Microstructure

To study the impact of altering the microstructure of aluminum particles, researchers often use computerized simulations. For instance, Vashishta et al. [31] created a paper that suggested the use of aluminum nanoclusters to increase the rate of reactivity with water, to produce hydrogen gas. Theoretically, aluminum anions Al_{16}^-, Al_{17}^-, and Al_{18}^- have a strong reaction with water. Therefore, the use of these molecules should increase the reaction rate with water. The experiment conducted used quantum molecular dynamics (QMD) for its simulations. This study encompassed the calculation of its molecular states using the projector- augmented wave method. The QMD simulation used was completed at 1273.15 ^oC. The simulation conducted was able to show the moles of hydrogen gas produced, from Al_{16}^-, Al_{17}^-, and Al_{18}^-. Al_{16}^-, and Al_{17}^- produced 3 moles of hydrogen gas, whereas, Al_{18}^- produces 6 moles of hydrogen gas. The simulation also showed that it took approximately 20ps for the reaction to take place. The designed hydrogen production simulation was well done; however, the study can be enhanced by verifying the simulated results with experimental values.

In another study conducted by Vashishta et al. [32], their research suggests a viable method using nanotechnology to increase the reaction rate between aluminum and water to produced hydrogen. Theoretically, aluminum anions Al_{12}^- and Al_{17}^- have a strong reaction with water; therefore, the use of these molecules should also increase the reaction rate with water. AB Initio was used to conduct a molecular dynamics analysis. The simulation assumed room temperature to be approximately 26.9 ^oC. Afterwards, the temperature was raised to 226.9 ^oC and 726.9 ^oC, to check for the dissociation of water molecules. During the simulation, it was observed that these aluminum molecules react rapidly with the water it was submerged into. The molecular analysis showed that 6 H_2O reacted with Al_{17}^- and that $5H_2O$ reacted with Al_{12}^-. At highly elevated temperatures up to 726.9 ^oC (1000 K), the dissociation of water molecules was not detected within the simulation. The study does not

quantify the amount of hydrogen gas produced from the use of these aluminum molecules, but instead focused primarily on the interaction of molecules at various temperatures.

2.2 Hydrogen Production Using Variations in Aluminum Particle Size and Shape

In recent history, there have been numerous studies that examined the effect of altering the size and shape of aluminum particles. These studies identified if there were any notable trends or significant findings in regards to the reaction rate and hydrogen yield shrinking when particle size. In theory, one can deduce that this would be ideal in facilitating a chemical reaction, as using a smaller aluminum particle size would increase the overall surface area aluminum exposed to the water.

To verify the hypothesis that decreasing aluminum particle size should have a positive impact on the overall reaction, Razavi-Tousi et al. [33] conducted a study entitled, "Effect of ball size on the steady-state of aluminum powder and efficiency of impacts during milling." The study provides an analysis of the size of balls used during the milling process to produce hydrogen. The analysis includes changes in morphological features, imperfections, and the formation of flat particles. The aluminum powder created for hydrogen production has a purity of 99.8%. A potential control agent of stearic acid was required to mitigate additional cold welding and agglomeration at the start of milling. The mill used a speed of 200 RPM., with a ball powder ratio (BPR), of 30:1. The milling process was split into eight different sections by time, 0.25, .50, 1, 2, 4, 7, 11, and 19 hours. To study the impact the different balls would have, four different types of vials were used (1 to 4). The ratio and speed of the mill were not changed; however, the amount and size of balls change. Vial 1 had 202- 6mm, 19- 10mm, 28- 16mm, and 8- 18mm diameter aluminum balls. All of vial 2 contained 28- 16mm, and vial 3 contained 337- 6mm ball, vial 4 contained 225- 6mm balls, 21- 10mm, and 2- 18mm balls. Following the completion of the study, it was noted that the milling process flattens the particles, and additional milling will harden the particles. Noticeable imperfections observed in the aluminum from all vials include grain boundaries and dislocations. After comparing the milling efficiency of the vials, it was determined that the vials which had a mixture in ball size produced numerous low energy impacts. Low energy impact displayed a positive effect on efficiency. After the completion of the experiment, it was noted that the study could be

improved by then measuring the amount of hydrogen produced from each milling strategy. This was important to quantify, as the end goal of the study should be to produce hydrogen from a metal that was milled effectively.

Yavor et al. [34] conducted a study in which the aluminum powder utilized were spherical and within nano/ micro in size. The experimental temperature range of the powders was between 20-200^{o}C to test the impact of variations within the aluminum temperature. This study used ultrasonic waves is an agitator during the reaction process. The completed experimental setup for the hydrogen reactor was novel. It consisted of a hot water storage tank, a conical shape reactor, and an ultrasonic rod. As expected, the nano aluminum particles produced a higher hydrogen yield, due to their smaller size. This proved that larger particles size and low reactant temperature is not an ideal method to facilitate this chemical reaction. The study was unique due to its experimental apparatus. However, the study can be enhanced through testing aluminum production in alternative mediums, or adding reaction promoters such as NaOH to inhibit the formation of the oxide layer.

2.3 Hydrogen Production Using Various Water Mediums

There have been several studies in which changing the water medium was the main parameter of the research conducted. The idea varying the water medium was based on the premise that fresh or treated water may not always be readily available for hydrogen production processes. However, saltwater accounts for 96.54% of the total water available on earth, whereas only 2.53% of the water on earth is fresh. Furthermore, it should be considered that only 0.36% of freshwater is readily available. The majority of freshwater, which is unavailable, is located within glaciers and can be found within polar regions. Additional freshwater would be considered to be groundwater or moisture within the atmosphere [35]. Saltwater is sometimes viewed as an untapped resource for its potential to be converted into fresh water through the desalination process. However, the use of saltwater within hydrogen production can be viewed as an excellent opportunity to expand on salt water's useful outputs given its abundance.

For instance the work published by Rosenband et al. [36] studied the impact of changing the water medium. The work conducted by these researchers investigated the aluminum and water reaction's ability to produce hydrogen, through the use of novel aluminum

powder. A series of experiments were conducted, to identify the effectiveness of the aluminum powder. The conducted experiments used various water temperatures. Following this, a comparison with other aluminum- water reactions were conducted. This study emphasized the impact the type of water medium has on the aluminum samples used, including sea, tap, and distilled.

As previously demonstrated by numerous researchers, the use of gallium within metal alloys has great potential in effectively produce hydrogen. Other researchers have also identified gallium as an effective element within alloys, and have conducted studies which focus on gallium in particular. For instance, in a study conducted by Lu et al. [37], seawater and aluminum plates, which were activated using Ga- In alloy, were tested. The experimental design included the use of aluminum plates of the dimensions $10mm \times 10mm \times 10mm$. The seawater used within the experiment was artificially created by simply adding NaCl to the water, and had a starting temperature of 20^{o}C. The NaCl concentration was varied to add another metric to the study; each time, the aluminum plate submerged into the water. As expected, as the NaCl concentration increased within the water, the hydrogen production rate increased as well. By weight composition, the water medium was 0% NaCl in the first run. However, the concentration increased to 15%. The corresponding hydrogen production rate increased from 0.6 mL/min to 3mL/ min. The study conducted confirmed the use of NaCl as an effective reaction promoter. However, the study can be enhanced if researchers established how hydrogen production changes at higher temperatures.

Hydrogen production through the use of seawater was also tested by Pudukudy et al. [38], however, rather than using pure and new aluminum, waste aluminum used. Also, CaO was added to the reaction process to alter the environment the experiment was conducted within. The use of CaO added another level of complexity, and novelty to the experiment. Numerous experiments were conducted, which varied parameters such as the amount of NaCl added, temperature, the amount of aluminum, the form of aluminum (powder, foil, cans, and wires), comparing the results of various water mediums, and changing the amount of CaO added to the process.

The study conducted was extremely comprehensive, and the novelty of the research enhanced the study as well. To briefly summarize the effect salt has, the mass of NaCl was varied between 0g and 0.25g. It was determined that 0.15g of NaCl within the 20mL of seawater at 60^{o}C was optimal. 0.15g of NaCl was established as the ideal amount of salt if the goal is to maximize the amount of hydrogen yielded, and the hydrogen production rate. Following this, researchers aimed to identify which form of aluminum compliments 0.15g of NaCl the most. It as determined that Al powder was the best option when comparing the hydrogen production rate. A possible reason for this is the increased surface area, which using aluminum powder offers. At the end of the study, researchers compared the volume hydrogen produced, from various water mediums to the seawater they simulated with NaCl. The water containing NaCl produced a substantially greater volume of hydrogen compared to tap water and distilled water over 130 min. In this test 1g of CaO was added, and the test volume of aluminum used was 0.05g. It was later indicated that adding 3 or 4 grams of CaO will produce a significantly higher percent hydrogen yield, at nearly 100%. As previously stated, the study is very comprehensive and detailed. However, it would be interesting to measure the performance with other additives.

2.4 Hydrogen Production Using Various Aluminum Alloys

To identify if the use of aluminum alloys are more beneficial in hydrogen production compared to pure aluminum powder, researchers have conducted several studies to determine the effectiveness. For instance, Ilyukhina et al. [39] conducted a study that compared low energy activation and high energy activation of aluminum to produce hydrogen gas. Aluminum was selected as a reactant with water to produce hydrogen gas at different room temperatures, due to its abundance, low price, and overall safety. In this study, the room temperature was varied, and metal activation was achieved by adding Ga-In to create an alloy. The two different scenarios considered were low energy and high energy treatment.

The room temperature for high energy treatment was 21^{o}C, 40^{o}C, and 59^{o}C. The room temperature for low energy treatment was 24^{o}C, 41^{o}C, and 61^{o}C. After the experiment was completed, the aluminum was analyzed using an electron microscope, an X-ray spectrometer, X-ray powder diffraction, and a differential scanning spectrometer. The high

energy treatment of aluminum was able to cause an increase in its reactivity with water compared to low energy treatment; therefore, more hydrogen was produced. Maximum hydrogen production at high energy and low energy activation of aluminum is achieved at 11 mL/ (g min), and 1280 ml/ (g min). Although high energy activation of aluminum produces considerably more hydrogen gas, the study does not compare exact room temperature values.

In another study, Fan et al. [40] investigated another aluminum alloy and measured its effectiveness using other parameters. The alloy studied contained aluminum, lithium, and bismuth, and was used to generate hydrogen from its reaction with water. By conducting this experiment, researchers were able to identify the composition of the alloy that would be most effective in producing hydrogen. The impact temperature had on the reaction process was also studied. Aluminum was selected as a metal to produce hydrogen for this experiment due to it being recyclable and relatively affordable and its approximate cost of $3/ kg. The addition of lithium provided the benefit of being able to produce increased amounts of hydrogen. This was evident when lithium was used with aluminum, there was a decrease grain size within the alloy, therefore improving hydrogen production. Metals such as bismuth do not react with water and can hinder the growth of an oxide layer on the aluminum. Different weight compositions were used while adjusting the press pressure, and thickness of the sample, to determine the most cost-effective alloy. Several experiments were conducted for 30 minutes each, in which three different temperature ranges were used. It was determined that an alloy containing the weight composition of Al-20wt.%Li-5wt.%Bi was the most effective alloy. It was able to produce 1340mL of hydrogen with a hydrogen generation rate of 988 mL/ min per gram of Al used. This experiment did prove that this alloy was capable of producing more hydrogen, compared to pure aluminum used.

Furthermore, higher temperature experiments proved to be more effective in producing hydrogen. To conduct a more comprehensive study, additional combinations of an alloy's weight can be used. Furthermore, aluminum alloys containing different elements can be studied alongside this aluminum alloy to identify if there are more effective combinations.

In another study conducted by Fan et al. [41], researchers tested various aluminum alloys with different weight composition between aluminum and bismuth. The four different weight percentages of bismuth were 10, 16, 23, and 30. The hydrogen yield percentage and generation rate was compared at various times, to determine the effectiveness of the alloy. Distilled water was the water medium used, and NaCl was selected as a salt reaction promoter. Based on the information provided, the alloy which had a weight composition of 16%, had the highest hydrogen gas conversion yield of 89.88% at 30 minutes and the greatest hydrogen generation rate of 940 mL/ min, when only distilled water at room temperature was used. However, after 1M of NaCl was added to the water to identify how the reaction promoter may change the experimental results. The alloy with a composition of 16% still produces the highest conversion yield at 92.75%. However, the weight composition of 10% proved to have the highest hydrogen generation rate of 1010 mL/ min. Based on the results collected from researchers, it was clear that 16% weight composition showed the most promising results. To identify the optimal conditions to produce the aluminum sample, researchers also varied the milling time. The different milling times used were 2, 5, 10, and 20 hours. After this, their hydrogen conversion yield was compared over 60 minutes. The alloy milled for 10 hours, produced the greatest yield of 84.20% and had a generation rate of 880 mL/ min. Lastly, a microscopic analysis was conducted to identify changes within the microstructure of the aluminum particles milled at different times. The research conducted was detailed and well thought out. This was evident as researchers successfully determined an optimal alloy composition, then determined optimal conditions for its production as well. However, the study can be enhanced by comparing other aluminum alloys to the alloys that were studied. For instance, a comparison to an alloy containing aluminum and gallium would provide a more comprehensive study.

Another study which aims to find the optimal aluminum alloy composition was a study conducted by Zhao et al. [42]. The experiment introduced hydrogen production using an alloy containing aluminum and calcium. Five variations were implemented, to find the optimal mix between aluminum and calcium. The aluminum percent compositions of the samples were 0, 5,10, 15, and 20. In which each experimental trial conducted over 3000 seconds, with temperatures ranging from 10^{o}C to 80^{o}C. The test sample was also produced

using ball milling, and NaCl was added to improve the hydrogen yield. The significant finding from this experiment was the aluminum composition of 20% had the highest hydrogen yield percentage at 47.87 %. However, the addition of 5% of NaCl to the alloy, will result in a substantial increase in the hydrogen yield percentage. If the 20% aluminum is combined with NaCl, this will result in the hydrogen yield percentage is 96.5 %. Similar to the previous experiment, the study would benefit greatly by comparing different metal alloys while using NaCl.

Although the use of aluminum compounds is a standard method to facilitate hydrogen production, a composite powder containing aluminum and other metals can be investigated. In a 2011 study conducted by Dupiano et al. [43], researchers aimed to compare the different aluminum- metal oxide powders with varying rates of reaction to identify the amount of hydrogen produced for comparison. To carry out this experiment, various milled aluminum- metal oxide powders heated to 80^{o}C then to room temperature for 16 hours. The metals reacted with water to produce hydrogen (Al- water split reaction). Compounds include ($AlMoO_3$, $AlBi_2O_3$, AlCuO, AlMgO and $AlAl_2O_3$). In order to measure the hydrogen produced, a water displacement flask was used. Subsequently, X-ray diffraction and microscopy were used to analyze the products of the reaction. It was identified that $AlBi_2O_3$ has the fastest reaction rate, and produced the highest yield percentage of hydrogen gas compared to others. This study can be improved by varying the temperatures of the metal powders more and increasing the overall time of the experiment. Also, a cost comparison between the various aluminum- metal oxide powders, would aid in determining the most feasible option.

In a very novel study where the primary goal was to test various aluminum alloys, Xu. et al. [44] used unique test samples. All samples used were derived from the idea of using a combination of aluminum, lithium hydride, and a metal oxide. Amongst the various samples used, the weight composition used for the lithium hydride remained constant at 5%. One sample served as a reference in which no metal oxides were added, the other metal oxides added were Ga_2O_3, Bi_2O_3, In_2O_3, ITO, TiO_2, and γ-Al_2O_3. All metal oxides previously had a weight composition of approximately 5%. To quantify the effectiveness of the various compositions used, researchers measured the total H_2 yield, the conversion

efficiency, as well as the hydrogen production rate as a metrics to draw their conclusion. All samples used were tested using water at 25^{o}C. Based on the results collected from Xu. et al. [44], the presence of metal oxides was necessary to get effective results. The alloy without metal oxides produced only 475 mL of hydrogen gas total, with a conversion efficiency of 3.8%, and a production rate of only 78.3 mL/ min. However, after the alloy was added the experimental result was substantially more effective. Overall the alloy containing Ga_2O_3 performed the best overall. Its hydrogen yield was 1357 mL with a conversion efficiency of 98.6 % and a production rate that was by far the best amongst all the other alloys of 3857 mL/min. It should be noted that the alloy containing Bi_2O_3 produced a very close hydrogen yield and conversion efficiency of 1355 mL and 98.5 %, respectively. The conducted test was extremely novel in regards to the alloy used; however, the test was performed using a water temperature of approximately 25^{o}C. The water temperature used is relatively low; therefore, a possible area of improvement within the study is varying the water temperature.

2.5 Hydrogen Production Using Waste Aluminum

The switch to hydrogen as an energy carrier has significant benefits as a means to reduce the ecological impact of energy production. The hydrogen generation process can be enhanced by using recycled aluminum instead of aluminum that has been mined and prepared specifically for hydrogen production.

The idea of using waste aluminum cans for hydrogen production was investigated by Martinez et al. [45] in a study entitled, “Recycling of aluminum to produce green energy.” The experiment aimed to generate hydrogen gas with high purity. To do this NaOH, and H_2O was reacted with recycled aluminum. By using different ratios of aluminum and NaOH, it can be identified what ratios produce the most hydrogen gas, and predict the amount of energy in Watt-hours the hydrogen gas will provide. The experimental apparatus used to generate hydrogen was a Kipp generator. The Kipp generator used contained NaOH and aluminum. The NaOH at the top of the container pressurized the middle section of the Kipp generator, where aluminum was present. Hydrogen was produced in the pressurized middle section and then leaves through a tube afterwards. As the hydrogen exits the middle section, the pressure reduced. The hydrogen that exits the pressurized middle section exits

through a pipe connected to a bubbler system. The complete experimental setup is depicted in Figure 2.1.

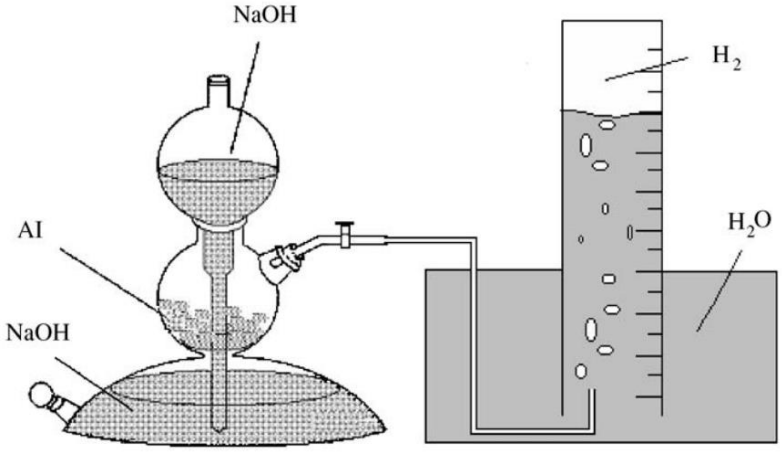

Fig. 2.1 Experimental setup designed by Martinez et al. [45]

All experiments were conducted from 0 to 180 minutes, with different Al/NaOH ratios. The ratios used were 3.00, 2.00, 1.50, 1.25, and 1.10. Subsequent to the completion of all experiments, it was noted that the ratio of 3.00 produced the most hydrogen after 180min. Approximately 1379 mL of hydrogen gas was produced at 180min. Whereas the ratio of 1.10 produced 755 mL of hydrogen gas, after 180min. The ratio of 3.00 is also capable of producing the most energy (Wh) after 180min, at 4.14 Wh. The ratio of 1.10 is projected to produce the least energy 2.27 Wh. This study assumed that 1L of hydrogen gas was capable of producing 3Wh of energy. The financial analysis of this study was limited, as it only shows the cost for the average Mexican person and the production cost for 3 Al/NaOH ratios.

In another study, Swamy et al. [46] investigated the ability to convert aluminum foil to powder, for hydrogen production. The concept of using aluminum foil was derived from the idea of households wasting aluminum and aluminum's ability to be recycled. This paper introduced the idea of using scrap aluminum to produce aluminum powder to make hydrogen. The aluminum foil prepared through the milling process reacted with water having a temperature 35- 80^{o}C. Aluminum samples with a mass of 0.7 grams were immersed in 0.750 L of deionized water to complete the experiment. The temperatures used during the experiment were 35^{o}C, 50^{o}C, 65^{o}C, and 80^{o}C. Following the completion of the experiments, the aluminum foil milled with NaCl had a high amount of reactivity

with heated water. The test at 80^{o}C experienced the most significant increase in the reaction rate and had the highest hydrogen yield over 120 minutes. The study can be enhanced by studying the effects of pre-heating aluminum samples or using various water mediums in conjunction with recycled aluminum.

Hiraki et al. [47] conducted a life cycle assessment, in conjunction with an experiment where the goal was to reduce metallic waste and produce hydrogen gas. In order to study the feasibility of hydrogen production using waste aluminum, a unique experimental apparatus was developed. The experimental apparatus used consisted of the following main components, a flow meter, magnetic stirrer, sample powder in an alkaline solution, thermocouple, and pH meter. The experimental set up is depicted in Figure 2.2.

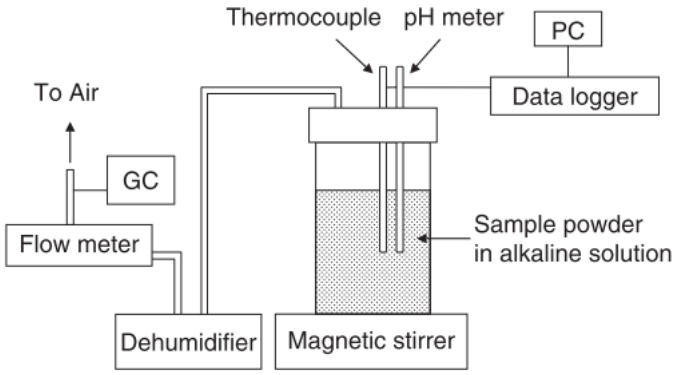

Fig. 2.2 Experimental setup designed by Hiraki et al. [47]

In total, five different simulations were studied. The initial temperature of the aqueous solution in each trial was 36.4 ^{o}C, 18.1^{o}C, 40.1 ^{o}C, 50.1 ^{o}C, and 60.1 ^{o}C in the respective order; the experiments were carried out. The concentration and volume of the solution remained constant throughout. However, the weight to mass ratio and the molar mass ratio for the first run was different. The chemical reaction was facilitated using a magnetic stirrer. The experiments were conducted for over 40 minutes. Qualitatively, hydrogen bubbles became immediately visible. The hydrogen gas generated had a purity of 99.9 %. After the reaction took place, the PH of the solution incrementally decreased. The incremental decrease was due to the $Al(OH)_4^-$ yield. However, there was a notable increase in the PH after the 1200 second mark. Furthermore, as expected, the aqueous solution at the higher temperatures experienced the most significant degree of reaction (%). The use

of other aqueous solutions can be explored with a similar experimental setup up to draw additional comparisons.

In another study conducted by Ho et al. [48], the feasibility of using waste aluminum to generate hydrogen is studied. The waste aluminum used was hydrolyzed cans that were previously submerged in an alkaline solution; NaOH was used to remove the aluminum-oxide layer. Before the start of the experiment, the aluminum cans were pre-treated using sulfuric acid (H_2SO_4). In order to study the effectiveness of aluminum cans, it was compared to aluminum powder. The powder used during the experiment was much smaller, being smaller than 45um. However, it should be considered that the waste aluminum and powder both have a purity of 99.5%. The study varied the temperature of the aluminum powder and can waste from 50^{o}C to 70^{o}C. The results of using aluminum powder and aluminum cans were very comparable. The aluminum powder produced was able to achieve a maximum hydrogen production rate of 1360 mL/min at 70^{o}C, however, the waste aluminum was able to achieve 1350 mL/min. Considering that pure aluminum in the form of waste produced a similar amount of hydrogen, and requires less energy to produce, this study established waste aluminum as a viable option for this type of hydrogen production. It should also be noted that aluminum cans containing nickel as an additive were able to produce significant results as well. This study was successful in investigating and proving that hydrogen production using waste aluminum is a viable and even more sustainable option. However, this study used distilled water, which required more energy to manufacture. In order to conserve energy, the use of sea/ saltwater in conjunction with waste aluminum is an opportunity to determine if there are even more ways to make this production technique more sustainable.

2.6 Novel Hydrogen Production Methods

By using the chemical reaction between aluminum and water, there were numerous methods to produce hydrogen gas. In the past, researchers have aimed to introduce new and novel methods of hydrogen production to build and contribute to past research done. Typically, researchers measure the performance of systems or the hydrogen production technique by varying the water medium, aluminum alloy composition, aluminum particle size, microstructure, and experimental setup.

In a study conducted by Elitzur et al. [49], researchers investigated the effectiveness of using aluminum in conjunction with urine to produce hydrogen gas. In theory, hydrogen production via urine does have merit considering urine is approximately 95% water [50]. This method of hydrogen production can also be considered a subcategory of hydrogen production through aluminum water hydrogen production since urine is a derivative of water. It should also be considered that similar to saltwater, urine is an indefinite resource as numerous multicellular organisms excrete it as waste. To test its effectiveness as a solvent, researchers conducted a parametric study in which they varied urine temperature from 25^{o}C to 60^{o}C, while also varying the mass by a factor of 2. As expected, the urine temperature of 60^{o}C produced the highest hydrogen yield at approximately 90%. At the end of the study, it was concluded that the use of urine is capable of achieving 2200 Wh/kg of Al if a fuel cell having a 50% efficiency is being used. The study also claimed a high rate of hydrogen production capable of reaching up to 700 ml/min per gram of aluminum. At the beginning of the study, it states the urine composition used for the test. However, it should be noted that the composition of urine depends heavily on what was consumed during the day by the living organisms, as well as its general health. Therefore, to enhance the study variations in urine composition can be studied.

2.7 Variations in Water Temperature

Most of the experiments previously summarized in Sections 2.1 to 2.6, were conducted using variations in water temperature. This was done to identify how effective hydrogen can be produced from an aluminum water reaction, with temperature as the varying property. Based on the previously examined studies, the increase in temperature of the reactants usually results in a higher yield percentage, and hydrogen production rate. The increase in reaction temperature forces the molecules to reach a more excited state, therefore forcing the reaction to take place at a faster rate.

2.8 Oxide Layer Reduction Techniques

The formation of the oxide layer on aluminum is viewed as the largest barrier researchers must overcome to produce hydrogen from an aluminum water reaction. Through the introduction of reaction promoters, and aluminum treatment techniques to the chemical reaction, the effect of the formation of the oxide layer can be reduced. Chemical reaction promoters and aluminum treatment techniques are summarized in Figure 2.3.

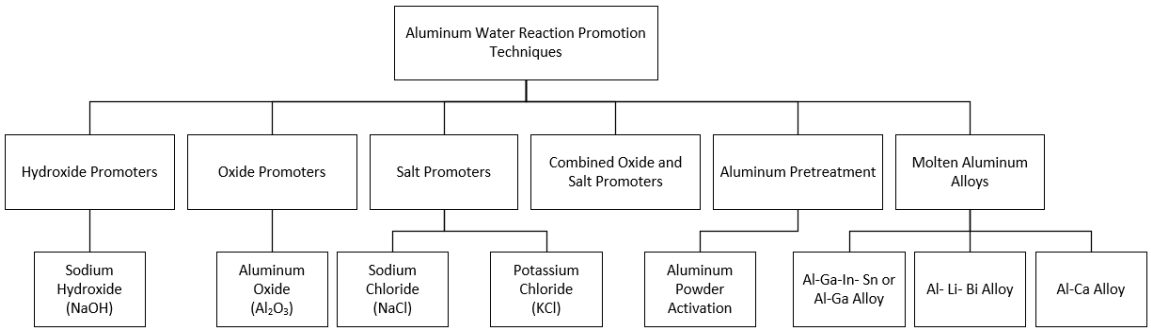

Fig. 2.3 Aluminum water reaction promotion techniques (data from [7])

2.9 Hydroxide Promoters

Typically, NaOH is the hydroxide promoter selected to be added to an aluminum water reaction. NaOH added to the reaction is typically in pellet form, and it dissolves into water to form hydroxide ions. The interaction between NaOH, aluminum, and H_2O molecules is depicted within the following chemical equations:

$$2Al + 2NaOH + 2H_2O \rightarrow Na_2Al_2O_4 + 3H_2 \quad (2.1)$$

$$2Al + 6NaOH + xH_2O \rightarrow Na_6Al_2O_6 + xH_2O + 3H_2 \quad (2.2)$$

$$2Al + 2NaOH + 6H_2O \rightarrow 2NaAl(OH)_4 + 3H_2 \quad (2.3)$$

The above chemical equations were obtained from the U.S. Department of Energy, in a report entitled, “Reaction of Aluminum with Water to Produce Hydrogen” [7].

To study the effectiveness of aluminum and aluminum alloy’s ability to generate hydrogen for fuel cell applications, Soler et al. [51]conducted a study where changing the hydroxide promoter properties was a primary area of the study. The study used KOH and NaOH as the two hydroxide reaction promoters implemented during the experiment. The experiment consisted of 0.1 grams of aluminum foil compressed into a spherical shape, then submerging it into a reaction vessel containing 75 cm^3 water, and its respective hydroxide promoter. Another dimension added to the study was varying the concentration of the reaction promoter. According to researchers, they were able to achieve the maximum hydrogen production rate using NaOH as the hydroxide promoter, with a concentration of 5 M, and with a water temperature of 348 K.

2.10 Oxide Promoters

Oxide promoters, such as Al_2O_3, have been proven to show resistance to the formation of the aluminum oxide layer. In the past, the researcher has found that Al_2O_3 in powdered form is considerably effective on the water with a temperature of 10 to 90^oC, with the water concentration ranging at a pH level of 4 to 9. In a US patent entitled, "Hydrogen Generation From Water Split Reaction," the inventor Chaklader [52] compared an aluminum compound that had a 20% weight composition of Al_2O_3, ability to produce hydrogen compared to pure aluminum. As expected, the sample containing 20% weight composition of Al_2O_3 produced significantly more hydrogen than pure aluminum. Aluminum oxide exists mainly in the following four forms [7]:

- Alpha alumina- α- Al_2O_3
- Gamma alumina- γ- Al_2O_3
- Bayerite- $Al(OH)_3$
- Boehmite- AlO(OH)

Amongst the four aluminum oxide powders listed, α- Al_2O_3 has the greatest ability to ability to produce hydrogen. However, a study conducted by Deng et al. [53] γ- Al_2O_3 is was used to produce hydrogen. The conducted study found that γ- Al_2O_3 was able to react to water at standard temperature continuously and pressure conditions. Additional studies were also conducted at water temperatures, which exceeded 40^oC. The chemical reaction used by Deng et al. [53] is a stage process, shown in the following equations:

$$Al_2O_3 + H_2O \rightarrow 2AlOOH \tag{2.4}$$

$$2Al + 6AlOOH \rightarrow 4Al_2O_3 + 3H_2 \tag{2.5}$$

In Equation 2.4, Al_2O_3 is converted to AlOOH after it becomes fully hydrated. After this, the AlOOH layer surrounding the aluminum particle reacts to form hydrogen bubbles. It should also be noted that hydroxide ions are also formed on the metal's surface. To visualize the chemical reaction process more accurately, Deng et al. have created the following schematics, which correspond with Equations 2.4 and 2.5.

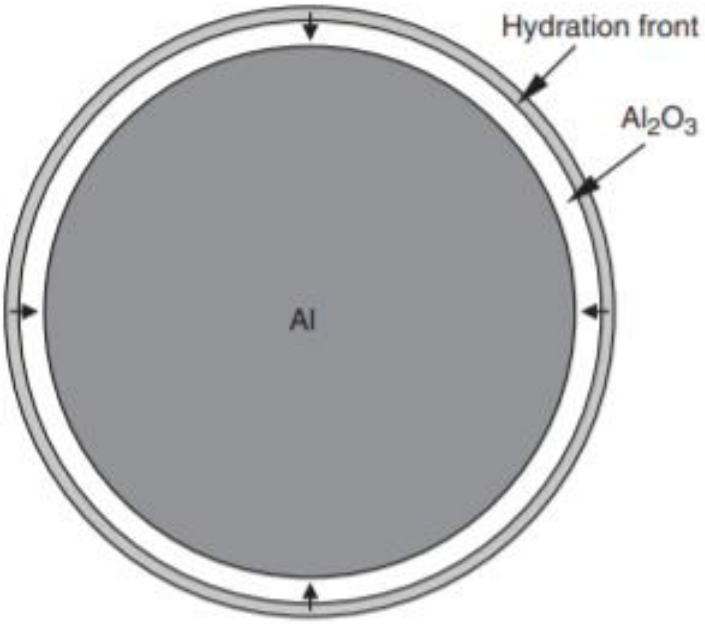

Fig. 2.4 Water reaction with alumina coated aluminum particle (Before ALOOH Growth, Stage 1) [7]

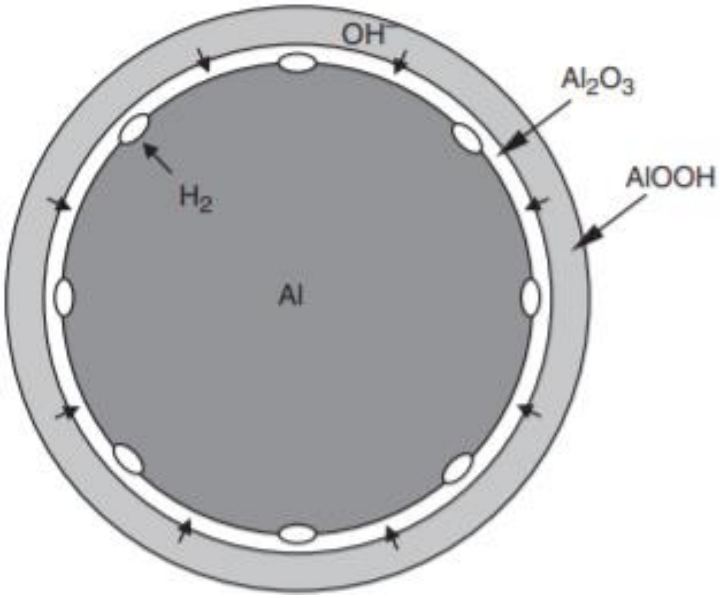

Fig. 2.5 Water reaction with alumina coated aluminum particle (after AlOOH growth, and formation H_2 bubbles, stage 2) [7]

2.11 Salt Promoters

Ideally, the salt promoter should be inorganic and water-soluble. The addition of inorganic salts to the reaction process causes the aluminum oxide layer to deteriorate. Commonly used salts are sodium chloride and potassium chlorides, as they are widely considered to

be the most effective salts for removing the oxide layer [7]. In 2005, Canadian inventors Troczynski et al. [54], introduce hydrogen production strategies using the chemical reaction between aluminum and water. The introduced aluminum water reaction uses inorganic salts as a catalyst within the chemical reaction. Troczynski et al. [54] conducted a test that compares the effectiveness of NaCl and KCl. The experiment used a water temperature of 55^{o}C for 120 minutes. The aluminum powder used was balled milled with one salt and was compared to the results of aluminum milled with another salt throughout different runs. Early in the experiment, Sodium Chloride was found to be the more effective catalyst compare to Potassium Chloride in its respective run. However, as the experiment progressed, Potassium Chloride proved to be the more effective catalyst in terms of generating hydrogen over at a faster rate.

In a study conducted by Irankhah et al. [55], the effect of using various salt promoters to facilitate the reaction between aluminum and water was studied extensively. The salt promoters used and compared during the study included NaCl, KCl, and $BaCl_2$. The salts were melted down with aluminum particles to form aluminum alloys. All three alloys were tested under the same conditions to determine the most suitable or ideal alloy composition. All alloys were ball milled for 5 hours; then, the hydrogen production was compared for 1200 seconds. It was determined that KCl produced the maximum hydrogen generation rate of 856.9 mL/min. However, $BaCl_2$ had the greatest average hydrogen production rate at 229.2 mL/min. Lastly, NaCl was able to produce the largest cumulative amount of hydrogen gas at 1641 mL/min. Therefore, it was deduced that all three salt promoters used by researchers have merit, but NaCl will give the greatest amount of hydrogen gas. To simulate non-isothermal test conditions, the temperature of the water medium fluctuated, to identify how it would impact the amount of hydrogen generated. Amongst the three water temperatures used 65^{o}C, 75^{o}C, and 80^{o}C it was observed that the greatest temperature of 80^{o}C produced the most hydrogen.

Furthermore, to add another dimension to the study, researchers conducted a comparison between the aluminum alloys that contained NaCl and waste aluminum foil with aluminum powder and aluminum powder that had salt within it. As expected, the sample containing aluminum powder with salt produced the best results in terms of the amount of hydrogen

produced, since it contained a reaction promoter while also being in powdered form. The experiments, the amount of research conducted by Irankhah et al. [55], was well executed and detailed; however, the study can be enhanced by using various water mediums.

2.12 Combined Oxide and Salt Promoters

To maximize the reaction yield, different methods to reduce the oxide layer can be used in conjunction with each other. The positive attributes of using oxides and salt promoters individually have been expressed earlier in chapter 2. However, inventors of a 2006 patent, Anand et al. [56] studied the effect of combining these techniques. In their study, authors combine salt and oxides at 20^{o}C. Researchers determined that the ideal salt and oxide promoter available were NaCl and CaO. The conducted experiments varied the amount of CaO added in each trial from 0% to 20% for five runs. The results showed that the ideal amount of calcium oxide should be between 0.5 to 4%, and a 1 to 1 ratio between aluminum and NaCl is optimal for the designed system. Under these experimental conditions, the hydrogen generation rate was 0.001 g H_2/ s [56].

To study the effect of using oxides in conjunction with salt promoters, Wang et al. [57] examined this by primarily using aluminum with CaO, and NaCl. In order to create variation within the experiment, the mass percentages were varied to identify an optimal composition, capable of giving the most significant hydrogen yield. Wang et al. observed that when the water temperature started at approximately 60^{o}C, the composition that provided the most significant hydrogen yield was Al-9% CaO-9% NaCl. It should be noted that this mass composition was the only one listed to have the same amount of NaCl and CaO. Subsequently, Wang et al. used the same mass ratio but changed the composition of aluminum to an alloy, in order to identify a more optimal composition. These alloys consisted of Sn, Ga, and In, and tests were conducted at 60^{o}C and 25^{o}C. By comparing the results shown by Wang et al. [57], it can be stated that the 60^{o}C water was preferred over 25^{o}C, and the alloy Al- Ga- In- Sn with the respective ratio of 96: 1: 1: 2 produce the most hydrogen.

2.13 Aluminum Pre-Treatment

Aluminum activation is also a commonly used strategy to maximize the amount of hydrogen generated within an aluminum water chemical reaction. To effectively activate

aluminum, it can be ball milled while being submerged in water, then implementing a rapid heating and cooling process. This form of aluminum treatment was conducted by inventors Watanabe et al. [58], in which 5g of aluminum particles were used to generate hydrogen over 50 hours. The results of the experiment showed that aluminum after metal activation was significantly more effective compared to hydrogen production without activation [58].

2.14 Molten Aluminum Alloys

The use of molten aluminum alloys has the potential to mitigate the formation of the oxide layer. Alloys derived aluminum- gallium is considered to be a viable option. However, gallium has been linked to fatal lung complications [59]; therefore some avoid the use of gallium within research. Hydrogen reactors that utilize molten aluminum integrate a sprayer system embedded within the reactor to facilitate the dispersion of the molten aluminum alloy [60]. Molten aluminum alloys can bypass the formation of the oxide layer, as it is more difficult to form on aluminum while it is a molten state. Since the oxide layer does not form, the aluminum can start reacting with water upon contact [61][62].

To study the effectiveness of using molten aluminum to produce hydrogen, researchers Shemev et al. [63] conducted a series of tests. The aluminum temperature used during the study had a starting temperature, which ranged from 1100 to 4000^{o}C, and was confirmed using a thermocouple contained within a blind steel jacket. To safely and effectively work at these high temperatures researcher used a stainless steel reactor. The aluminum samples used during the experiment had a mass of 60g. During the experiment, water entered the process through the use of a syringe and was converted into steam. The hydrogen yield when the steam had a flow rate of 0.01 g/s had a relatively low yield of 40%. However, it should be noted that the hydrogen yield was able to substantially increase as high 100% when KOH was added to the molten aluminum. The study conducted by researchers can be enhanced by studying the effect of using various aluminum alloys within the reactor system and then providing a comparison of the yield percentages.

CHAPTER 3: EXPERIMENTAL APPARATUS AND PROCEDURE

In this section, the experimental setup and processes used to collect results were introduced. This section presented a novel hydrogen production strategy, based on the chemical reaction between aluminum and water. The novelty of this thesis project pertained to the unique experimental setup. The distillation setup enables water to be recycled back within this system to increase the overall efficiency of the process.

3.1 Principles of Design

Before the start of the experiment, an experimental schematic was designed to establish the needed components, the arrangement of components, and the entire experimental process. In Figure 3.1, the various stages in the experimental setup were established.

Before state 1, N_2 gas was released from a compressed cylinder at a pressure and flow rate of 18 kPa and 15L/ min before. After state 1, N_2 gas released Al powder, into the 500mL reaction vessel. The chemical reaction within the 500mL reaction vessel was highly exothermic. Therefore, hydrogen gas, and evaporated water rose through the Vigreux column and the 200mm Liebig condenser. Simultaneous to this, a peristaltic pump moves cold water at a flow rate of 400.1 mL/min into the condenser. Water then left the condenser at state 5, where it entered the reservoir. This embedded cycle repeats when water is withdrawn from the reservoir at state 7. At state 4, saturated water and hydrogen gas left the Liebig condenser. The saturated water and the hydrogen gas can be separated by using a distillation head, at the intersection of state points 4,8, and 9. At state point 8, condensed water entered the 500mL flask, and hydrogen gas moved along with state 9, where it will entered a volumetric flow meter. The volumetric flowmeter designed by Alicat recorded changes the pressure, temperature and volume as a rate. However, the primary issue of only using a flow meter was its inability to verify the composition of the gas. Ideally, only hydrogen should flow through the meter; however, the system is not without the absence of air, and the presence of nitrogen gas. Therefore, after the gas leaves the flowmeter at state 10, it is guided through an L tube to release the hydrogen in front of a gas sensor. The gas sensor measured the concentration of hydrogen in the environment in ppm.

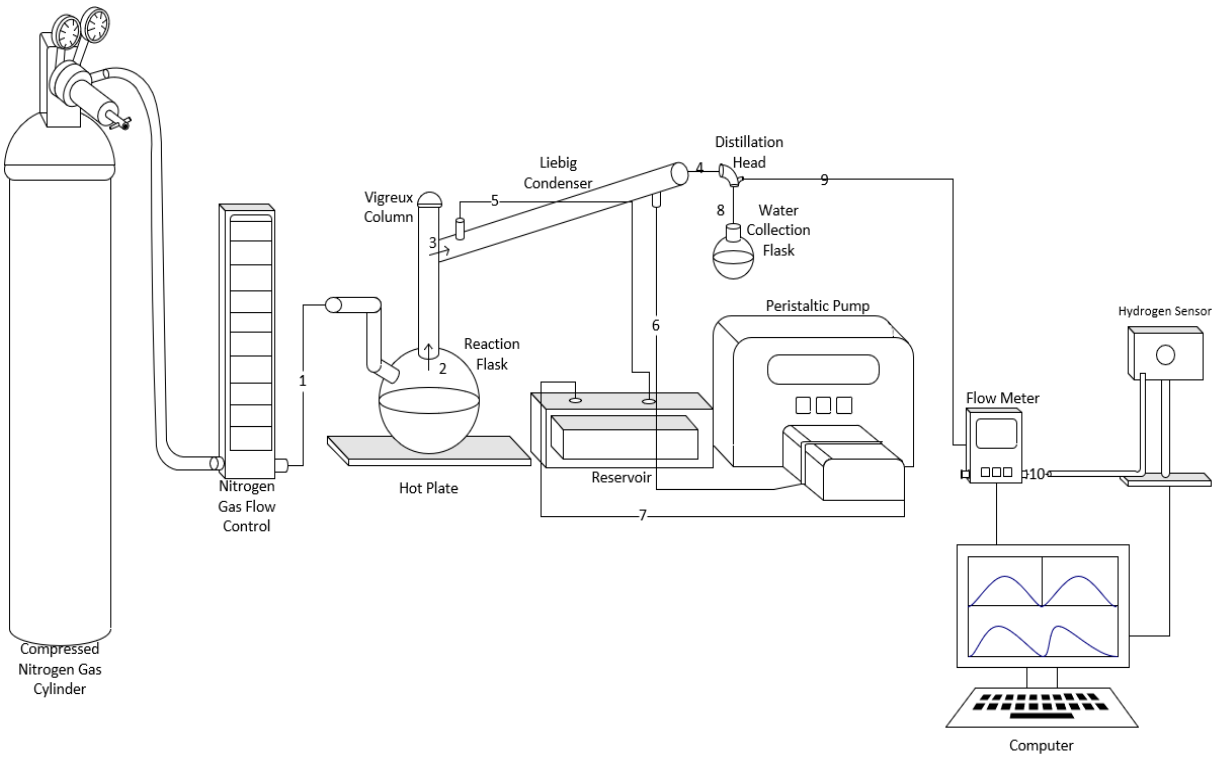

Fig. 3.1 Schematic of system design

After the system schematic was completed, the design of the experimental set up was then considered. During this process, it was acknowledged that for the system to operate effectively, two work stations were required. The experimental testing station located within the fume hood and a data acquisition station where the concentration, volumetric flow, mass flow, pressure, and temperatures of hydrogen gas being generated from the system were recorded. Figure 3.2 provides an image of the experimental setup located within the fume hood and its major components. Various variations of this experimental setup were also tested to find the most suitable design. Several different powder sprayer systems, hot plates, and pumps were considered.

Initially, a spray gun system was considered; however, after the powder is released from the spray gun, a substantial amount of aluminum powder was stuck in its powder storage system. This caused the idea of the spray gun system to be re-evaluated, the improved spray system should have a less complex storage compartment, that would be easy to clean between experimental trials. The different hotplates were used and considered during the experimental setup design process. Due to the experiment having to be conducted within a

fume hood for safety reasons, cold air blew unto the reaction vessel during the warm-up period. Therefore, during the initial testing process, it was difficult for the reaction vessel to achieve the necessary temperature because it was being cooled by convection. At this point, two feasible solutions to mitigate this issue were proposed. Potential solutions to this issue consisted of; using an insulating jacket over the reaction vessel or using a hot plate with a larger surface area. The insulating jacket proposed would be made out of fibreglass; however, this idea was discontinued because of the flakey nature of the material. A hot plate with a larger surface area was available within the laboratory and did not leave any debris behind within the fume hood; therefore, it was deemed the ideal option for the experiment. Before considering the peristaltic pump, a submersible pump was used. The submersible pump was substantially cheaper; however, it presented numerous issues. The submersible pump initially purchased was unable to tune to a specific flow rate. Also, the pump was prone to issues such as cavitation and other forms of damage since its internal components came in direct contact with the water.

Fig. 3.2 Experimental testing work station

The data acquisition station operated simultaneously with the experiment being conducted. In order to keep a log and interpret the raw data obtained from the hydrogen sensor, the PK Port accessory was purchased. The PK port accessory was compatible with the older Windows XP operating system; therefore, an older desktop computer was acquired and placed on the left side of Figure 3.3. This part of the experimental set up was primarily responsible for recording the concentration of the gas passing through the system. Quantities such as the volumetric flow, mass flow, and changes in pressure were recorded and analyzed using flow vision software acquired from ALICAT. The flow vision software was compatible with the flowmeter and was capable of providing real-time updates similar to PK port accessory and PK Port software. A smaller laptop computer was used to record and analyze this data, shown on the right side of Figure 3.3.

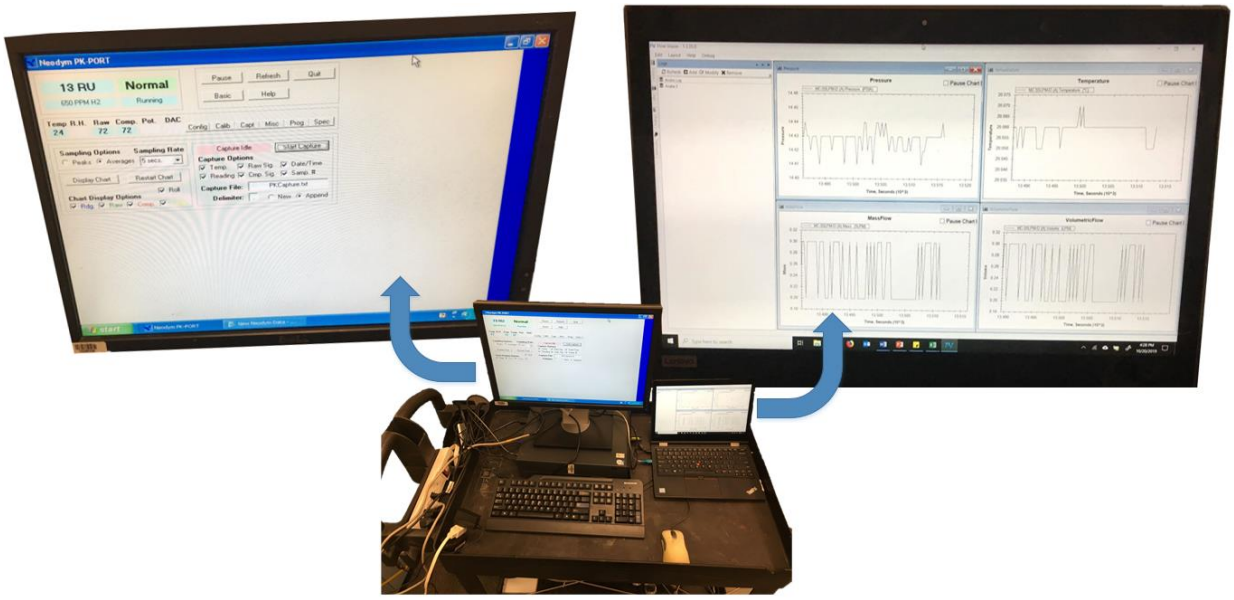

Fig. 3.3 Data acquisition station

3.2 Key System Components and Observation Devices

To construct the physical prototype, major system components, along with several others, were implemented. Components used for data acquisition and system control have been provided within this section. Additional components such as valves, pipes, and electrical wires that were not within this section.

To verify the hydrogen production rate, the M- Series Flow Meter was implemented within the system. The M-Series Flow Meter is shown in Table 3.3, and its operating conditions and performance have been summarized in Tables 3.1 and 3.3, respectively. The Alicat M-Series Flow Meter is capable of acquiring temperature, pressure, and volumetric flow data of the gas passing through its chamber.

Table 3. 1 M- Series Flow Meter Operating Conditions (data from [64])

Operating Conditions	**M-Series Mass Flow Meter**
Mass Reference Conditions (STP)	25ºC & 14.696 psi (standard — others available on request)
Operating Temperature	−10 to +60 ºCelsius
Humidity Range (Non–Condensing)	0 to 100%
Maximum Internal Pressure (Static)	145 psi
Maximum Allowable Instantaneous Differential Pressure Across Device (Inlet to Outlet)	75 psi
Proof Pressure	175 psi
Mounting Attitude Sensitivity	None
Ingress Protection	IP40

Table 3. 2 ProtiSen^{TM} Hydrogen Sensor Operating Conditions (data from [65])

Parameter	**Min.**	**Type**	**Max.**	**Units**	**Notes**
Accuracy	5	3	-	%	Percent range, still air
Linearity	5	3	-	%	Percent range, still air
Air Velocity Error	-	1	1.5	%	Percent range, 3 m/s
Oxygen Requirement	5	21	-	%	
HMDS Tolerance	100/ 50 10/500	-	-	ppm/h	
Operating Temperature	-40	-	+80	ºC	
Operating Humidity	0	-	99	%RH	Non- condensing
Warm- up Time	-	2	10	s	
Response Time (T90)	-	2	3	s	
Recovery Time (T10)	-	5	10	s	
Input Voltage 5-16 VDC	5	-	16	VDC	Option I2- switch mode PSU
Power Consumption	-	750	800	mW	At 12 VDC supply

To effectively capture the concentration of the hydrogen gas produced, after it released into the fume hood environment, the ProtiSen hydrogen sensor was implemented at the very end of the experimental setup. An image for the ProtiSen^{TM} sensor is provided in Table 3.3. The manufacturer data and operating conditions have been summarized in Tables 3.3 and 3.2, respectively.

An essential aspect of testing the experimental system was to identify how effectively it can operate under varying temperature conditions. It is also crucial to verify various temperatures within the system, such as the water temperature within the reservoir, and the water temperature within the reaction vessel. Initially, the implementation of thermocouples within the system was considered; however, the addition of thermocouples may cause the system to experience leakage if the thermocouples were used. Furthermore, due to the addition of NaOH within the reaction vessel, the NaOH can react with the thermocouple material, thus causing it to deteriorate.

In order to mitigate the issues previously listed, a temperature gun can be used as an alternative. After the trigger was pulled, a laser points at the location the temperature is being read from. Following this, the temperature at that particular point, along with the average temperature is reading is displayed.

Thus, there is no need to have contact with the device and the medium. Although this method of temperature collection is non-invasive, it was important not to point the infrared thermometer at the glass of the reaction vessel, when taking a reading, as the reflection may distort collect values. The Master Craft Digital Temperature Reader used within the experiment provides the ability to collect values quickly. An image of the Master Craft Digital Temperature reader has been shown in Table 3.3. General information of the used infrared thermometer has also been summarized in Table 3.3.

The experimental set up utilizes the BT100-1L Longer pump over conventional or cheap submergible pumps. The BT100-1L is a peristaltic pump is not prone to common pump problems such as cavitation. The peristaltic pump moved water through the tubes connected the condenser directly. Since water is being moved through the tubes, it does not come into contact with the pump's components; this provides the added benefit of reducing the possibility of contamination, and cavitation. Furthermore, experiment parameters can easily be tuned and adjusted using its rotating knob and the buttons

underneath its digital display screen. The device's interface and features enabled the experiment parameter to be set accurately. An image of the BT100- 1L Peristaltic Pump used for the experiment has been provided, along with the pump data being summarized in Table 3.3.

The theoretical mass of reactants NaOH and aluminum were calculated using mole ratios, and the molar mass of the respective compound. However, to verify that the correct mass was being added to the 500mL reaction vessel, they were weighed using the Mettler Toledo, AB204- FACT scale.

The scale has a protective transparent shield around three sides to encase the material being weighed. This blocked air currents and dust particles from landing on the section being weighed. An image for the scale has been provided, with the scales' data summarized in Table 3.3.

Testing the system under varying water temperature conditions was a significant component of the research being conducted. Therefore, a hotplate has been integrated within the design to elevate the temperature of the water within the reaction vessel for the various trials. The reaction can also be improved if the hot plate is capable of magnetic stirring. By agitating the mixture, while a reaction is taking place, this should facilitate the reaction to occur quicker. The Fisher Scientific Isotemp Hotplates with Stirring is capable of this. This hot plate was selected amongst others with the same capabilities due to its surface area. During the design process of the experimental setup, it was determined that the experiment should be conducted within a fume hood with a safety shield. The air within the fume hood has a velocity of approximately 1.3m/s. Therefore, while the solution is being heated from the plate, it was also being cooled from air convection. The use of a plate with a large surface area or cloaking the reaction vessel with insulation mitigated this issue and allowed the water to reach its required temperature quicker.

After identifying the main chemical reaction between aluminum, water, and sodium hydroxide, Equation 2.3 was selected and used throughout experimental runs. By analyzing at the mole ratios of Equations 2.1 to 2.3, it established that all three reactions would produce the same amount of hydrogen; however, Equation 2.3 required a smaller amount of sodium hydroxide compared to Equation 2.2, and the additional water required for Equation 2.3 helped the reaction to take place.

Table 3. 3: Experimental components and description

Equipment Name	Equipment Image	Parameter	Specification
M- Series Flow Meter (data from [64])		Accuracy at calibration conditions after tare	± (0.8% of Reading + 0.2% of Full Scale)
		High Accuracy at calibration conditions after tare	± (0.4% of Reading + 0.2% of Full Scale) High Accuracy option not available for units ranged under five sccm or over 500 slpm.
		Accuracy for Bidirectional Meters at calibration conditions after tare	± (0.8% of reading + 0.2% of total span from positive full scale to negative full scale)
		Repeatability	± 0.2% Full Scale
		Zero Shift and Span Shift	0.02% Full Scale / ºCelsius / Atm
		Operating Range / Turndown Ratio	0.5% to 100% Full Scale / 200:1 Turndown
		Maximum Measurable Flow Rate	up to 128% Full Scale (Gas Dependent)
		Typical Response Time	10 ms (Adjustable)
		Warm-up Time	< 1 Second
Neodym ProtiSen™ Hydrogen Sensor (data from [65])		Target Gas (in the air)	Hydrogen (in the air)
		Sensor Type	Catalytic (with filter)
		Detection Range	0-40,000 ppm
		Resolution	200 ppm
		Visual Indication	Bicolour LED (red/ green)
		Signal Type	Enclosed State
		Enclosure	Anodized aluminum
		Connector	Molex Mini- fit Jr. 4- min
		Weight	50g
		Temperature range	-30 -480ºC (-22 - 896ºF)
		Accuracy at ambient 23ºC ±2ºC (74ºF ± 4ºF)	±3ºC (-30 – 0ºC/ ± 6ºF (-22º – 32ºF)

Master Craft Digital Temperature Reader (data from [66])			±2ºC or 2% (0 – 100ºC)/ ± 4ºF or 2% (32º – 212ºF), ±3ºC or 3%/ ± 6ºF or 3% for other range
		Repeatability	1 % of reading or 1
		Response Time	500msec, 95% response
		Spectral response	8- 14um
		Emissivity	0.1-1.0 adjustable
		Operating Temperature	0- 50ºC (32-122ºF)
		Relative Humidity	10-95% RH noncondensing
		Storage Temperature	-20 – 60ºC (-4 – 140ºF)
		Weight/ dimensions	155 g; 165 x 72 x 41 mm
		Power	9 V block battery
		Battery life (alkaline)	12 hours
		Display spot size	8:1
BT100-1L Longer Peristaltic Pump (data from [67])		Speed	1-100.0 rpm
		Speed Precision	0.1 rpm
		Communication Interface	RS485
		Output Torque	2 Nm
		Display Mode	128*64 graphic LCD display
		Applicable Power	Applicable Power: AC 220 V +/- 10% 50Hz +/- 1Hz Applicable Power: AC 110 V +/- 10% 60Hz +/- 1Hz
		Power Consumption	≤ 50W
		Operating Consumption	Temperature 0-40ºC
		Relative humidity	< 80 %
		Drive Dimensions (L x W x H)	205 x 155 x 227 (mm)
		Drive Weights	5.34 Kg
		IP Rating	IP 31
		Readability	0.1mg
		Max capacity	220 g
		Repeatability	0.1 mg
		Linearity	0.2 mg

Mettler Toledo, AB204-S/ FACT (data from [68])		Sensitivity temperature drift (10ºC… 30ºC)	2.5 ppm/ ºC
		Setting time, typical	4 s
		Adjustment weight	Built-in
		Backlight	Yes
		External dimensions of balance (W/D/H)	245 x 321 x 344 mm
		External dimensions of packaging (W/D/H)	419 x 494 x 521 mm
		Weighting pan	(Diameter symbol) 80 mm
		Usable height of the draft shield	237 mm
		Net weight (with packaging)	6.4 kg (9.1 kg)
Fisher Scientific Isotemp Hotplates With Stirring (data from [69])		Type	Stirring Hotplate
		Top Plate Size and Material	10in x 10in Ceramic
		(Volts/ Amps/ Watts/ Freq./ Phase)	120/ 11.7/ 1410/ 60/ 1
		Temperature Range	5- 400ºC
		Speed Range	60- 1200 rpm
		Top Plate Capacity	6L flask/ 35 lbs

3.3 Test Samples

Throughout the various experimental runs, several experimental samples were used. The primary experimental samples used have been summarized in Table 3.4.

Table 3. 4 Experimental samples used in the tests.

Name of Test Sample	Test Sample	Packaging	Description
Instant Ocean Sea Salt	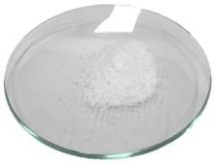 Sea salt	 Sea salt packaging	To simulate seawater aquarium, sea salt was purchased and can be added to distilled water to simulate water taken from the sea. The composition of the sea salt used consists mainly of chloride, sodium, sulphate, magnesium, and potassium ions.

Sodium Hydroxide Powder	 NaOH pellets	 NaOH packaging	This thesis introduces sodium hydroxide pellets as a means to stop or slow down the formation of the oxide layer. The sodium hydroxide pellets used have a purity of ≥98%. The sodium hydroxide packaging, along with the pellets, is displayed.
Aluminum Powder	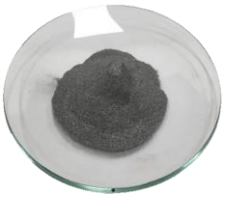 Aluminum powder	 Aluminum powder packaging	To carry out the experiment, the aluminum powder has been ball milled to a size of < 149 microns, with a purity of 99.8%, which was utilized. The aluminum powder and the corresponding packaging is displayed.

It should be noted that the experiment mainly used great value distilled water as it's the main water medium. However, to simulate seawater, it was mixed with the instant ocean sea salt shown in Table 3.4. The tap water used in the experiment was easily attainable from any faucet within the laboratory.

3.4 Hydrogen Production Strategy

After the principal chemical reaction was established, the reaction kinetics and thermodynamics of the reaction were then studied. Ideally, hydrogen production through aluminum and water should occur in an inert environment to prevent the air from reacting with the aluminum powder. The aluminum oxide layer formed on the exterior surface of aluminum is often considered to be the largest barrier within the reaction process and can slow down the rate of reaction. Therefore, the more inert the environment is, the harder it will be for an oxide layer to form on the exterior surface of the aluminum.

To create an inert experimental environment, the molecules surrounding the reaction must be chemically stable. Chemical stability is achieved when all electrons are bonded, or when the valance shell of electrons is full. There were several options of gases available to create

an inert environment listed below, with their corresponding Bohr Rutherford diagram. The Bohr Rutherford diagram was selected as a simple approach to show the interactions between electrons and the amount of the electrons in the valance shell.

Table 3. 5 Chemically stable molecules Bohr Rutherford diagram

Bohr-Rutherford Diagram	**Molecule Name**
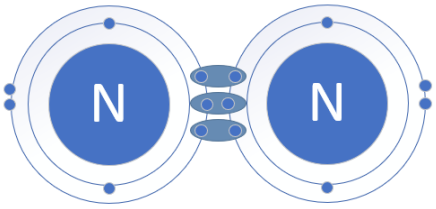 Nitrogen gas Bohr Rutherford diagram	Nitrogen Gas (N_2)
 Helium Bohr Rutherford diagram	Helium (He)
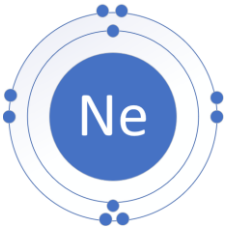 Neon Bohr Rutherford diagram	Neon (Ne)
 Argon Bohr Rutherford diagram	Argon (Ar)
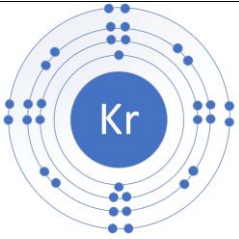 Krypton Bohr Rutherford diagram	Krypton (Kr)

In this experiment, N_2 was selected because it is a more cost-effective option. Furthermore, due to nitrogen's abundance, it is relatively easier to acquire compared to other gases listed in Table 3.5. There was also a strong correlation between the cost and the abundance. Table 3.6 provides the abundance of the various inert gases within the atmosphere.

Table 3. 6 Inert gas abundance within air (data from [70])

Gas	Abundance within the air (%)
Nitrogen Gas (N_2)	78.09
Oxygen Gas (O_2)	20.95
Argon (Ar)	0.93
Carbon Dioxide (CO_2)	0.03
Neon (Ne), Helium (He), and Krypton (Kr)	Trace amounts

The nitrogen cylinder used within the completion of this thesis project is shown in Figure 3.5, with the corresponding gage used beside it.

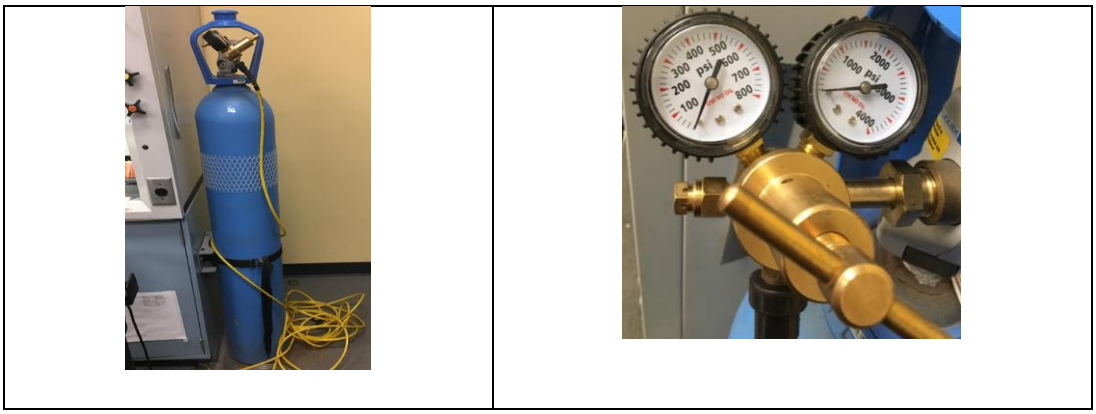

Fig. 3.5 Nitrogen gas cylinder with gauge

3.5 Error Analysis

To effectively analyze the created system, it was important to conduct an error analysis. Each component used within the system has been calibrated to have a certain level of accuracy. The accuracy of various system components was stated in Chapter 3 and summarized in Table 3.7. by using their respective manuals.

Table 3. 7 Experimental component error analysis

Experimental Error		
Component	**Experimental Conditions**	**Component Error/Accuracy**
BT100- 1L Peristaltic Pump	Speed Precision (ranging from 1-100rpm) Assume experiment operates at 80 rpm	0.1rpm (10-0.01)% error at 80rpm is 0.0125%
Alicat Scientific (M-Series)	Accuracy at calibration conditions after tare	± (0.8% of Reading + 0.2% of Full Scale)
	High Accuracy at calibration conditions after tare	± (0.4% of Reading + 0.2% of Full Scale) High Accuracy option not available for units ranged under 5 sccm or over 500 slpm.
	Accuracy for Bidirectional Meters at calibration conditions after tare	± (0.8% of reading + 0.2% of the total span from positive full scale to negative full scale)
	Repeatability	± 0.2% Full Scale
	Zero Shift and Span Shift	0.02% Full Scale / ^{o} Celsius / Atm
	Operating Range / Turndown Ratio	0.5% to 100% Full Scale / 200:1 Turndown
	Maximum Measurable Flow Rate	up to 128% Full Scale (Gas Dependent)
	Typical Response Time	10 ms (Adjustable)
	Warm-up Time	< 1 Second
ProtiSen	Still Air	% 5
Mettler Toledo AB204-S	Repeatability or readability	0.1mg, if measuring the mass of 9g error can be 0.011%
	Linearity	±0.2mg
Fisher Scientific Stirring Hotplate	Heating Specifications (Temperature Display vs. Actual Average Temperature)	± 10.0°C
	Stirring Speed Specifications (600 ml of water in a 100 ml glass flask above 200 rpm)	± 2.0%
Mastercraft Temperature Reader	For -30 – 0^{o}C	±3^{o}C
	For 0 – 100^{o}C	±2^{o}C or 2% (0 – 100^{o}C)
	For other ranges	±3^{o}C or 3%

The values taken for each component can impact the final result of the experiment differently compared to other components. For instance, a 5% error in the ProtiSen sensor may have a more substantial impact compared to another piece of equipment.

The uncertainty value of the various system components was calculated, to conduct an error analysis effectively. The uncertainty value of the various system components has been summarized in Table 3.8.

Table 3. 8 System component uncertainty value

Measurement Device	**Measured Quantity**	**Selected Reference Point**	**Absolute Bias Error**	**Relative Bias Error**	**Value Uncertainty (%)**
Alicat Scientific Flowmeter	Volumetric Flow	14 LPM	0.112	0.008	0.0265
Neodym ProtiSen	ppm	500 ppm	25.000	0.0500	0.0500
Metler Toledo	Mass	8.89 g	0.0009779	0.001	0.0087
Master Craft Temperature	Temperature	70 ^{o}C	0.140	0.002	0.0156

The specified equation used to calculate the uncertainty value for the various system components was the following:

$$U = \sqrt{\sum_x \left(\frac{\delta_x}{\delta_y}\right) \times U_x^2} \tag{3.1}$$

A common source of error considered within the creation of hydrogen production systems is leakage. Hydrogen is the smallest element on the periodic table and has a covalent radius of only 37pm [71]. Furthermore, it is colourless and odourless, therefore making it increasingly difficult to detect. To mitigate hydrogen gas leakage between fittings, clips were placed over components to hold them in place. Also, Teflon tape was used around screws and glass fittings, which has the potential to leak hydrogen gas. Furthermore, grease was added around the insertion points of the glass fittings to prevent leakage, and aid in the separation of fittings when the system required cleaning between experimental trials.

Furthermore, the transfer of aluminum powder and sodium hydroxide from one container to another serves as a potential issue. During the transfer process, the particles of the respective substance being measured got stuck to the measuring plate, after which it can be difficult to recoup. Although the amount lost during the transfer process is relatively insignificant, it can be established as a potential source of error.

CHAPTER 4: THERMODYNAMIC ANALYSIS AND MODELING

In this chapter entitled " Thermodynamic Analysis and Modeling," the principles regarding a system thermodynamic analysis will be outlined.

4.1 Thermodynamic analysis

This section will outline and conduct a brief thermodynamic study on the designed aluminum- water reaction recovery system. This section consisted of the energy balance equations, that were considered during the design of the system. Although the water within the system has the potential to be recycled, and the hydrogen has the potential to be captured, within the experiment, they were not. During and after the completion of the experimental trials, the water was disposed of, and the hydrogen gas was released into the fume hood. Therefore, the designed system was assumed to be an open system. The various state points used within the thermodynamic analysis were depicted in Figure 3.1 of Chapter 3 of the thesis.

The first step of the thermodynamic analysis was establishing the system's balance equations, in regards to mass, energy, entropy, and exergy. The balance equations for the various system components have been encapsulated in Table 4.1, Table 4.2, Table 4.3, and Table 4.4, respectively. The balance equations depicted are crucial in displaying how mass and energy are conserved throughout the system. In this regard, the mass balance equations of the system were defined in Table 4.1. The mass balance equations displayed in Table 4.1, can easily be applied because the various components represent control volume experiencing a process.

Table 4. 1 System mass balance equations

Component	Mass Balance Equations
500 mL Reaction Vessel	$\dot{m}_{(N)1} + \dot{m}_{(Al)1} + \dot{m}_{(H_2O)1} + \dot{m}_{(NaOH)1} = \dot{m}_{(N)2} + \dot{m}_{(H_2O)2} + \dot{m}_{(H_2)2} + \dot{m}_{NaAl(OH)_2}$
Vigreux Column	$\dot{m}_{(N)2} + \dot{m}_{(H_2O)2} + \dot{m}_{(H_2)2} = \dot{m}_{(N)3} + \dot{m}_{(H_2O)3} + \dot{m}_{(H_2)3}$
Liebig Condenser	$\dot{m}_{(N)3} + \dot{m}_{(H_2O)3} + \dot{m}_{(H_2)3} + \dot{m}_6 = \dot{m}_{(N)4} + \dot{m}_{(H_2O)4} + \dot{m}_{(H_2)4} + \dot{m}_5$
Cold Water Reservoir	$\dot{m}_5 = \dot{m}_7$
Distillation Head	$\dot{m}_{(N)4} + \dot{m}_{(H_2O)4} + \dot{m}_{(H_2)4} = + \dot{m}_{(H_2O)8} + \dot{m}_{(N)9} + \dot{m}_{(H_2)9}$
Peristaltic Pump	$\dot{m}_7 = \dot{m}_6$
Flowmeter	$\dot{m}_9 = \dot{m}_{10}$

The energy balance equations of the system were defined in Table 4.2. The energy balance equations show that the amount of energy entering the control volume will be the same amount of energy leaving the control volume. The energy passing through the control volume is also dependent on the work or heat entering and leaving each component.

Table 4. 2 System energy balance equations

Component	**Energy Balance Equations**
500 mL Reaction Vessel	$\dot{m}_{(N)1}h_{(N)1} + \dot{m}_{(Al)1}h_{(Al)1} + \dot{m}_{(H_2O)1}h_{(H_2O)1} + \dot{m}_{(NaOH)1}h_{(NaOH)1} + \dot{Q}_{heater} = \dot{m}_{(N)2}h_{(N)2} + \dot{m}_{(Al)2}h_{(Al)2} + \dot{m}_{(H_2O)2}h_{(H_2O)2} + \dot{m}_{(NaOH)2}h_{(NaOH)2}$
Vigreux Column	$\dot{m}_{(N)2}h_{(N)_2} + \dot{m}_{(H_2O)2}h_{(H_2O)2} + \dot{m}_{(H_2)2}h_{(H_2)2} = \dot{m}_{(N)3}h_{(N)_3} + \dot{m}_{(H_2O)3}h_{(H_2O)3} + \dot{m}_{(H_2)3}h_{(H_2)}$
Liebig Condenser	$\dot{m}_{(N)3}h_{(N)3} + \dot{m}_{(H_2O)3}h_{(H_2O)3} + \dot{m}_{(H_2)3}h_{(H_2)_3} + \dot{m}_6h_6 = \dot{m}_{(N)4}h_{(N)4} + \dot{m}_{(H_2O)4}h_{(H_2O)4} + \dot{m}_{(H_2)4}h_{(H_2)} + \dot{m}_5h_5$
Cold Water Reservoir	$\dot{m}_5h_5 = \dot{m}_7h_7$
Distillation Head	$\dot{m}_{(N)4}h_{(N)4} + \dot{m}_{(H_2O)4}h_{(H_2O)4} + \dot{m}_{(H_2)4}h_{(H_2)_4} = \dot{m}_{(H_2O)8}h_{(H_2O)8} + \dot{m}_{(N)9}h_{(N)9} + \dot{m}_{(H_2)9}h_{(H_2)9}$
Peristaltic Pump	$\dot{m}_7h_7 + \dot{W}_{pump} = \dot{m}_6h_6$
Flowmeter	$\dot{m}_{(N)9}h_{(N)9} + \dot{m}_{(N)9}h_{(N)9} = \dot{m}_{(N)10}h_{(N)10} + \dot{m}_{(N)10}h_{(N)10}$

Table 4.3 Defined the entropy balance equations of the various system components. The entropy balance equations of each system component can be used to identify the total amount of entropy generated within the system.

Table 4.4 Lists the exergy balance equations for system components. The exergy balance equations shown within Table 4 were used to establish the amount of useful energy available within the system, and the amount of useful energy that was lost due to irreversibilities.

Table 4. 3 System entropy balance equations

Component	Entropy Balance Equations
500 mL Reaction Vessel	$S_{gen} + \dot{m}_{(N)1}s_{(N)_1} + \dot{m}_{(H_2O)1}s_{(H_2O)1} + \dot{m}_{(H_2)1}s_{(H_2)1} + \dot{m}_{(Al)1}s_{(Al)1} + \left(1 - \frac{T_0}{T_s}\right)Q_{heater} = \dot{m}_{(N)2}s_{(N)_2} + \dot{m}_{(H_2O)2}s_{(H_2O)2} + \dot{m}_{(H_2)2}s_{(H_2)2}$
Vigreux Column	$S_{gen} + \dot{m}_{(N)2}s_{(N)_2} + \dot{m}_{(H_2O)2}s_{(H_2O)2} + \dot{m}_{(H_2)2}s_{(H_2)2} = \dot{m}_{(N)3}s_{(N)_3} + \dot{m}_{(H_2O)3}s_{(H_2O)3} + \dot{m}_{(H_2)3}s_{(H_2)}$
Liebig Condenser	$S_{gen} + \dot{m}_{(N)3}s_{(N)3} + \dot{m}_{(H_2O)3}s_{(H_2O)3} + \dot{m}_{(H_2)3}s_{(H_2)_3} + \dot{m}_6 s_6 = \dot{m}_{(N)4}s_{(N)4} + \dot{m}_{(H_2O)4}s_{(H_2O)4} + \dot{m}_{(H_2)4}s_{(H_2)} + \dot{m}_5 s_5$
Cold Water Reservoir	$S_{gen} + \dot{m}_5 s_5 = \dot{m}_7 s_7$
Distillation Head	$\dot{m}_{(N)4}s_{(N)4} + \dot{m}_{(H_2O)4}s_{(H_2O)4} + \dot{m}_{(H_2)4}s_{(H_2)_4} = \dot{m}_{(H_2O)8}s_{(H_2O)8} + \dot{m}_{(N)9}s_{(N)9} + \dot{m}_{(H_2)9}s_{(H_2)9}$
Peristaltic Pump	$S_{gen} + \dot{E}x_7 = \dot{m}_6 s_6$
Flowmeter	$S_{gen} + \dot{m}_{(N)9}s_{(N)9} + \dot{m}_{(N)9}s_{(N)9} = \dot{m}_{(N)10}s_{(N)10} + \dot{m}_{(N)10}s_{(N)10}$

Table 4. 4 System exergy balance equations

Component	Exergy Balance Equations
500 mL Reaction Vessel	$\dot{E}x_{Q_{heater}} + \dot{E}x_{(N)1} + \dot{E}x_{(H_2O)2} + \dot{E}x_{(H_{2)2}} = \dot{E}_{heater_{(N)2}} + \dot{E}x_{(H_2O)2} + \dot{E}x_{(H_{2)2}} + \dot{E}x_{D,RV}$
Vigreux Column	$\dot{E}x_{(N)2} + \dot{E}x_{(H_2O)2} + \dot{E}x_{(H_2)2} = \dot{E}x_{(N)3} + \dot{E}x_{(H_2O)3} + \dot{E}x_{(H_2)3} + \dot{E}x_{D_{VC}}$
Liebig Condenser	$\dot{E}x_{(N)3} + \dot{E}x_{(H_2O)3} + \dot{E}x_{(H_2)3} + \dot{E}x_6 = \dot{E}x_{(N)4} + \dot{E}x_{(H_2O)4} + \dot{E}_{x_{(H_2)4}} + \dot{m}_5 h_5 + \dot{E}x_{D,LC}$
Cold Water Reservoir	$\dot{E}xh_5 = \dot{E}xh_7 + \dot{E}x_{D,CW}$
Distillation Head	$\dot{E}x_{(N)4} + \dot{E}x_{(H_2O)4} + \dot{E}x_{(H_2)4} = \dot{E}x_{(H_2O)8} + \dot{E}x_{(N)9} + \dot{E}x_{(H_2)9} + \dot{E}x_{D,DH}$
Peristaltic Pump	$\dot{E}xh_7 + \dot{W}_{pump} = \dot{E}x_6 h_6 + \dot{E}x_P$
Flowmeter	$\dot{E}x_{(N)_9} + \dot{E}x_{(N)9} = \dot{E}x_{(N)10} + \dot{E}x_{(N)10} + \dot{E}x_{D,FM}$

The following general equation defines the exergy destroyed within the system:

$\dot{E}x_D = T_o S_{gen}$

In the previously stated equation, the ambient temperature of the system is represented by the variable T_o and is assumed to 25°C, as it considered to a temperature where exergy is at a dead state [72]. The variable S_{gen} represents the entropy generated within the equation.

For a full system description and the experimental design of the various state points and component descriptions, please refer to Chapter 3 of the document.

4.1.1. System Heat Addition

To effectively elevate the temperature of the aqueous solution during the experiment, a hot plate was utilized. The following general equation can define the heat addition from the hot plate used for heat addition:

$$Q = mc_p\Delta T$$

However, this equation must be modified to suit the system analyzed. The mass value of the equation should take into consideration the mass of the sodium hydroxide and water within the reaction vessel. During the 6 and 3 gram aluminum powder test, the stoichiometric reaction required that the combined mas between the sodium hydroxide and the water be approximately 20.89g and 10.445g, respectively. Also, the specific heat capacity of water and sodium hydroxide varied at different temperatures as well; therefore, that must be considered. The temperature within the fume hood was about 25°C. Consequently, the specific heat capacity of the water and sodium hydroxide was considered at approximately the same temperature of 25°C. According to Engineering Equation Solver (EES) the specific heat capacity of water and sodium hydroxide at room temperature at 4.181 and 1.999 $\frac{J}{g^oC}$. However, the starting temperature and final temperature of the water and sodium hydroxide experience the same, since they both have the same target temperatures. To expand on the initial equation, the heat addition from the hot plate can first be summarized in the following equation:

$$Q_{heater} = Q_{water} + Q_{NaOH} \tag{4.1}$$

In which the heat added to the water and sodium hydroxide take into consideration their respective masses and specific heat capacities. However, the change in temperature for

both reactions considered to be the same. The sample heat addition from various experimental trial conditions has been summarized in the following tables.

Table 4. 5 Heat addition from various experimental trails (3g aluminum sample used)

m_{Al} g	m_{H_2O} Distilled g	m_{NaOH} g	C_{p,H_2O} $\frac{J}{g^oC}$	C_p $\frac{J}{g^oC}$	T_i C	T_f C	Q_{H_2O} kJ	Q_{NaOH} kJ
3	6	4.45	4.181	1.99	25	40	0.3763	0.3763
3	6	4.45	4.181	1.99	25	45	0.5018	0.5018
3	6	4.45	4.181	1.99	25	50	0.6272	0.6272
3	6	4.45	4.181	1.99	25	55	0.7526	0.7526
3	6	4.45	4.181	1.99	25	60	0.8781	0.8781
3	6	4.45	4.181	1.99	25	65	1.004	1.004
3	6	4.45	4.181	1.99	25	70	1.129	1.129
3	6	4.45	4.181	1.99	25	75	1.254	1.254
3	6	4.45	4.181	1.99	25	80	1.38	1.38
3	6	4.45	4.181	1.99	25	85	1.505	1.505

Table 4. 6 Heat addition from various experimental trails (6g aluminum sample used)

m_{Al} g	m_{H_2O} Distilled g	m_{NaOH} g	C_{p,H_2O} $\frac{J}{g^oC}$	C_p $\frac{J}{g^oC}$	T_i C	T_f C	Q_{H_2O} J	Q_{NaOH} kJ
6	12	8.89	4.181	1.99	25	40	0.7526	0.1599
6	12	8.89	4.181	1.99	25	45	1.004	0.2132
6	12	8.89	4.181	1.99	25	50	1.254	0.2665
6	12	8.89	4.181	1.99	25	55	1.505	0.3198
6	12	8.89	4.181	1.99	25	60	1.756	0.3731
6	12	8.89	4.181	1.99	25	65	2.007	0.4264
6	12	8.89	4.181	1.99	25	70	2.258	0.4797
6	12	8.89	4.181	1.99	25	75	2.509	0.533
6	12	8.89	4.181	1.99	25	80	2.76	0.5863
6	12	8.89	4.181	1.99	25	85	3.011	0.6396

4.2 System Energy Efficiency

To determine if the system was operating effectively, the system's efficiency must be taken into consideration. The system's efficiency can be defined using a variety of methods. Within the context of this experiment, the system's efficiency can be defined using various molecule's enthalpy of formations, as well as the energy input of system components.

The standard energy efficiency equation takes into consideration only the molecular energy input from the molecules and the energy that can be obtained from the produced hydrogen molecule. In all chemical reactions, the reactants consist of aluminum, water, and sodium hydroxide. All molecules, with the exception of aluminum, has an enthalpy of formation. The enthalpy of formation of aluminum is 0 kJ/mol, due to its naturally exiting in a solid-state in nature, and it is not composed of other atoms. The enthalpy of formation of the water, and sodium hydroxide aqueous are considered to be -292.74 kJ/mol and -469.2 kJ/mol, respectively.

The efficiency of the chemical reaction was determined using, the lower heating value (LHV) of hydrogen gas must be considered if the intended use of hydrogen as a fuel. The LHV for hydrogen gas is considered to be -242 kJ/mol; it is the energy. It is released during the combustion process of hydrogen.

The following equation represents the combustion of hydrogen gas:

$$H_2(g) + \frac{1}{2}O_2(g) \rightarrow H_2O(l) + (-242\frac{kJ}{mol}) \tag{4.2}$$

Based on the previously defined molecular enthalpy of formations of the reactants, and the energy released during the combustion of hydrogen. The following equation defined the standard efficiency equation of the process:

$$\eta_{standard\ energy\ efficiency} = \frac{N_{H_2}LHV}{N_{H_2O}h_{f,H_2O}+N_{NaOH}h_{f,NaOH}} \tag{4.3}$$

It should be noted that LHV represents the lower heating value, and N_{H_2}, N_{H_2O}, and N_{NaOH} represent the moles of hydrogen that were generated and the moles of water and NaOH used in the reaction process. By multiplying the LHV with the moles of hydrogen produced, the amount of energy that can be harnessed as fuel can be calculated. The variables

represent the enthalpy of formations of water and NaOH were h_{f,H_2O} and $h_{f,NaOH}$. As seen in Equation 4.3, the enthalpies of formation of the water and NaOH were multiplied by the number of moles, and added together, to identify the amount of energy added to the process. The enthalpy of formation values was summarized in Table 4.7. Here, the values assume the environment to be at 25°C and environmental pressure of 101.325 kPa.

Table 4. 7 Chemical enthalpy of formation (data from [73])

Substance	Chemical Enthalpy of Formation (kJ/mol)
Aluminum (Al)	0
Water- liquid (H_2O)	-292.74
Water-gas (H_2O)	-241.8
Sodium Hydroxide- solid (NaOH)	-469.2

The standard energy efficiency equation can be modified further to take into consideration the amount of heat added to the reaction from the vessel. The heat addition from the heater was previously defined in Equation 4.1. By taking into consideration the heat addition from the hot plate, the thermal efficiency of the system can be determined. The following equation defined the thermal energy efficiency of the process:

$$\eta_{thermal} = \frac{N_{H_2} LHV}{N_{H_2O} h_{f,H_2O} + N_{NaOH} h_{f,NaOH} + Q_{heater}} \quad (4.4)$$

As previously shown in Tables 4.5 and 4.6, the heat addition from the heater is dependent on the specific heat capacity of water and sodium hydroxide.

However, to define the overall efficiency of the experimental process. The overall efficiency equation for the process should take into consideration the water that has been recovered as a result of the distillation head.

The overall thermal efficiency of the system is defined using the following equation:

$$\eta_{overall\ energy} = \frac{N_{H_2} LHV}{(N_{H_2O} - N_{recvered,H_2O}) h_{f,H_2O} + N_{NaOH} h_{f,NaOH} + Q_{heater}} \quad (4.5)$$

It should be noted that the energy from the pump was not taken into consideration, as it is relatively small and negligible. The defined energy equation takes into consideration the water recovered, which can be recycled for later use. The water that was recycled did not

contribute to the reaction process. Therefore, it is subtracted from the total mass of the water, which was the initial input into the system.

4.3 System Exergy Analysis

Subsequent to analyzing the system energetically, a system exergy analysis was conducted. The system exergy analysis established the amount of energy available within the system, and how effectively it was being harnessed. Other properties such as entropy generated, and exergy destroyed was also investigated.

4.3.1 System Exergy Efficiency

In order to define the exergy efficiency, the enthalpy of formation terms within equation 4.3.1 was replaced using the standard chemical exergy terms, defined by $e^{0}_{x,ch}\left(\frac{kJ}{mol}\right)$. The standard exergy efficiency equation is displayed within the following:

$$\eta_{standard\ exergy\ efficiency} = \frac{N_{H_2} e_{x,H_2}}{N_{H_2O} e_{x,H_2O} + N_{NaOH} e_{x,NaOH} + N_{Al} e_{x,Al}} \tag{4.6}$$

The standard chemical exergy for each term has been summarized in Table 4.8. Here, the values assume the environment to be at 25^{o}C and environmental pressure of 101.325 kPa.

Table 4. 8 Standard Chemical Exergy (data from [74])

Substance	Standard Chemical exergy (kJ/mol)
Hydrogen-gas (H_2)	236.09
Aluminum (Al)	795.7
Water- liquid (H_2O)	0.9
Sodium Hydroxide (NaOH)	74.9

Following this, the overall system energy equation can be modified to create the overall system exergy equation. The overall system exergy equation is as follows:

$$\eta_{overall\ exergy} = \frac{N_{H_2} ex,H_2}{(N_{H_2O} - N_{recvered,H_2O}) e_{x,H_2O} + N_{NaOH} e_{x,NaOH} + N_{Al} e_{x,Al} + Q_{heater}} \tag{4.7}$$

4.3.2 System Exergy Destroyed

The exergy destruction of a system provides a measure of irreversibility and the amount of energy that was lost during the process. The exergy destroyed within a system can be defined using a variety of equations mathematically. As previously discussed, the exergy

destroyed within a system can be defined using just the ambient temperature, and the amount of entropy generated, as seen in the basic equation below:

$$Ex_D = T_o S_{gen}$$

This basic equation can also be rearranged to solve for the entropy generated within the system.

The overall exergy efficiency of a system can be used to define the exergy destruction, as seen in the following equation:

$$Ex_D = (1 - \varphi) Ex_{in} \quad (4.8)$$

In Equation 4.8, φ represents the decimal value of the exergy efficiency and Ex_{in} represents the total exergy input in the system. After considering what Ex_{in} represents, Equation 4.8 can then be expanded to fit the following:

$$Ex_D = (1 - \varphi)((N_{H_2O} - N_{recvered,H_2O}) e_{x,H_2O} + N_{NaOH} e_{x,NaOH} + N_{Al} e_{x,Al+\ Q_{heater}}) \quad (4.9)$$

Furthermore the Ex_D and Ex_{in} within the system can be used to find the exergetic sustainability index of the system developed. The sustainability index is a ratio of the exergy output to the exergy that was wasted within the system.

The formula for sustainability index is as follows:

$$\theta = \frac{Ex_{out}}{Ex_D} \quad (4.10)$$

The exergy that was wasted within the system is simply represented by the exergy that was destroyed, and the exergy output is dependent on the standard chemical exergy of hydrogen gas, and the amount of exergy that was produced.

4.4 Thermodynamic System Reference Data

To understand the thermodynamic aspects of the aluminum water reaction at various temperatures, the U.S. Department of energy has compared the thermodynamic properties of 2 different reaction equations, where the aluminum temperature ranged from 0°C to 1000°C. The results have been summarized in Tablea 4.9 and 4.10. It should be noted that the chemical equations have been divided by a factor of 3 to ensure that only 1 mole of

hydrogen will be produced. Table 4.8 contains the reaction properties where the bayerite is the product, and Table 4.9 contains the properties of the reaction where alumina is the product.

Table 4. 9 Thermodynamic reaction properties for bayerite product (data from [7])

$2/3Al + H_2O = 2/3Al(OH)_3 + H_2$			
Temperature (ºC)	**ΔH (kJ/ mol H_2)**	**ΔS (J/K)**	**ΔG (kJ/ mol H_2)**
0	-277	26.2	-284
100	-284	3.29	-286
200	-291	-12.1	-285
300	-298	-25.1	-283
400	-306	-38.0	-280
500	-316	-51.8	-276
600	-328	-66.8	-270
700	-350	-90.9	-262
800	-369	-109	-252
900	-391	-128	-240
1000	-417	-149	-232

Table 4. 10 Thermodynamic properties for alumina product (data from [7])

$2/3Al + H_2O = 2/3Al_2O_3 + H_2$			
Temperature (ºC)	**ΔH (kJ/ mol H_2)**	**ΔS (J/K)**	**ΔG (kJ/ mol H_2)**
0	-272	62.1	-289
100	-275	51.1	-294
200	-279	43.1	-299
300	-283	35.5	-303
400	-288	27.3	-306
500	-294	18.1	-308
600	-303	7.80	-310
700	-320	-11.3	-309
800	-333	-23.7	-308
900	-348	-37.1	-305
1000	-366	-51.6	-304

CHAPTER 5: REACTION KINETICS ANALYSIS AND MODELING

In this section, the reaction kinetics of aluminum and water's chemical reaction to produce hydrogen gas will be analyzed and discussed. The reaction kinetics considers the factors which contribute to the rate of the chemical reaction, the energy associated with it, and other various factors that can impact the expected yield.

5.1 Aluminum Water Chemical Reactions

This thesis examined the chemical reaction between water and aluminum to produce hydrogen gas. The three main chemical reactions between water and aluminum are represented by the following equations, with the corresponding visual representation of the molecules interacting underneath it.

$$2Al + 6H_2O \rightarrow 2Al(OH)_3 + 3H_2 \quad (5.1)$$

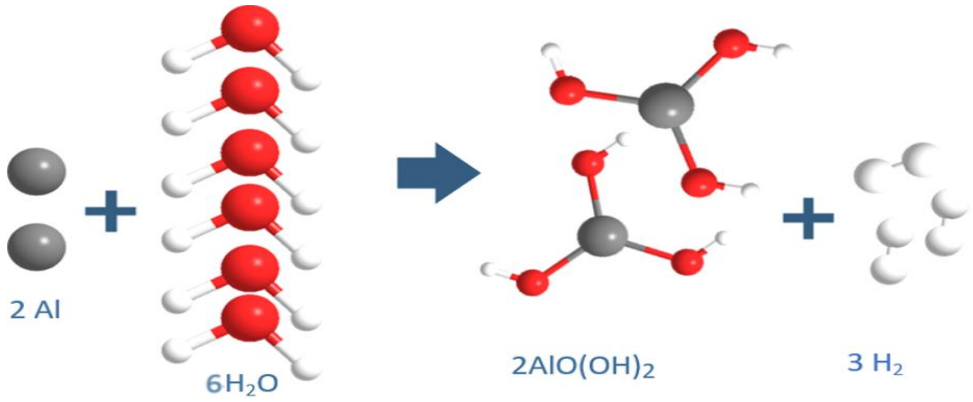

Fig. 5.1: Chemical reaction 1 visual representation

$$2Al + 4H_2O \rightarrow 2AlO(OH)_2 + 3H_2 \quad (5.2)$$

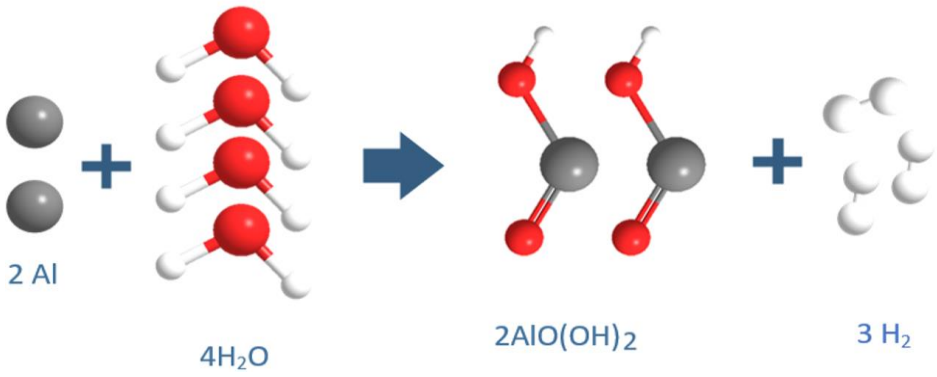

Fig 5.2 Chemical reaction 2 visual representation

$$2Al + 3H_2O \rightarrow Al_2O_3 + 3H_2 \quad (5.3)$$

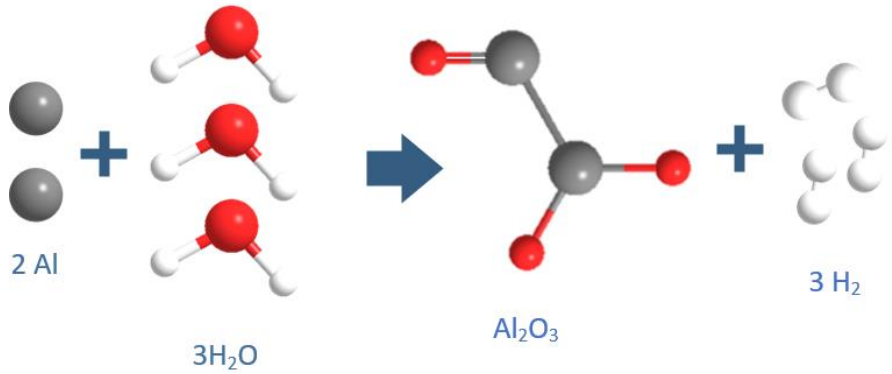

Fig. 5.3 Chemical reaction 3 visual representation

As previously stated, aluminum reacts with water to produce hydrogen. However, the chemical reaction is inhibited by the formation of the oxide layer. A simplified schematic of the chemical reaction is shown within the following figure.

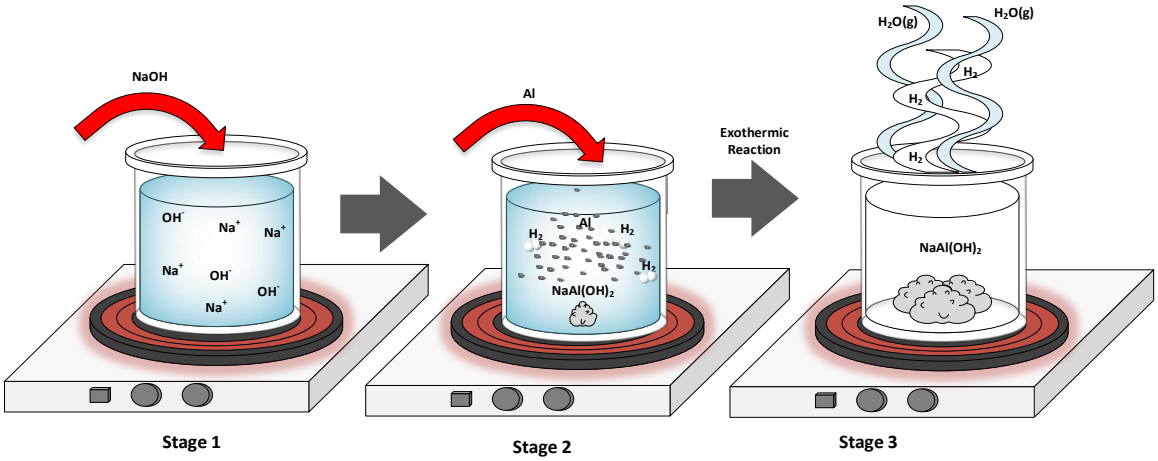

Fig. 5.4 Chemical reaction process

5.2 Aluminum Water Oxide Layer

The aluminum oxide layer formed on the exterior surface of the aluminum that should be taken into consideration. The work conducted by Jeurgens et al. [75] was examined, to study the growth and kinetics associated with the formation of the oxide layer. The formation of the oxide layer on the exterior surface of the aluminum metal was compartmentalized in the following stages:

- absorption
- dissociation
- nucleation
- growth

Initially, when aluminum comes in contact with oxygen molecules, aluminum atoms become bonded to oxygen molecules to form a thin aluminum oxide layer. The structure of the oxide layer formed is dependent on the temperature and length of time the oxidation process occurs. For instance, at a lower temperature, the oxide layer is considered to aluminum deficient; however, at higher temperatures, the oxide layer is considered to be aluminum enriched. In the aluminum deficient oxide layer, the layer has the chemical composition of Al_2O_3; however, at higher temperatures, it becomes γ- Al_2O_3. Although the formation of the oxide layer has positive uses such as the mitigation of corrosion, and electronics technology.

In the three chemical reactions shown, different mole ratios are implemented between the aluminum and water. The different mole ratios result in 3 moles of hydrogen being produced. However, there is a variation in the type of waste product produced. For instance, possible waste products from the reaction include barite [$Al(OH)_3$], boehmite [$2AlO(OH)_2$], and alumina [Al_2O_3] in Equations 4.1, 4.2, and 4.3 respectively. The moles of aluminum in these three reactions do not change. However, the level of hydration in the equation varies, as shown by the change in the moles of water used.

5.3 Determining Hydrogen Production Rate

The system's hydrogen production rate can be determined, theoretically and experimentally. Section 5.3.1 explains the analytical process used in the past to generate hydrogen, and Section 5.3.2 explains how the hydrogen production rate can be determined experimentally.

5.3.1 Determining Hydrogen Production Rate Theoretically

A viable method of determining the effectiveness of the chemical reaction between aluminum and water is through the calculation of the degree of reaction percentage, which

was calculated previously by Hiraki et al. [47]. Hiraki et al. expressed the degree of a chemical reaction using the following equation:

$$f = \frac{\frac{V_{H_2}}{n_{H_2}}}{22.4\times10-3\left(\frac{T_a}{273}\right)}\left(\frac{W_{Al}}{M_{Al}}\right)^{-1} \times 100 \quad (5.4)$$

In Equation 5.4, the variables $\left(\frac{W_{Al}}{M_{Al}}\right)$ refers to the ratio of the weight of aluminum over the molar mass of aluminum. The variable represents the ambient temperature environment in which the experiment was conducted in T_a, where it is by dividing by 273 K. 22.4×10^{-3} m^3 in the denominator position, represents the volume of the 1 mole of hydrogen gas at standard conditions for temperature and pressure (STP). The degree of the reaction expressed the rate at which hydrogen is produced as a percentage, relative to is maximum theoretical yield.

The rate at which a chemical reaction takes place, where it is temperature-dependent is dictated by Arrhenius equation shown below:

$$k = Ae^{\frac{E_A}{RT}} \quad (5.5)$$

In the Arrhenius equation shown above, k is the rate constant, A refers to the pre-exponential factor, e is Euler's number, E_A is the activation energy, R is the ideal gas constant, and T is the temperature in kelvin. Non- isothermal conditions were simulated by varying the experimental temperature. Specifically, experimental trial temperatures ranged from approximately 293 K to 343 K, during the pre-heating of the NaOH and water solution.

As stated by Hiraki et al. [47], the shrinking core model can then be used to identify the various rate constants. The chemical reaction used between aluminum and water has the presence of NaOH. The reaction was highly dependent on the amount of aluminum added. Therefore, this reaction was considered to be the first order. The rate of which moles of aluminum reacted, using the shrinking core model that can be expressed using the following rate equation:

$$-\frac{d}{dt}\left(\frac{4}{3}\pi\frac{\rho_{Al}}{M_{Al}}r_c^3\right) = 4\pi r_c^2\frac{dn_{Al}}{dt} \quad (5.6)$$

In equation 5.6 shown above, r_c represents the radius of the unreacted aluminum molecule. Additional variables ρ_{Al},M_{Al}, and $\frac{dn_{Al}}{dt}$ represent the density, molar mass, and reaction rate moles of aluminum.

The rates on the left and right side of Equation 5.6 can be further simplified using reaction rate constants, the concentration of the solutions. In Equation 5.7 shown below, k_c is the mass transfer constant, and k_s is the reaction rate constant on the surface of the molecule. The numerator C_{NaOH} is the concentration of NaOH within the aqueous solution.

$$\frac{dn_{Al}}{dt} = \frac{C_{NaOH}}{\frac{1}{k_c}+\frac{1}{k_s}} \tag{5.7}$$

The relationship between the ratio of the reacted and unreacted radius of the aluminum molecule with the degree of the reaction.

$$\frac{r_c}{r_0} = (1-f)^{\frac{1}{3}} \tag{5.8}$$

The mass transfer constant can be found using Equation 5.9. By multiplying the inverse of the previous ratio expressed in Equation 5.8, with the initial mass transfer constant.

$$k_c = \frac{r_0}{r_c} k_{c0} \tag{5.9}$$

As a result of substituting Equations 5.8 and 5.9 into Equation 5.7, then integrating and simplifying the product, the equation will be 5.10.

$$r_0\{1-(1-f)^{\frac{1}{3}}\} = \left(\frac{C_{NaOH}M_{Al}}{\rho_{Al}}t\right)k_s \tag{5.10}$$

5.3.2 Determining Hydrogen Production Rate Experimentally

The hydrogen production rate can be calculated through graphical analysis. The graphical analysis uses time as the x-axis variable, and the hydrogen produced as the y-axis variable. By simply taking the slope of the line of best fit from its data points, the average hydrogen production can be calculated.

The general equation represents the slope of the line:

$$m = \frac{y_2-y_1}{x_2-x_1}$$

The process can then was expedited through the use of excel.

5.4 Determining Reaction Yield

As previously stated, the aluminum and water chemical reaction utilized was Equation 5.1, however, NaOH was a reaction promoter. The full chemical reaction was represented below:

$$2Al + 2NaOH + 6H_2O \rightarrow 2NaAl(OH)_4 + 3H_2 \quad (5.11)$$

The effectiveness of the chemical reaction was determined through the calculation of theoretical yield. To calculate the theoretical yield of hydrogen, the amount of reactants and products was taken into consideration. Identifying the limiting reactant of the reaction is crucial because it will get consumed first within the chemical reaction. Furthermore, the mole ratio between aluminum and other molecules will aid in determining the amount of reactants required for the reaction to take place.

Table 5. 1 Stoichiometric reaction properties

Scientific Name	Molecule Symbol	Stoichiometric Moles	Mole Ratio Relative to Al	Molecule Molar Mass (g/mol)
Aluminum	Al	2	1	26.982
Sodium Hydroxide	$NaOH$	2	1	39.997
Dihydrogen Monoxide (Water)	H_2O	6	3	18.015
Sodium Tetrahydroxyaluminate	$NaAl(OH)_4$	2	1	118.001
Hydrogen Gas	H_2	3	1.5	1.008

After the stoichiometric reaction properties were established, an equation to calculate the amount of hydrogen produced relative to the limiting reactant of aluminum was determined. The equation is as follows:

$$\frac{Al\ Experimental\ Mass}{Al\ Molar\ Mass} \times 1.5 mols \times H_2 Molar\ Mass = Theoretical\ H_2 Yield \quad (5.12)$$

Using Equation 5.11, the theoretical yield of hydrogen produced can be determined. The mass of the aluminum considered within the experiment was 3 g and 6 g. However, the mass of aluminum within Table 5.2 ranged between 1g and 10 g. The theoretical mass of

hydrogen produced, with the corresponding amount of aluminum added to the reaction, is shown in Table 5.2.

Table 5. 2 Theoretical hydrogen yield with respect to Al added

Mass of Al (g)	**H_2O required mass (g)**	**NaOH required mass (g)**	**H_2 Yield (g)**	**$NaAl(OH)_4$ Yield (g)**
1	2.003	1.483	0.112	4.373
2	4.006	2.965	0.224	8.747
3	6.009	4.447	0.336	13.120
4	8.012	5.930	0.448	17.494
5	10.015	7.412	0.560	21.867
6	12.018	8.894	0.672	26.240
7	14.021	10.377	0.784	30.614
8	16.025	11.859	0.897	34.987
9	18.028	13.341	1.009	39.360
10	20.031	14.824	1.121	43.734

After determining the theoretical yield of hydrogen, the percent yield can also be determined. The percent yield is determined using the following general equation:

$$\%Yield = \frac{Actual\ H_2\ Yield}{Theoretical\ H_2\ Yield} \times 100\% \tag{5.13}$$

The actual yield was determined experimentally using a combination of measurement devices. The flow meter was used to determine the volumetric flow and the mass flow of hydrogen gas, after leaving the experimental distillation setup. A hydrogen gas sensor was placed on the other end of the experimental setup to measure the concentration of the gas, leaving the flowmeter. After the sensor reaches its baseline concentration of 500 ppm, the experimental trial was deemed complete. The summation of the hydrogen produced in terms of mass, moles, or volume from the experiment represents the actual yield from the process.

CHAPTER 6: RESULTS AND DISCUSSION

In this section, the research will outline the various test conditions conducted along with obtained results from each system test. The performed test depended on various factors such as the temperature of the sodium hydroxide water mixture, water medium (tap, distilled, or sea), and variations in aluminum powder mass. The volume of the water recovered from the process was also recorded to identify its overall impact on the system's efficiency.

6.1 Impact of Variations in Water Temperature

In this section, the researcher has successfully tested the impact water temperature has on the overall reaction process. To identify the effectiveness of the process at various water temperatures, hydrogen production rate, and % yield/conversion efficiency was considered.

The variations in water temperature test conditions consisted of using experimental aluminum samples, of the mass 3g and 6g within distilled water. The distilled water temperature ranged from 40^{o}C to 70^{o}C.

The test specifications amongst the various trails have been summarized in Table 6.1. It should be noted that all experiments were conducted within a fume hood to ensure the safety standards were upheld while conducting the experiment.

Table 6. 1Variation in water temperature test conditions

Trial Number	**Al Mass (g)**	**NaOH Mass (g)**	**H_2O Volume (ml)**	**H_2O Temp. (^{o}C)**	**Pump Flow (ml/min)**
1	3.00	4.45	6.00	40	400.10
2	6.00	8.89	12.00	40	400.10
3	3.00	4.45	6.00	60	400.10
4	6.00	8.89	12.00	60	400.10
5	3.00	4.45	6.00	70	400.10
6	6.00	8.89	12.00	70	400.10

Figures 6.1 to 6.4 show the conversion efficiency and rate of hydrogen production studied at various water temperatures.

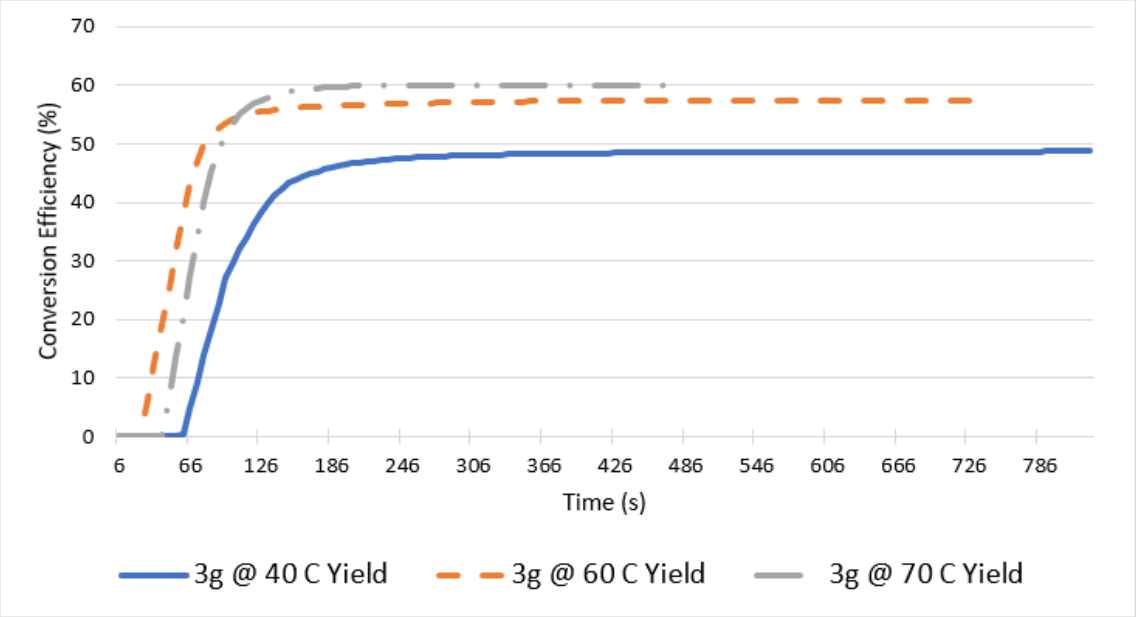

Fig. 6.1 Conversion Efficiency (3g Aluminum Samples), varying water temperature test conditions

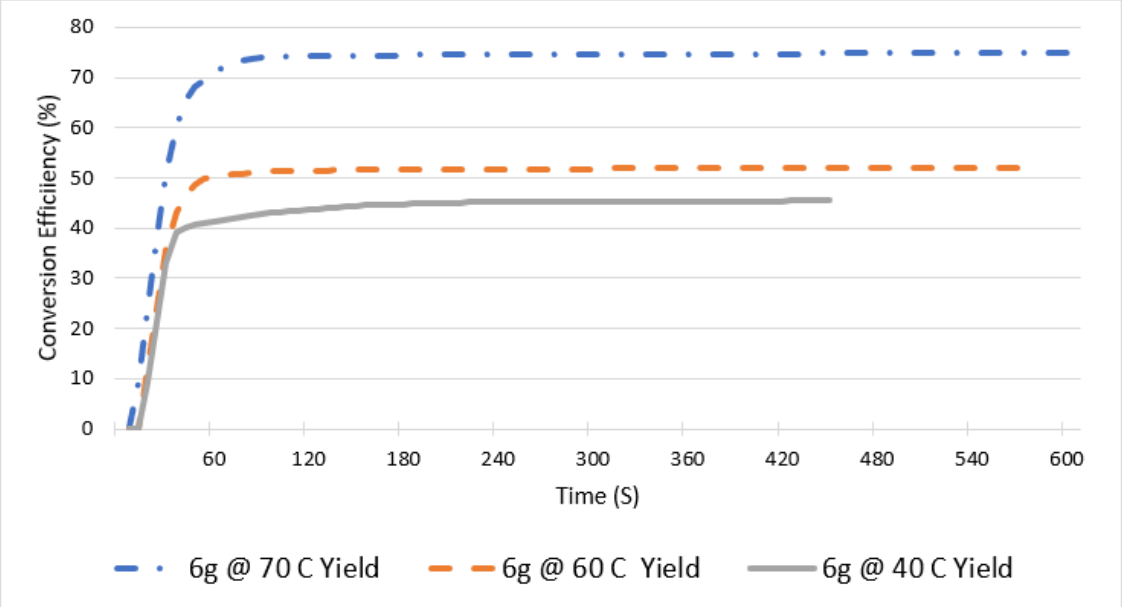

Fig. 6.2 Conversion Efficiency (6g Aluminum Samples), varying water temperature test conditions

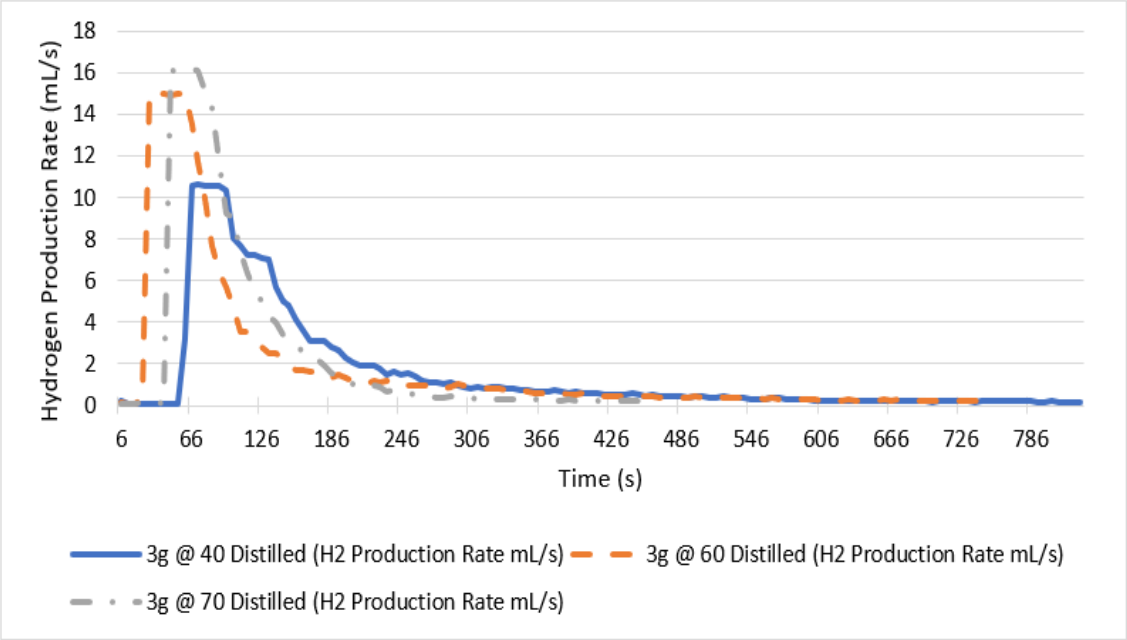

Fig. 6.3 Hydrogen production rate (3 g aluminum samples), varying water temperature test conditions

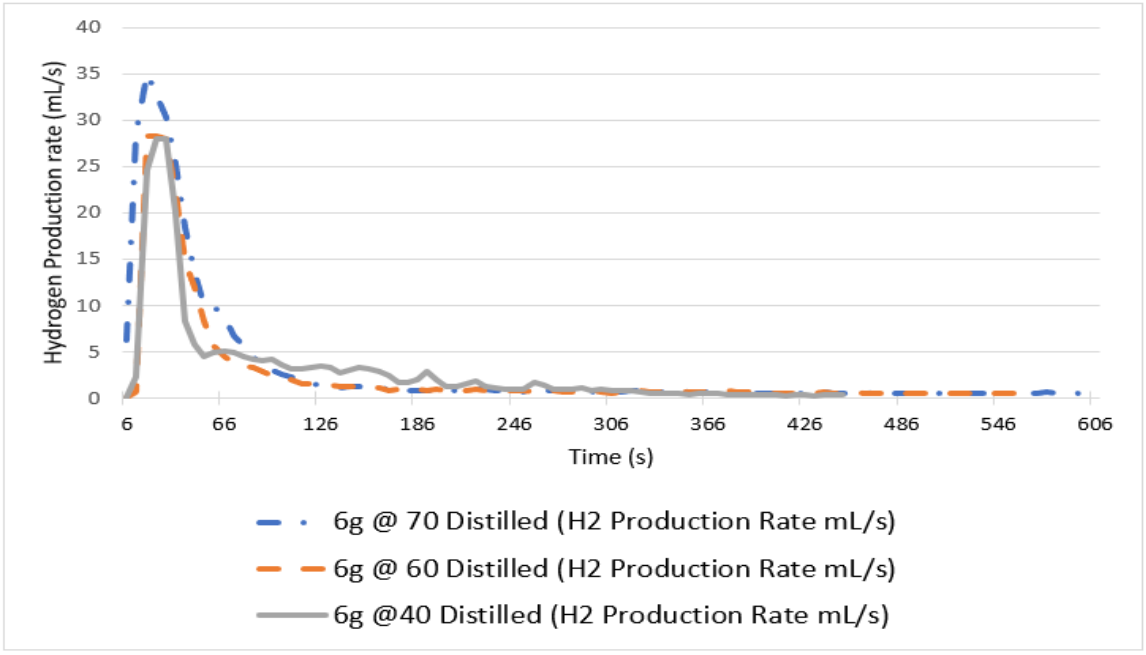

Fig. 6.4 Hydrogen production rate (3 g aluminum samples), varying water temperature test conditions

As expected, the hydrogen conversion efficiency, as well as the hydrogen production rate is significantly higher as temperature increases. This is expected as an increase in

temperature should have a positive effect on the overall reaction process, molecules taking place within the reaction process reach a more excited state.

Furthermore, it can also be noted that when conversion efficiency is at its maximum, the production rate is close to zero. The conversion efficiency provides a measure of how much hydrogen was produced, relative to the maximum theoretical amount that can be achieved. Therefore, when the production rate is at its lowest, most of the reaction has taken place. If most of the reaction has taken place, the conversion efficiency will be at its highest, and the production rate will decrease. This fact indicates that the conversion efficiency and production rate are inversely proportional to each other. After 400 seconds, the reaction has nearly concluded, as previously stated, a sensor reading of 500ppm, was selected as a baseline concentration to conclude the experiment.

Also, by observing these figures, the performance of the 6g aluminum sample and 3g aluminum sample were compared. Both graphs depict the same trend of increasing temperature resulting in greater overall yield and rate of production. However, it should be noted that the 6g sample did perform better than the 3g sample in terms of reaching a greater conversion efficiency and production rate. This can be attributed to a variety of reasons such as

- The trajectory of the aluminum particles was sprayed at
- The orientation of the water within the reaction vessel
- Possible leakage between pipes and fitting etc.

6.2 Impact of Using Various Water Mediums

In the section, tests were not conducted to identify the impact of using water at various temperatures but rather to observe the impact of using various water mediums. As water is a relatively abundant resource, it should be noted that distilled water is not always readily available; therefore, the use of saltwater during the experimental process should be investigated and compared to identify its effectiveness. The saltwater being used is artificial seawater. Another dimension is added to the study, through the utilization of tap water from the research facility was the best option to generate hydrogen. The tap water being used provide added another parameter to the study in terms of having a water medium

to make the comparison with. The starting temperature of water used during the reaction process was 70°C, as it showed to have promising results in terms of hydrogen production rate and the observed conversion efficiency.

The test conditions for the various water medium used have been established and summarized in Table 6.2.

Table 6. 2 Variation water medium test conditions

Trial Number	Al Mass (g)	NaOH Mass (g)	H_2O Volume (ml)	H_2O Temp. (°C)	Pump Flow (ml/min)
1	3	4.45	6.00 (Tap)	70	400.1
2	3	4.45	6.00 (Distilled)	70	400.1
3	3	4.45	6.00 (Sea)	70	400.1
4	6	8.89	12.00 (Tap)	70	400.1
5	6	8.89	12.00 (Distilled)	70	400.1
6	6	8.89	12.00 (Sea)	70	400.1

In order to compare the effectiveness of the various chemical reactions, various aspects such as the hydrogen production rate, reaction rate, and conversion efficiency were compared.

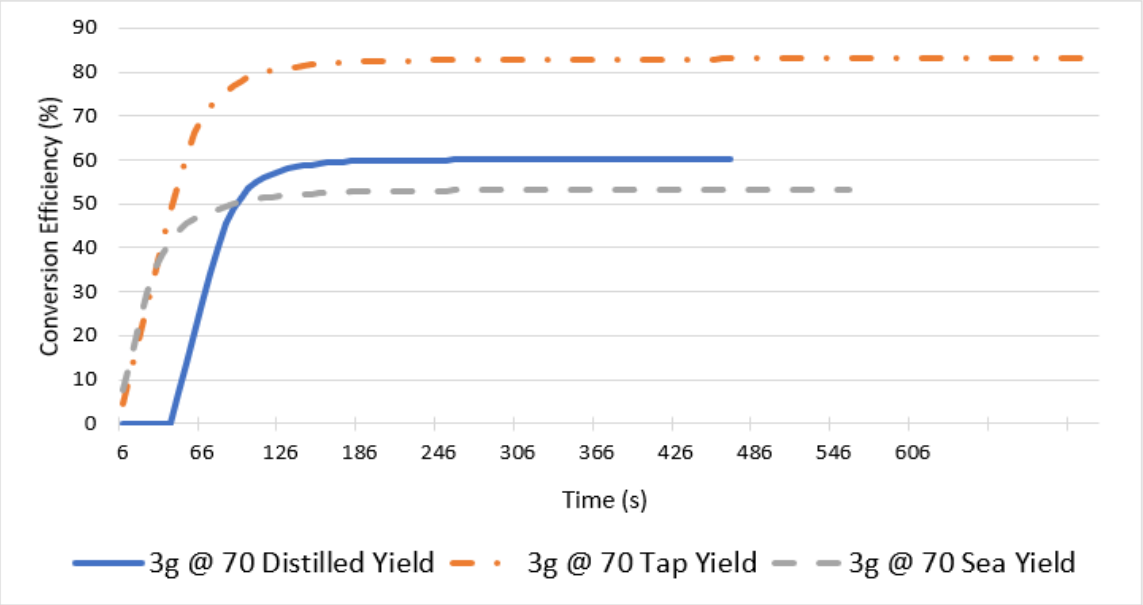

Fig. 6.5 Hydrogen Conversion efficiency (3 g aluminum samples), various water medium test conditions

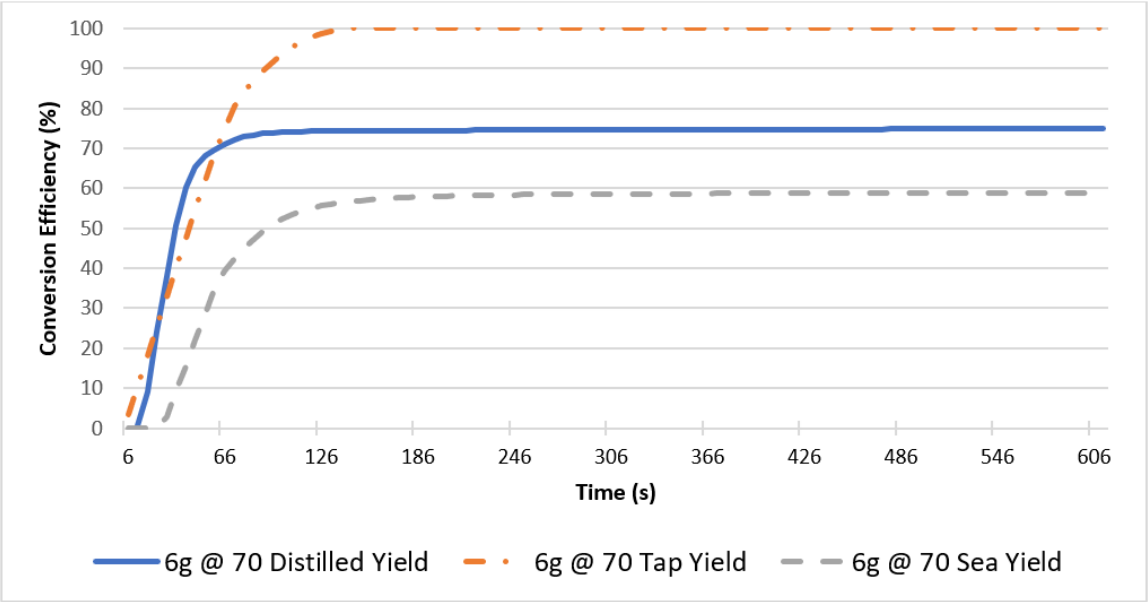

Fig. 6.6 Hydrogen conversion efficiency (6 g aluminum samples), various water medium test conditions

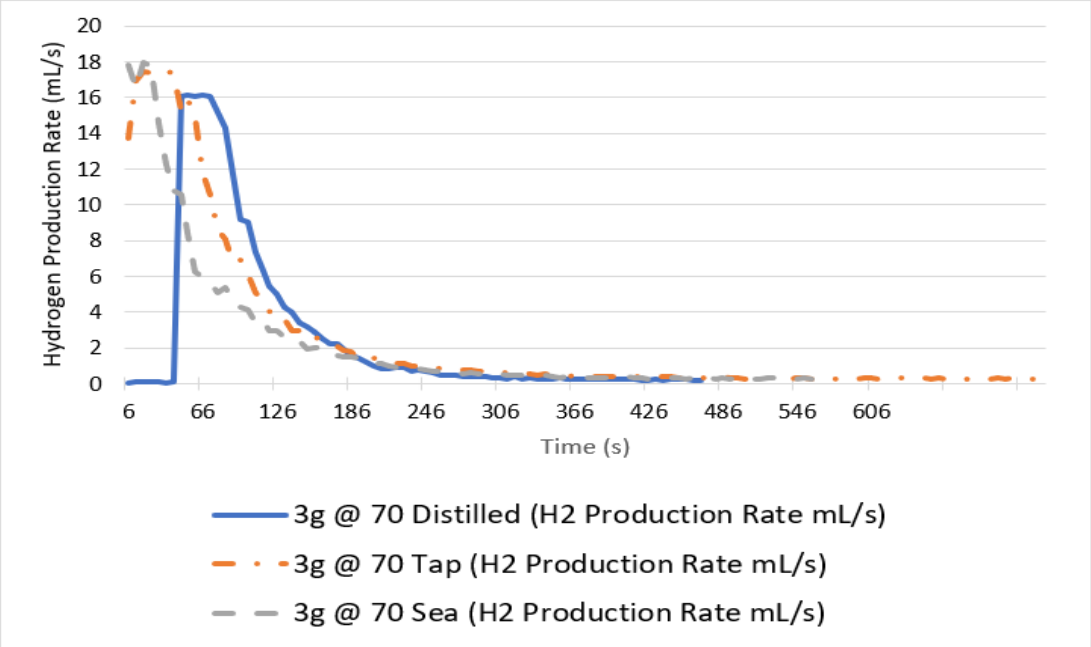

Fig. 6.7 Production rate (3g aluminum samples), various water medium test conditions

The results of studying the use of various water mediums were displayed in Figure 6.5 to 6.8. The graphs displayed within Figure 6.5 to 6.8 encapsulate a comparison of the measured hydrogen production rate and the calculated conversion efficiency as a means to assess the system's performance when using different water mediums. Based on the

conversion efficiency graphs, the tap water behaves more effectively in terms of conversion efficiency. A possible reason for this is due to tap water's composition. Tap water's mineral and ion composition likely contributed towards the splitting of water molecules to produce hydrogen. Given that tap water's composition can vary according to the specific location, it should be considered that the results obtained from this experiment can be heavily dependent on the region. This experiment was conducted within the town of Oshawa, Ontario Canada. Within the city of Oshawa, there are specific standards that building tap water must adhere to.

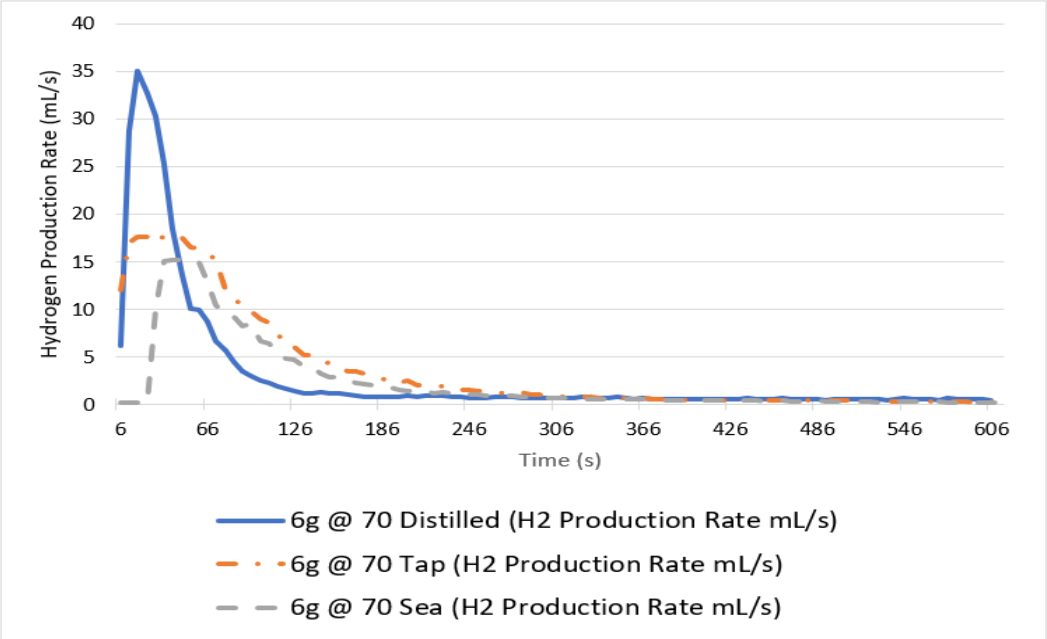

Fig. 6.8 Production rate (6g aluminum Samples), various water medium test conditions

According to the Guidelines for Canadian Drinking Water Quality, the tap water is evaluated based on the following parameters; microbiological, chemical and physical together, and radiological parameters. Microbiological parameters take into consideration bacteria, protozoa, and viruses. The chemical with physical parameters identifies what concentration of substances is acceptable, in reference to substances such as aluminum, ammonia, chlorine, and many other substances. However, the radiological parameters assess if cesium, iodine, lead, radium, radon and if other elements are present in the water [76].

In order to determine the composition of water within Oshawa, the city of Toronto was used as a reference.

Table 6. 3 Toronto Water Composition (adapted from [77])

Inorganic Substance	**Average amount (mg/L)**
Antimony	0.00021
Arsenic	0.0007
Barium	0.022
Beryllium	0
Boron	0.024
Cadmium	0.000006
Caesium	0.000001
Calcium	36.0
Chloride	27.9
Chromium	0.0006
Cyanide	0
Iron	0.063
Lead	0.005
Magnesium	9.1
Manganese	0.0002
Mercury	0
Molybdenum	0.0019
Nickel	0.0005
Nitrate	0.39
Nitrite	0.0004
Orthophosphate	2.2
Potassium	1.6
Selenium	0.00014
Silver	0
Sodium	15.1
Strontium	0.183
Sulphate	25.1
Terbium	0
Thallium	0
Thorium	0.00002
Tin	0.00001
Titanium	0.0019
Tungsten	0.0001
Uranium	0.0003
Vanadium	0.0003
Zinc	0.001

As seen in Table 6.3, the most prominent inorganic substance found tap water is calcium, which accounts for 36 mg/L of tap water's composition. The chemical reaction between tap water and calcium and water is as follows;

$$Ca + H_2O \rightarrow Ca(OH)_2 + H_2 \quad (6.1)$$

As seen in Equation 6.1, the calcium found in tap the water certainly contributed to the splitting of a water molecule produce hydrogen.

Recently, an increased amount of lead was detected within the water. However, the increased amount of lead found in the water does not cause for concern if the system were to be scaled up. Presently, 71% of the earth's surface is covered from water, 95.5% of which is saltwater, therefore the system would be consuming saltwater due to its abundance. Saltwater from the ocean has a much more consistent composition. Table 6.4 below provides a comparison between the artificially created ocean water, and real ocean water.

Table 6. 4: Artificial and real ocean composition comparison (adapted from [78])

Ion	**Artificial Ocean Composition (ppm)**	**Real Ocean Composition (ppm)**
Cl^-	19,290	19,353
Na^+	10,780	10,781
SO_4^{2-}	2,660	2,712
Mg	1,320	1,284
K^+	420	399
Ca^{2+}	400	412
CO_3^{2-}/HCO_3^-	200	126
Br^-	56	67
Sr^{2+}	8.8	7.9
Li^+	0.3	0.173
Ba^{2+}	<0.04	0.014
Mn^{2+}	<0.025	<0.001
Cd^{2+}	<0.002	<0.001

It should be noted that additional and trace amounts of substances can be found within ocean water. Furthermore, the salinity of artificial seawater is approximately 32 ppt, and the salinity of actual seawater is estimated at about 35 ppt. A comparison of the concentration, alkalinity, calcium and magnesium ion concentration is summarized in the following Table 6.5.

Table 6. 5 Artificial and real seawater property comparison (adapted from [78])

Criteria	Artificial Ocean Composition (ppm)	Real Ocean Composition (ppm)
Concentration ($g\ L^{-1}$)	38	35.169
Alkalinity ($mEq\ L^{-1}$)	3.0- 4.0	2.32
Calcium ion ($mg\ L^{-1}$)	349- 392	411.9
Magnesium ion ($mg\ L^{-1}$)	1,150- 1,310	1284

The significant finding from comparing the production rate of hydrogen, using various water mediums, was the distilled water's ability to reach the highest hydrogen production rate, at approximately 35mL/s.

6.3 Variations in Sodium Hydroxide Concentration

As previously stated previously, sodium hydroxide was selected as the main reaction promoter. Using sodium hydroxide as a reaction promoter is an effective method to eliminate the oxide layer formed on the exterior surface of the aluminum. Therefore, in order to study the impact sodium hydroxide has as a reaction promoter on the process, a test can be conducted, in which the amount of sodium hydroxide added is varied within the solution.

To the impact of sodium hydroxide, experiments consisted of 3g and 6g aluminum samples once again. However, the sodium hydroxide concentration varied by 50%. For instance, if 6g of aluminum powder is used, the trial required approximately 8.89g of sodium hydroxide for a stoichiometric reaction to take place. Therefore, the experimental trials conducted used approximately 4.45g and 13.34g of sodium hydroxide.

The test parameter of each trial for varying the sodium hydroxide amount has been summarized in Table 6.6.

Similar to the previously conducted studies, to measure the performance of the system, the conversion efficiency of the various trails and the hydrogen production rate was considered. The conversion efficiency and the hydrogen production rate were compared to the hydrogen production rate when a stoichiometric reaction was used.

Table 6. 6 Variations in Sodium Hydroxide Test Conditions

Trial Number	Al Mass (g)	NaOH Mass (g)	H_2O Volume (ml)	H_2O Temp. (°C)	Pump Flow (mL/min)
1	3.00	2.23	6.00	70	400.10
2	6.00	4.45	12.00	70	400.10
3	3.00	8.89	6.00	70	400.10
4	6.00	13.34	12.00	70	400.10

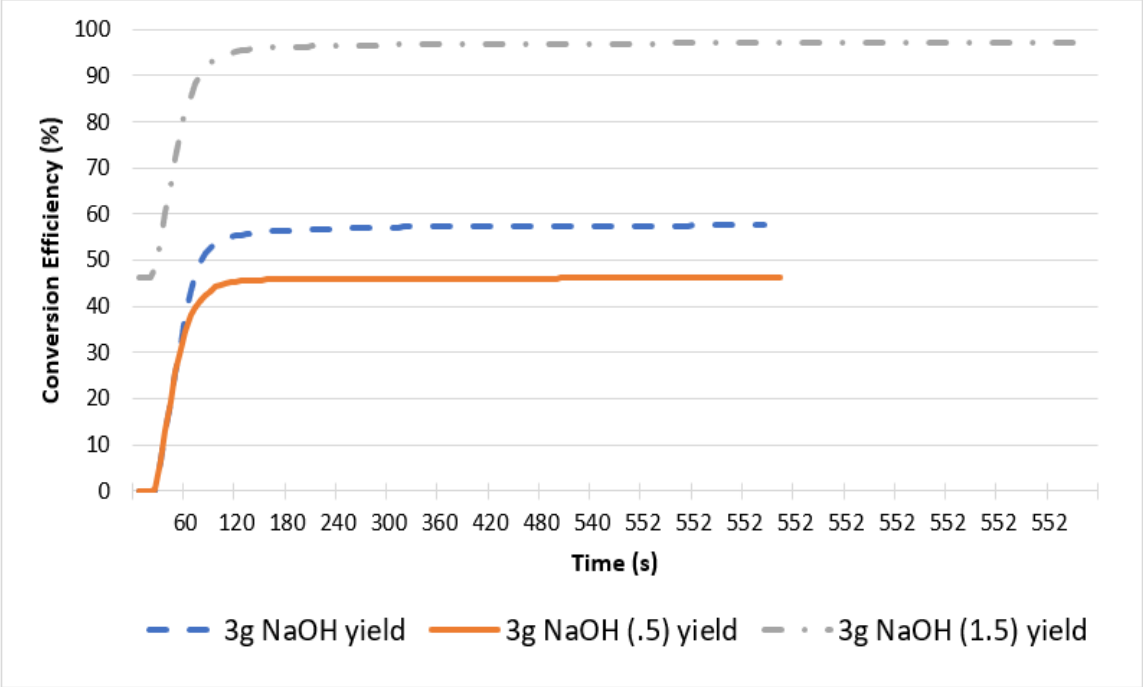

Fig. 6.9 Conversion efficiency (3g aluminum samples), variation in sodium hydroxide concentration

After completing the variations in sodium hydroxide test, a comparison of the conversion efficiency values was conducted. The trials which had a 50% increase in the sodium hydroxide was able to have a significantly higher conversion efficiency. The conversion efficiency values for the 3g and 6g samples, which had a 50% increase in sodium hydroxide was 97.15 % and 95.44 %, respectively. These conversion efficiencies were among the highest conversion efficiencies graphed. This is due to sodium hydroxide acting as a reaction promote. The increased presence of a reaction promoter, aids in the reaction taking place.

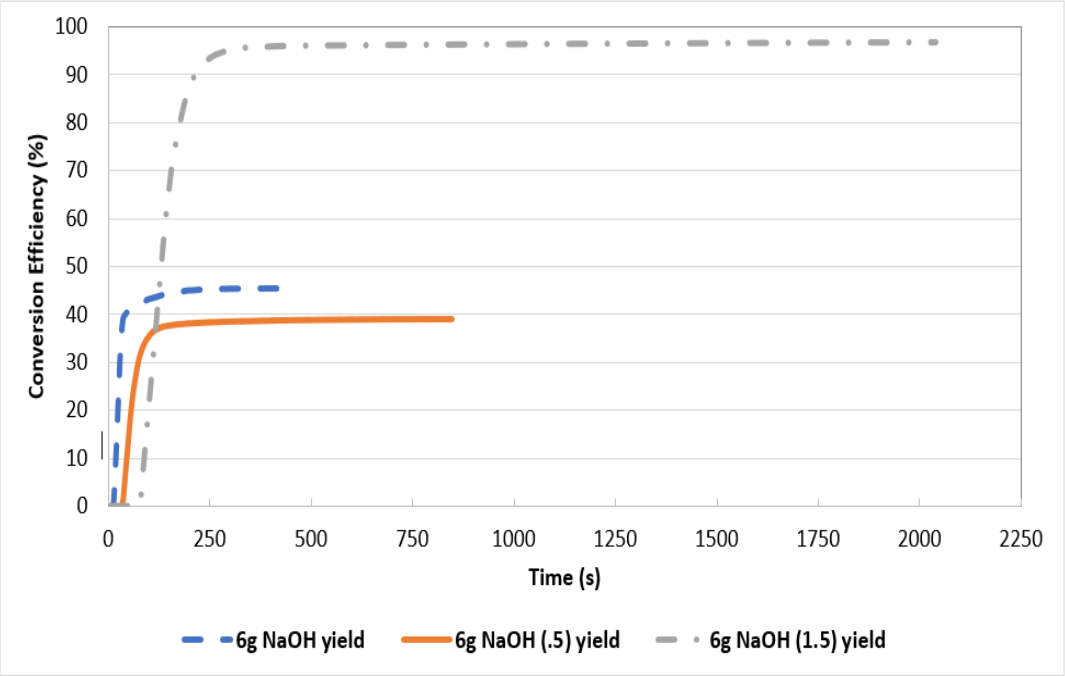

Fig. 6.10 Conversion efficiency (3g aluminum samples), variation in sodium hydroxide concentration

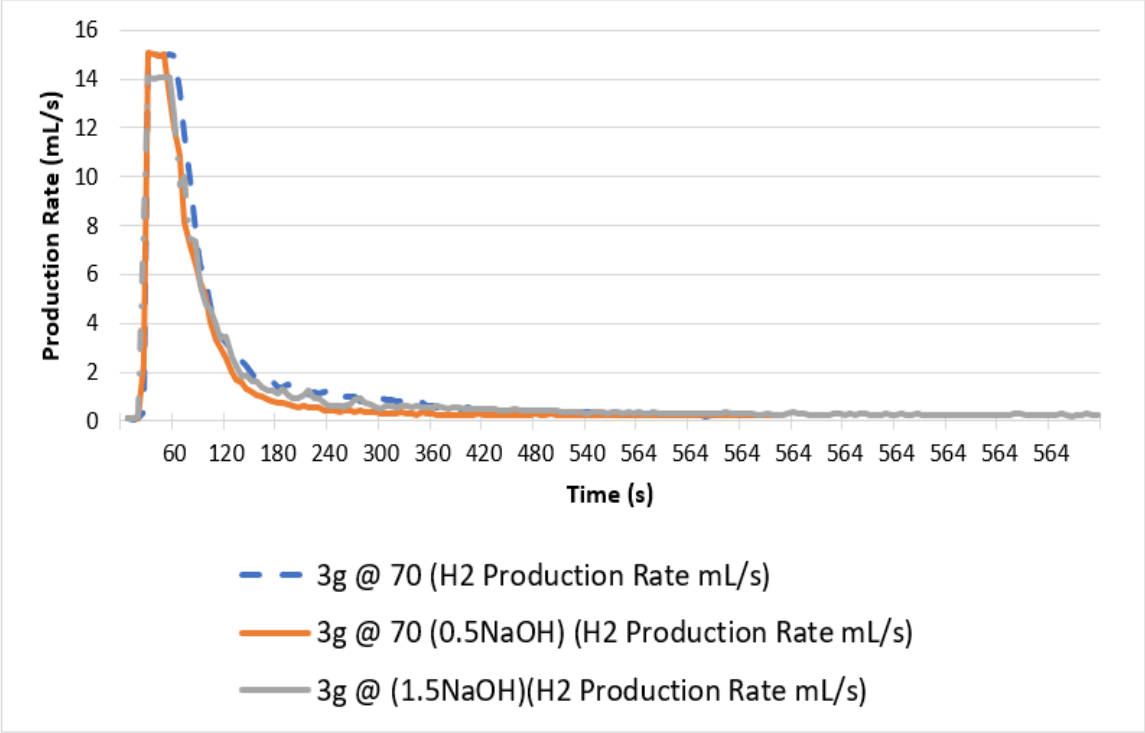

Fig. 6.11 Hydrogen production rate (3g aluminum samples), variation in sodium hydroxide concentration

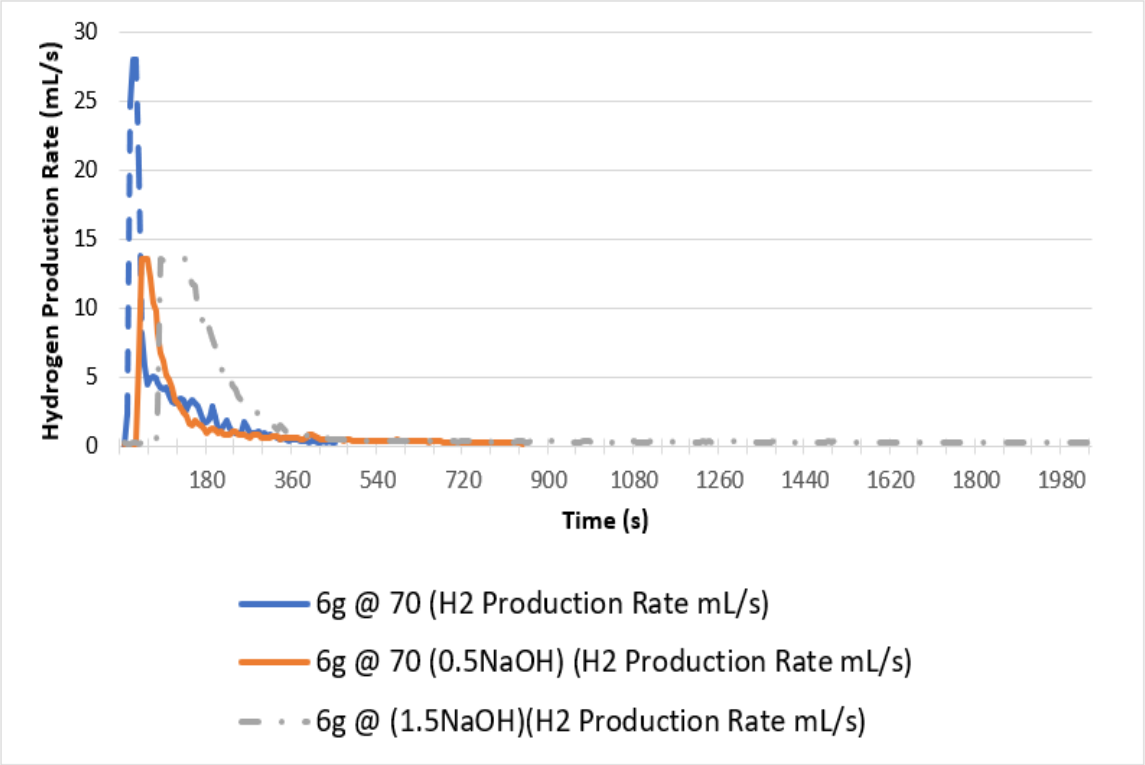

Fig. 6.12 Hydrogen production rate (6g aluminum samples), variation in sodium hydroxide concentration

6.4 Bench Marking and Comparing System Performance

As an important aspect of the study, it is important to assess the overall system performance and provide a comparison to other available systems/ studies that have been done previously.

Typically, within the topic of aluminum water, hydrogen production researchers and inventers often investigate system performance by using the conversion efficiency. Conversion efficiency is also referred to as the yield percentage. The yield percentage provides a measurement of the system's ability to reach the maximum theoretical yield of hydrogen from the aluminum water chemical reaction. Figure 6.13 below depicts the maxima and minima conversion efficiency of various researchers and compare them to each other.

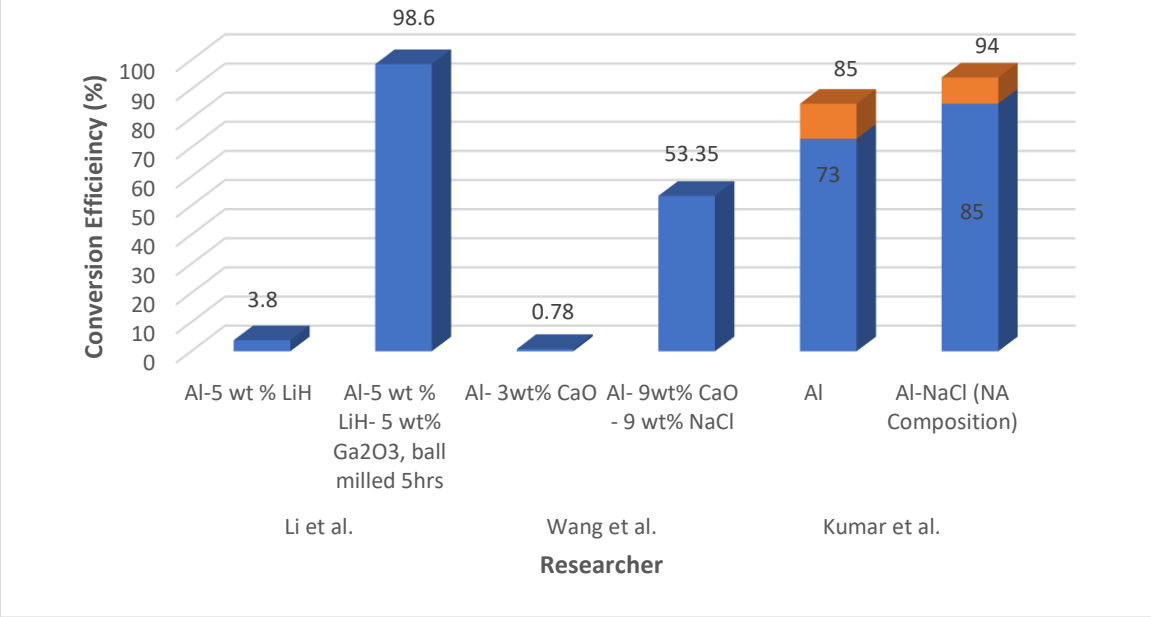

Fig 6.13 Conversion efficiency of aluminum water hydrogen production system

It should be noted that the conversion efficiency of the aluminum water chemical reaction can vary drastically. After, the completion of this thesis research project, it should be noted that the hydrogen production rate did vary drastically. The highest recorded conversion efficiency was 98.6%, and the smallest conversion efficiency observed was 0.78%.

After this, the researcher conducted a comparison of the maxima and minimax values of the hydrogen production rate from various pieces of literature. Figure 6.14 provides a graphical comparison of the hydrogen production rate from various researchers. Figure 6.14 compares the work of Li et al. [44], Irankhaha et al. [55], and Lu et al. [37]. By doing a comparison, it was established that the hydrogen production rate can vary drastically based on the specific test conditions of the system and also the conditions that were used to generate the test samples. It was noted ball milling with other metal that can potentially serve as excellent reaction promoters, and an effective method to create the aluminum test samples.

Figure 6.15, also serves to indicate that the hydrogen production rate achieved within the thesis is comparable to other pieces of literature. The maximum hydrogen production rate of 35.038 mL/ s is only behind the work conducted by Li et al. [44] and is more than Irankhaha et al. [55], and Lu et al. [37].

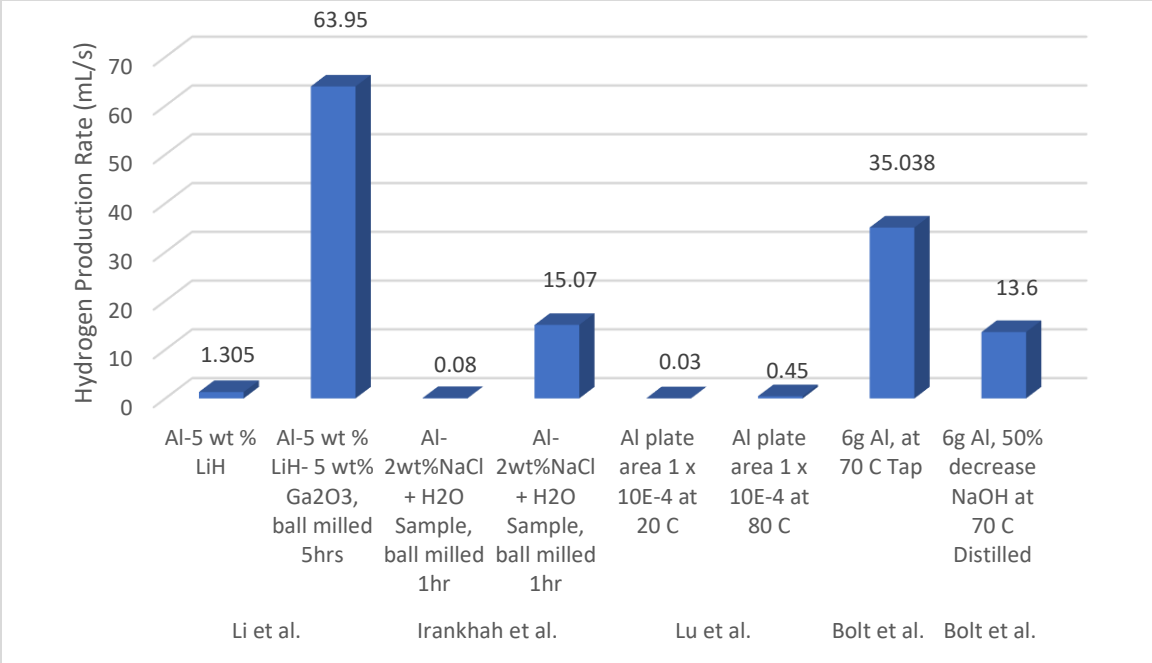

Fig 6.14 Benchmarking hydrogen production rate from aluminum water reaction

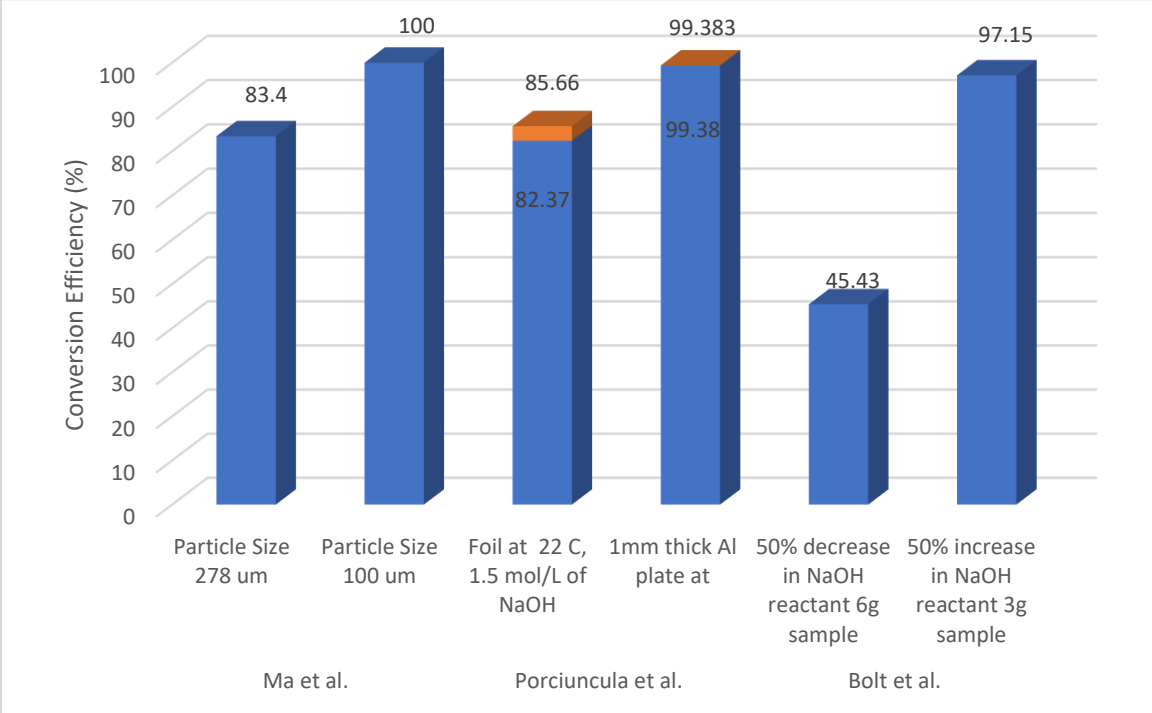

Fig. 6.15 NaOH reaction promoter system comparison

Figure 6.15 compared the work of Ma et al. [79], and Porciuncula et al. [80] to the presented. Based on the observed results, it can be stated that the designed novel hydrogen production system does produce comparable system results, with other systems that use NaOH as its reaction promoter. However, some systems have proved to provide more substantial results. This can be due to other experimental setups having a more refined approach to prevent potential hydrogen gas leaks.

6.5 Modeling Thermodynamic System

To determine if the system is energetically efficient, various ways to quantify system efficiency were previously established. This section aims to evaluate the various system energy efficiencies to determine if the system operates energetically efficient.

6.5.1 Evaluating System Energy Efficiency

As stated within the analysis section, to identify if the system's performance on a molecular level, the standard energy efficiency was calculated and compared for the variations in water temperature, composition, sodium hydroxide concentration test. Figures 6.16 to 6.21 provide a visual representation of this relationship.

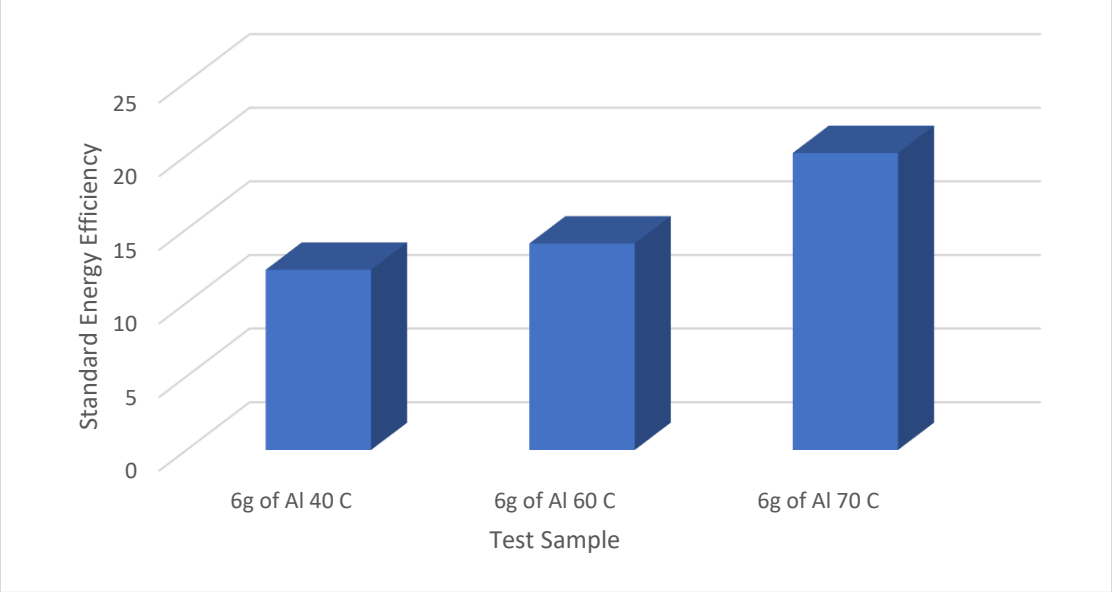

Fig 6.16: Comparison of standard energy efficiency, using 6 grams of aluminum (variations in water temperature)

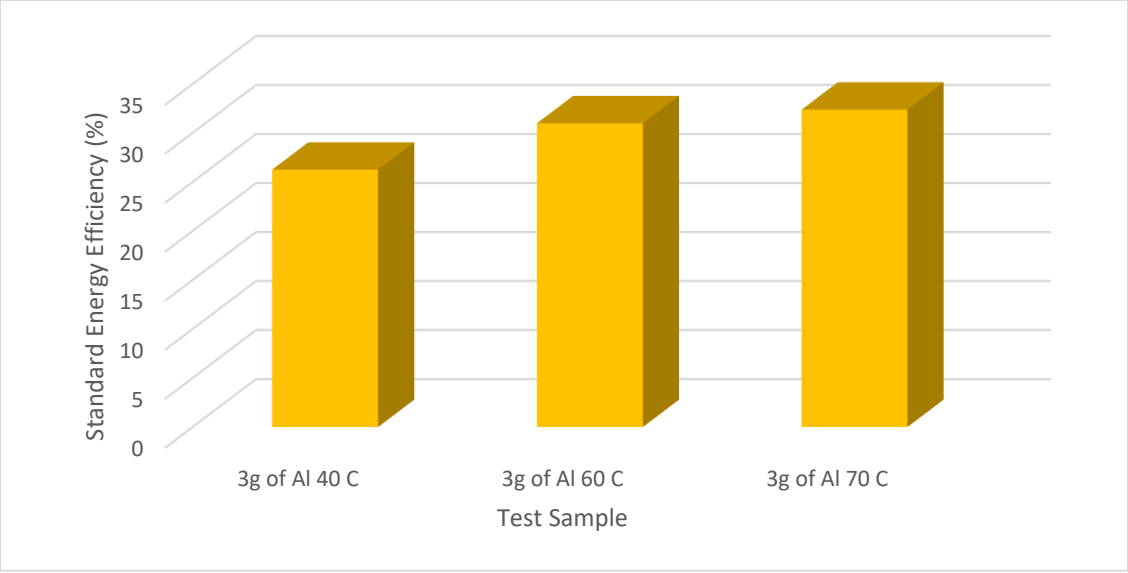

Fig 6.17: Comparison of standard energy efficiency, using 3 grams of aluminum (variations in water temperature)

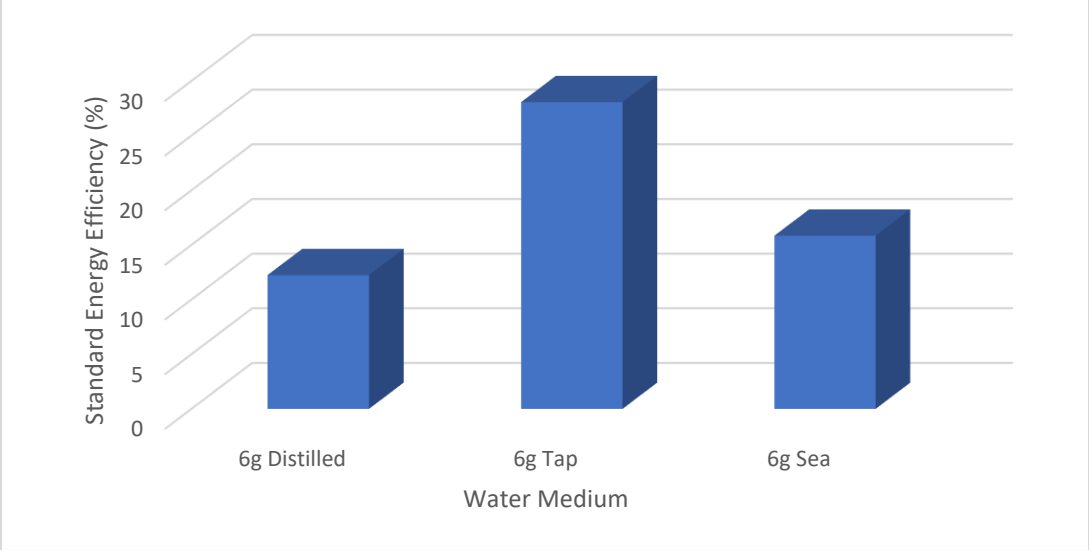

Fig 6.18: Comparison of standard energy efficiency, using 6 grams of aluminum (change in water medium testing)

The standard efficiency previously defined does not take into consideration the energy obtained from the heater, but only the enthalpy of formation of the molecules used within the reaction process, and LHV value taken from the hydrogen molecule. Therefore, preheating the aqueous solution to a temperature of 70^{o}C does not come at a high cost in terms of efficiency. Amongst the three and 6g aluminum varying water temperature test,

the 70°C samples had the most significant hydrogen yield; therefore, it had the highest standard efficiency.

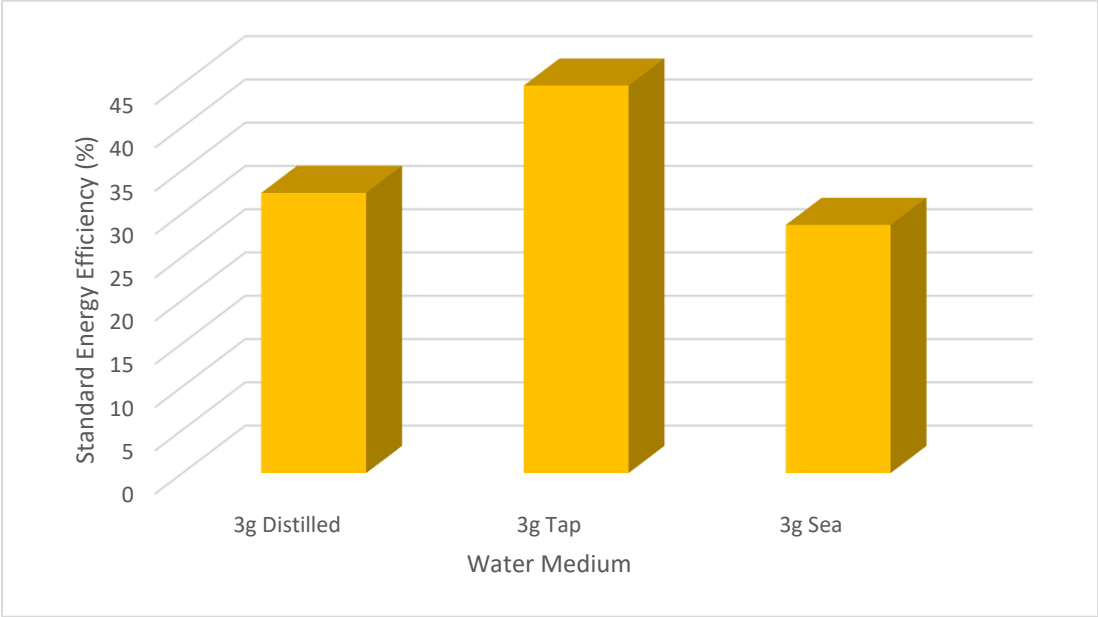

Fig 6.19: Comparison of standard energy efficiency, using 3 g of aluminum (change in water medium testing)

Based on Figure 6.18 and 6.19, the greatest standard efficiency was observed when using tap water samples to generate hydrogen. As previously stated, the tap water provided the most significant hydrogen yield.

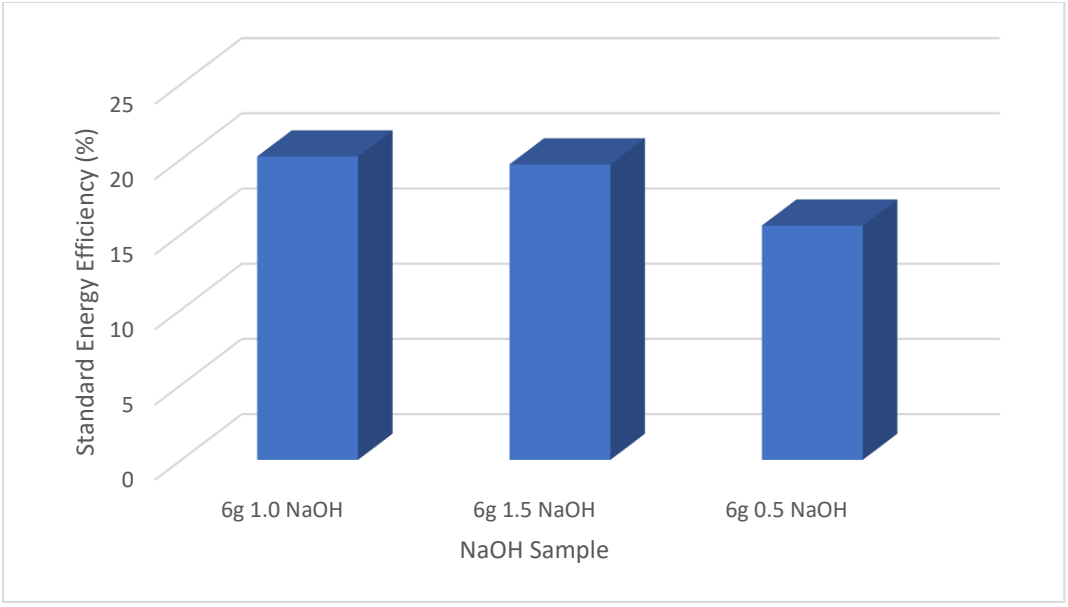

Fig 6.20: Comparison of standard energy efficiency, using 6 g of Al (change in NaOH)

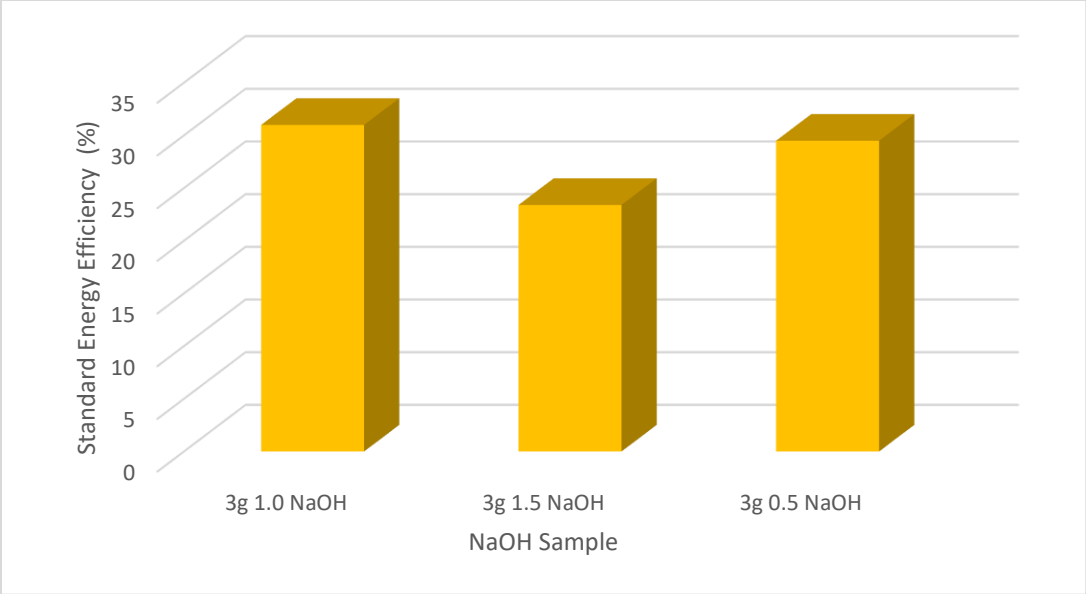

Fig 6.21: Comparison of standard energy efficiency, using 3 grams of aluminum (change in NaOH)

The observed standard efficiency when changing the sodium hydroxide concentration was greatly affected. The standard efficiency equation previously defined takes into consideration the added or reduced amount of energy of the NaOH as an input. Therefore, reducing the amount of NaOH will have a positive impact on standard efficiency. However, based on the experimental testing previously conducted, the increase in NaOH gave a higher conversion efficiency.

The overall system/ process efficiency was identified through the previously defined overall system efficiency equation. After this, the Engineering Equation Solver (EES) software was used to generate a parametric study in which the experimental results for the 3g and 6g aluminum samples were compared. The parametric study was conducted based on experimental results, the minimum and maximum hydrogen yields that were obtained at 40^{o}C and 70^{o}C were used. The study's temperature increased gradually until it reached approximately 70^{o}C. The study also assumed 15% of the water collected from the reaction process to be collected for potential recycling use. The results of this parametric study are displayed in Figure 6.22.

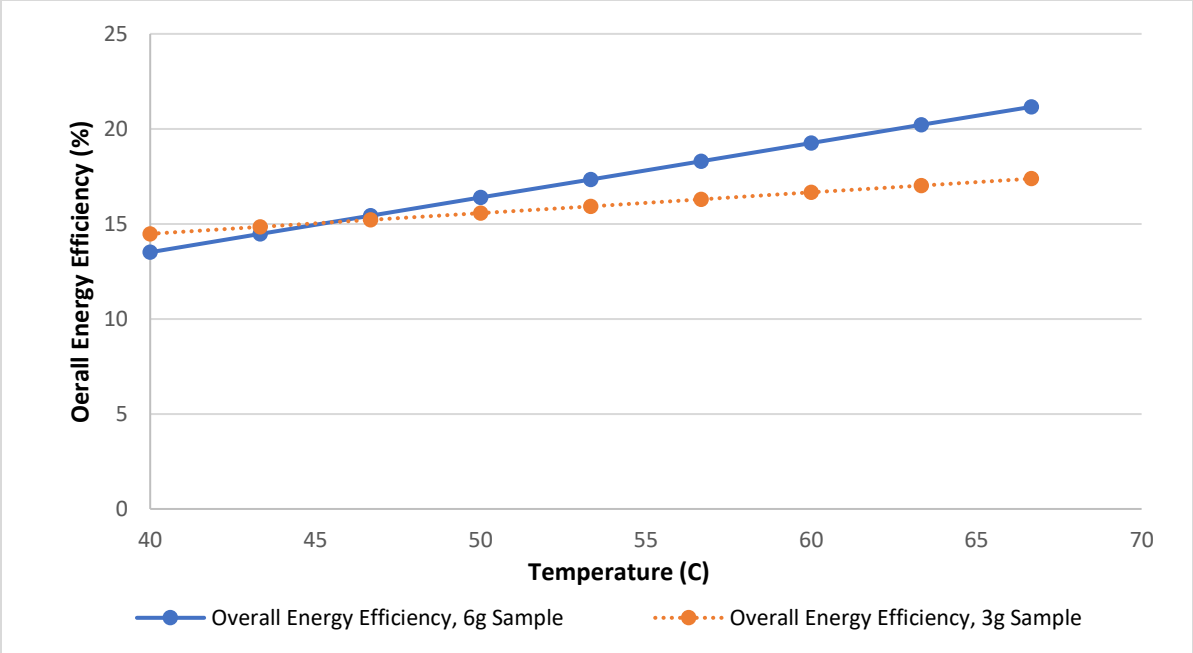

Fig. 6.22 Overall system energy efficiency, comparison of 6 and 3 grams aluminum samples within distilled water

Figures 6.22 displayed that the overall energy efficiency of the system increased gradually with temperature, regardless of the aluminum sample size. The correlation between water temperature and overall energy efficiency is likely due to the warm water temperature, forcing particles to reach a more excited state, which facilitates the chemical reaction to take place. The overall energy efficiency from the 3 gram samples is also higher after the 45^{o}C mark; this is likely due to more aluminum being consumed during the reaction process.

6.5.2 Evaluating System Exergy Efficiency

In order to evaluate the system exergy efficiency, the standard chemical exergy was considered for the various molecules. The exergetic efficiency graphs provide a visual representation of the maximum amount of energy that would be considered useful within the system [72].

As stated within the analysis section, to identify if the system's performance on a basic level was efficient, the standard exergy efficiency can also be calculated and compared for the variation in water temperature, mediums, and the NaOH concentration. Figures 6.23 to 6.28 provides a visual representation of this relationship.

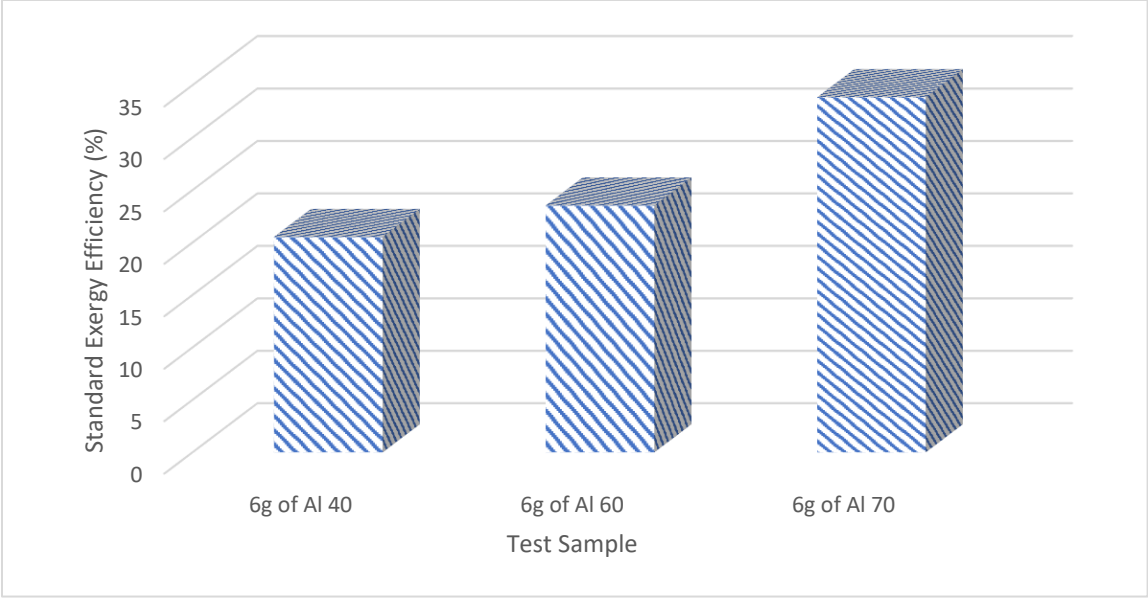

Fig 6.23 Comparison of standard energy efficiency, using 6 grams of aluminum (variations in water temperature)

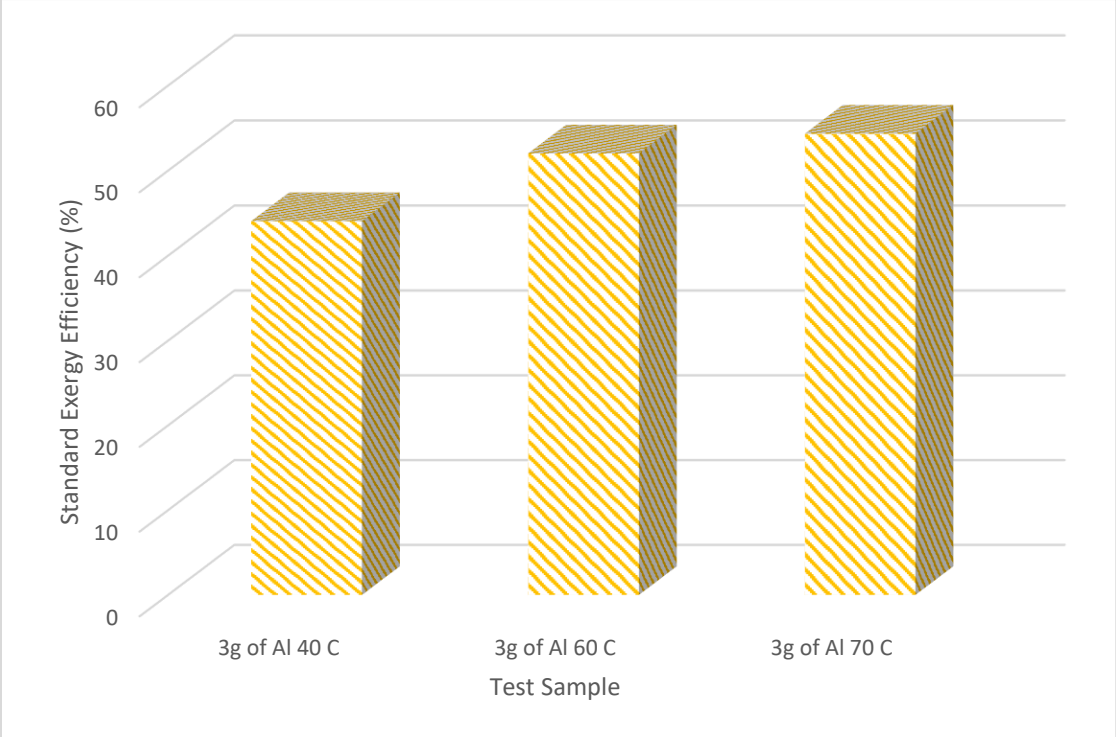

Fig 6.24 Comparison of standard exergy efficiency, using 3 grams of aluminum (variations in water temperature)

Based on the data encapsulated within Figure 6.23 and 6.24, the exergy efficiencies during the varying temperature tests for the 3g and the 6g samples were able to be obtained and compared. As expected, the early hypothesis of the exergetic efficiency increasing with water temperature was verified. As the water molecules increase in temperature, they reach a more excited state, therefore increasing the amount of useful energy that can be obtained from them.

The highest recorded molecular exergetic efficiency, amongst the 6g and the 3g samples, respectively were 33.86% and 54.35%. The smallest recorded exergetic efficiency of 20.54% and 44.06%.

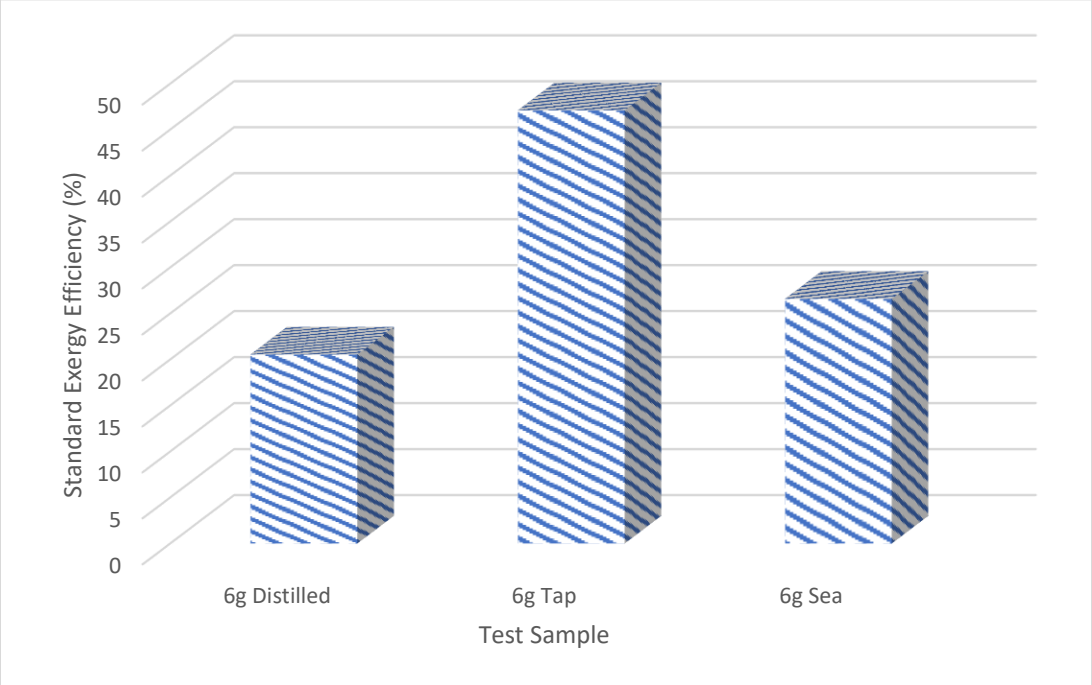

Fig 6.25 Comparison of standard exergy efficiency, using 6 grams of aluminum (change in water composition)

Figures 6.24 and 6.25 display the calculated standard exergy efficiencies when the water medium fluctuated. The tap amongst both trials produced the greatest exergetic efficiency, with seawater following it. The distilled water during the experiment is pure, and is without the presence of metal, non-metals, and minerals, unlike seawater and the tap water used. The composition changes found in seawater and tap water likely contributed to the splitting of water molecules to form hydrogen gas.

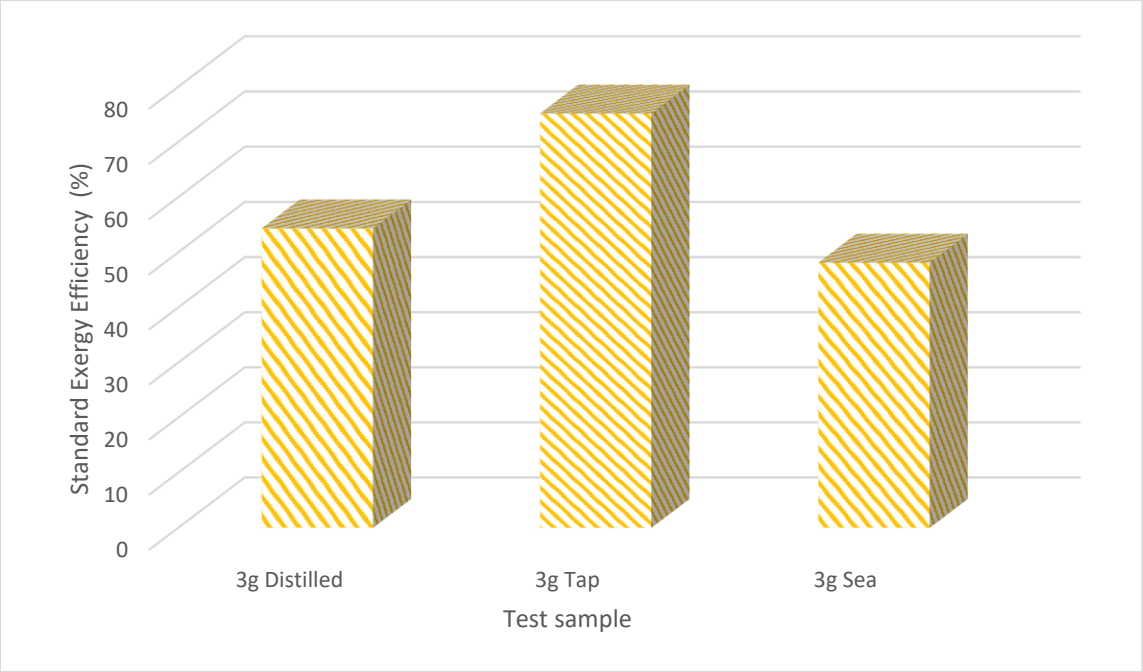

Fig. 6.26 Comparison of standard exergy efficiency, using 3 grams of aluminum (change in water composition)

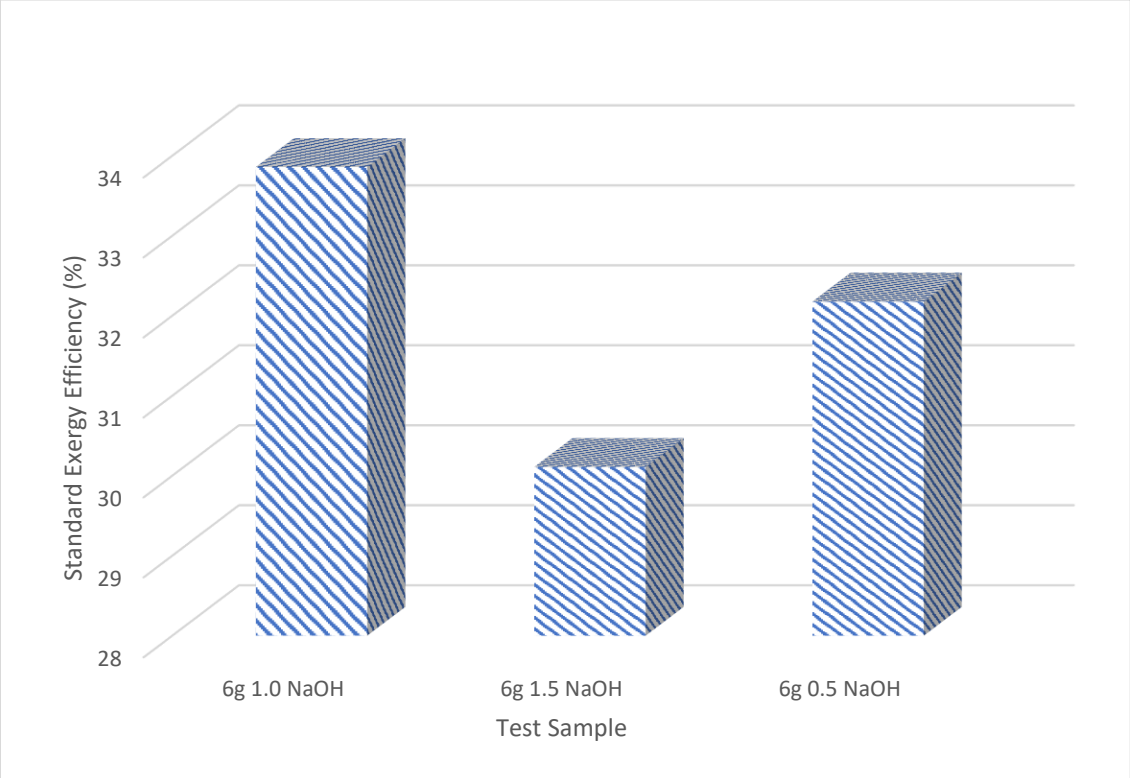

Fig. 6.27 Comparison of standard exergy efficiency, using 6 grams of aluminum (change in NaOH)

Furthermore, the NaCl and KCl that can be found in the tap and seawater have the ability to behave as reaction promoters, which can potentially help facilitate the reaction between water and aluminum. The largest exergetic efficiency recorded for the 6g and 3 g samples, respectively were 47.11 % and 75.15%. The smallest recorded exergetic efficiencies were 26.59% and 48.13 %, respectively.

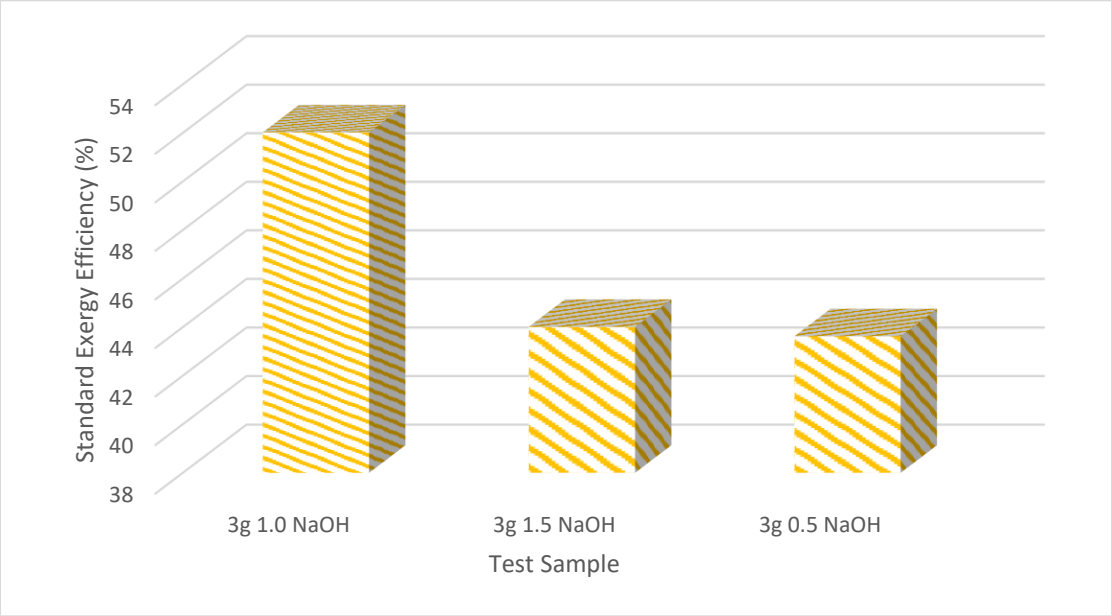

Fig. 6.28 Comparison of standard exergy efficiency, using 3 grams of aluminum (change in NaOH)

Following the change of water mediums test, the amount of sodium hydroxide added to the reaction was varied. The amount of sodium hydroxide added or reduced from the reaction process varied by approximately 50%. After varying, the amount of sodium hydroxide added, the results were compared to the initial reaction. The result showed among both graphs that the molecular efficiency in terms of exergy was at its highest when a stoichiometric amount of sodium hydroxide was added to the reaction. However, there was a noticeable discrepancy when comparing the 50% increase to a 50% decrease in sodium hydroxide between the 3 and 6g samples exergy efficiency. This discrepancy can be linked to the 50% decrease in sodium hydroxide for the 6g test, creating more space within the reaction vessel. Therefore, enabling the aluminum to be consumed more efficiently during the reaction process. The highest exergetic efficiency recorded during this experiment for

the 6g and 3g samples was 33.86% and 52.02%. The smallest recorded exergetic efficiency recorded was 30.11% and 43.63%.

After identifying the various standard exergy efficiencies amongst the three tests conducted, the overall exergy efficiencies were calculated for the varying temperature test results. A parametric study was conducted to identify the system's behaviour between 40°C to 70°C. This parametric study assumed 15% of the water was to be recovered at the end of each trial. The parametric study was based on the values obtained during the varying temperature test, where distilled water was used in conjunction with 3 and 6 g aluminum samples. The results of this study have been summarized in Figure 6.29.

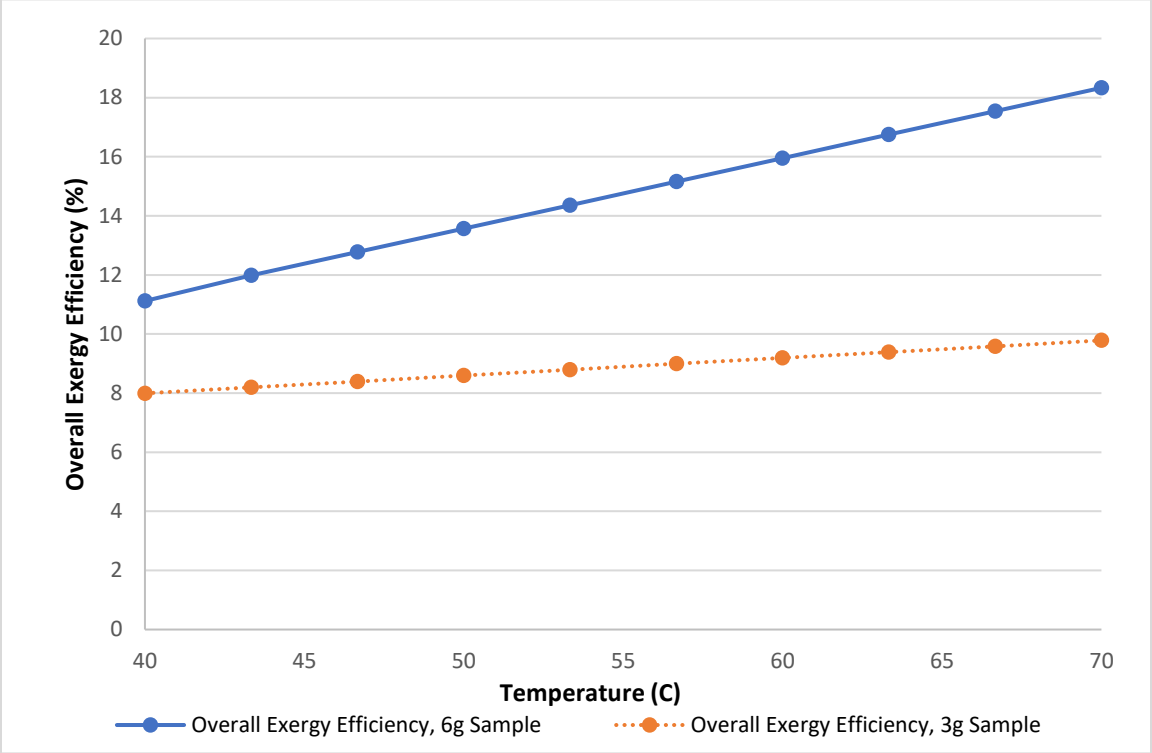

Fig. 6.29 Overall system exergy efficiency, comparison of 6 and 3 gram aluminum samples within distilled water

The results of the parametric study shown in Figure 6.30 closely mirror the result of the previously conducted parametric study, where the overall energy efficiency was compared. The overall exergy destruction for the 3 and 6 grams samples is shown in Figure 6.30. Based on Figure 6.30, it can be deduced that larger exergy destruction is displayed as mass and temperature increases.

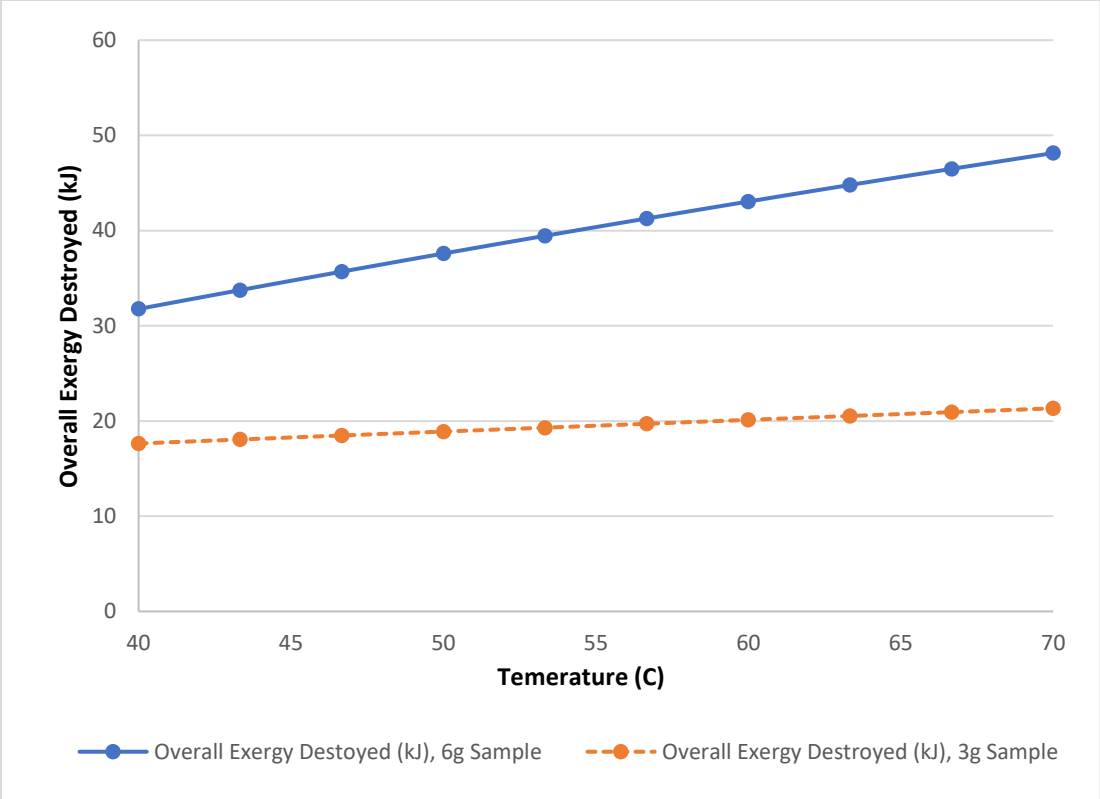

Fig. 6.30 Overall system exergy destroyed comparison of 6 and 3 gram aluminum samples within distilled water

Furthermore, the exergy destruction within the system linked to system efficiency, as seen in Equations 4.8 and 4.9. Furthermore, the increase in sample mass and exergy destroyed within the system were fundamentally linked to each other. If a larger sample-sized was used within the system, additional reactants would be also be used within the experiment. The increase in reactants within the process, therefore, results in an additional exergy input within the system.

The entropy generated within the system examines the change in entropy across the system. The change in entropy is derived by the system experiencing losses, the further the is from an idealized process, the greater the entropy generation rate will be. As seen in Figure 6.31, the entropy generation rate increases with a mass sample size, as seen in all of the entropy balance equations in Table 4.3. Furthermore, the specific entropy of reactants also increases with temperature; therefore, if the temperature of the water medium increases, entropy generated will increase as well.

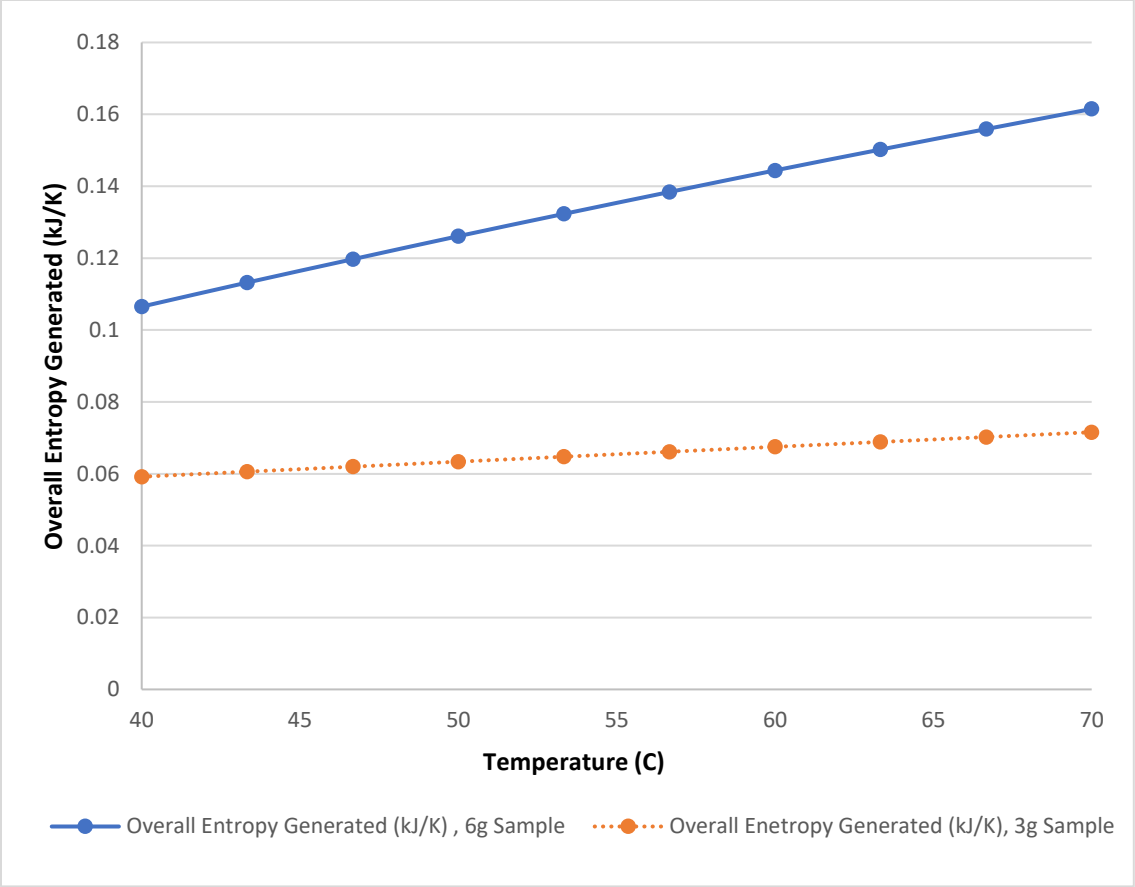

Fig. 6.31 Overall system entropy generated, comparison of 6 and 3 gram aluminum samples within distilled water

The calculated sustainability index within Figures 6.32, display the overall sustainability index for the system, at various water medium temperatures, ranging from 40^{o}C to 70^{o}C. The sustainability index is a good indicator to determine how sustainable the process is and determining if the process can be improved upon. The sustainability index can only be equal to one or greater if the exergy destruction is equal to or less than the exergy being produced during the reaction, through the standard chemical exergy of hydrogen.

Based on the results of Figure 6.32, it can be deduced that a greater sustainability index takes place at a greater temperature. This is justifiable, considering that temperature aids in chemical reactions taking place, as previously stated. Furthermore, the greatest sustainability index observed was 0.1833 at 70^{o}. The 3g curve followed a similar trend of the greatest sustainability index being at 70^{o}C as well; however, it is considerably smaller, only being 0.0978. In this future, this test can be improved by testing additional mass

samples to identify if the sustainability index will decrease when adding additional mass to the process.

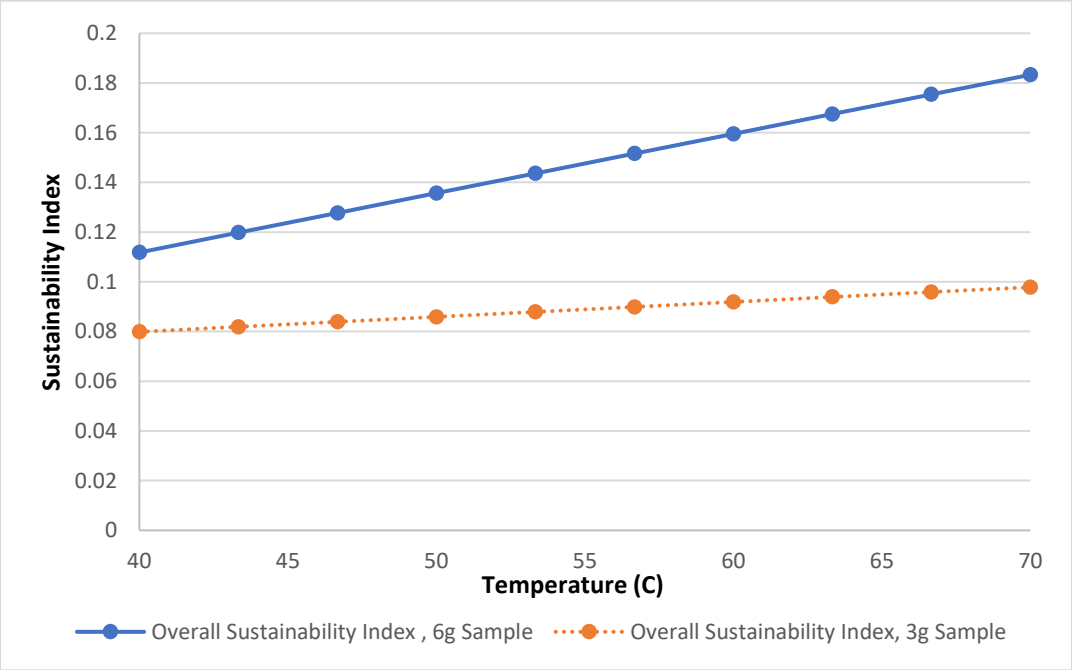

Fig. 6.32 Overall system sustainability index, comparison of 6 and 3 gram aluminum samples within distilled water

6.6 System Scalability

Based on the previously defined balance equations displayed in Chapter 4, the system was able to be modelled thermodynamically using the Aspen Plus software. The system generated within Aspen Plus was depicted in Figure 6.33 of the report. The system state point labelling scheme follows the initially designed schematic seen in Figure 3.1.

The initial model generated using the Aspen assumes the following:

- The pressure losses within the fittings, and bends are negligible
- The steady-state conditions are assumed, across also system components
- The average flow rate of reactants nitrogen gas, aluminum powder, sodium hydroxide and water was assumed to be stoichiometric rates per second.
- The system considers ambient temperature to be 25^{o}C
- The transient start-up period was not considered.

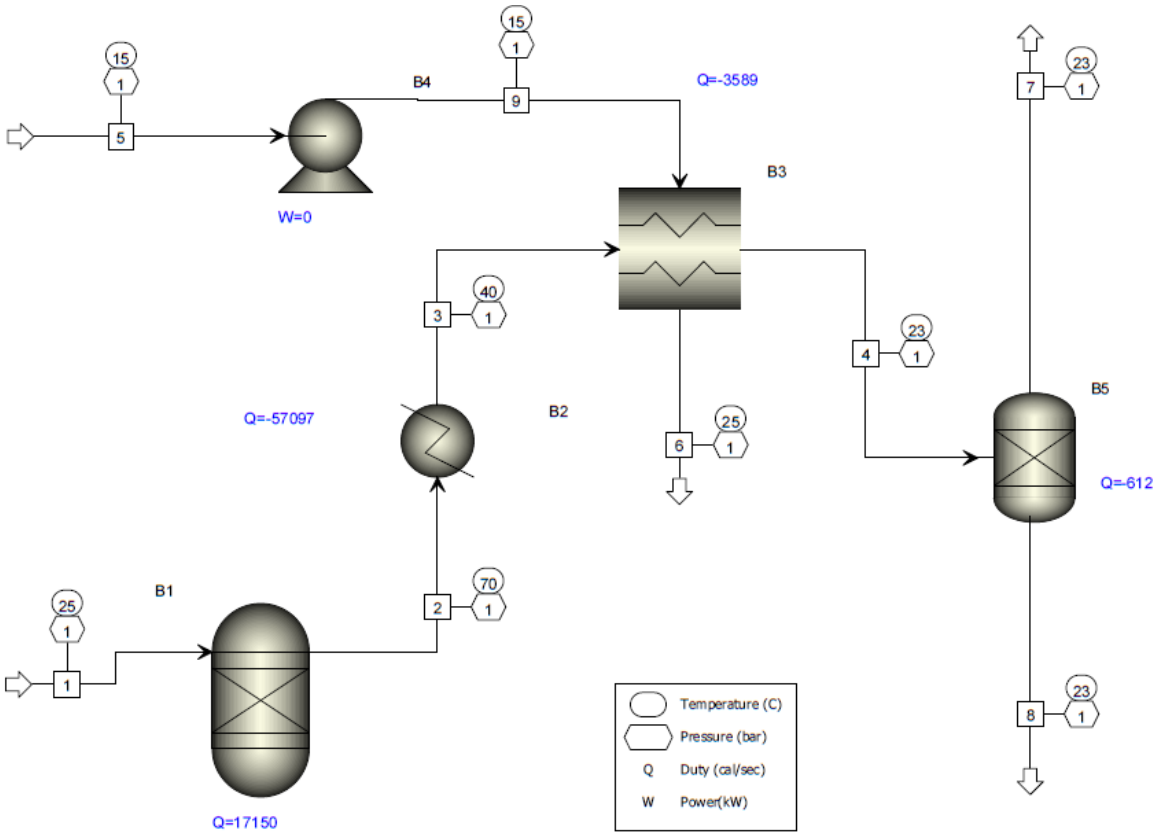

Fig. 6.33 System schematic generated within aspen plus software

Within the Aspen flow sheet depicted in Figure 6.33, the main reactor within the system was modelled as Gibbs free energy minimization approach-based reactor (B1). The gasses leaving the reactor passes through the Vigreux column, which is modelled as a heat exchanger, with approximated heat losses to the environment. Following this, the gaseous product consisting of hydrogen, nitrogen, and water vapour enters a condenser, which is modelled in aspen as a counter flow heat exchanger. Lastly, the condensed water and the gases are separated in a phase separator, which models a distillation head.

By making these system assumptions, a baseline was developed to estimate the various system state points. The state points and the corresponding mole fractions of the system generated within Aspen have been summarized in Tables 6.7 and 6.8 of this thesis accordingly.

Table 6. 7 Standard system state points

State Number	1	2	3	4	5	6	7	8	9
Temperature (C)	25	70	40	23.2701	15	25	23.2701	23.2701	15.0161
Molar Enthalpy $(\frac{kJ}{mol})$	-228.909	-246.366	-272.927	-274.597	-286.581	-285.828	-0.04879	-412.298	-286.58
Molar Entropy $(\frac{kJ}{mol\,k})$	-0.08562	-0.05273	0.20239	0.19567	-0.1658	-0.16324	-5.97E-5	0.29202	-0.16579
Mass Exergy $(\frac{kJ}{kg})$	-94.088	3804.640	-11.2857	1.1183	0.6036	0.0188	-16.1243	1.5655	0.0623

It should be noted that the negative values within Table 6.8 are due to the selected reference point of the Aspen Plus software.

Table 6. 8 Mole fractions of system molecules

Mole Fraction									
NA+	0	0	0	0	0	0	0	0	0
H2O	0.6	0.44	0.44	0.44	1	1	0	0.67	1
OH-	0	0	0	0	0	0	0	0	0
H+	0	0	0	0	0	0	0	0	0
H3O+	0	0	0	0	0	0	0	0	0
NAOH	0.2	0	0	0	0	0	0	0	0
H2	0	0.33	0.33	0.33	0	0	1	0	0
AL(OH)4-	0	0	0	0	0	0	0	0	0
AL	0.2	0	0	0	0	0	0	0	0
AL(OH)3	0	0	0	0	0	0	0	0	0
NA	0	0	0	0	0	0	0	0	0
NAALO2	0	0.22	0.22	0.22	0	0	0	0.33	0

Subsequent to the system state points being established, a parametric study was conducted to study how the system operates under varying environmental conditions.

6.7 Fuel Cell Integration

During the experimental design process, it was acknowledged that a possible application for the hydrogen generated would be its use within fuel cell technology. However, if the experimental set up were to be integrated within a fuel cell system design, thermal management issues can pose a challenge. As previously stated, the chemical reaction

between water, aluminum, and sodium hydroxide is highly exothermic. In order to mitigate issues associated with thermal management, effective methods to provide cooling to a fuel cell should be considered. As outlined by the United States Department of Energy, bus and stack cooling systems are effective methods to mitigate thermal management issues.

A stack cooling system can be used to control the temperature during the chemical reaction. The fuel stack cooling system schematic is outlined below:

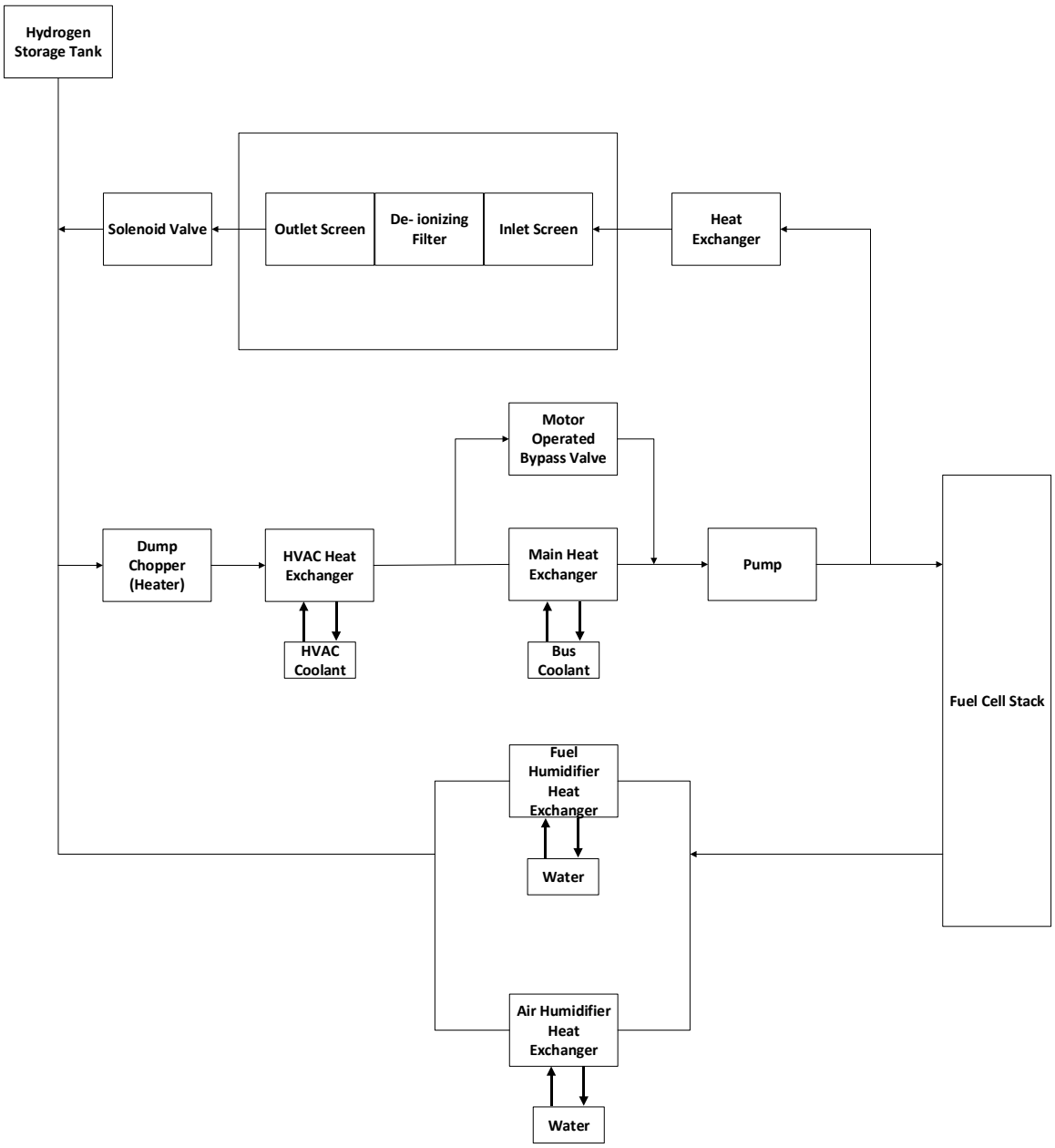

Fig. 6.34 Example of stack cooling system (adapted from [81])

The stack cooling system schematic designed by the United States DOE, utilizes a main coolant loop. The main coolant loop circulates the coolant through the fuel cell stack to absorb heat from the fuel cell stack.

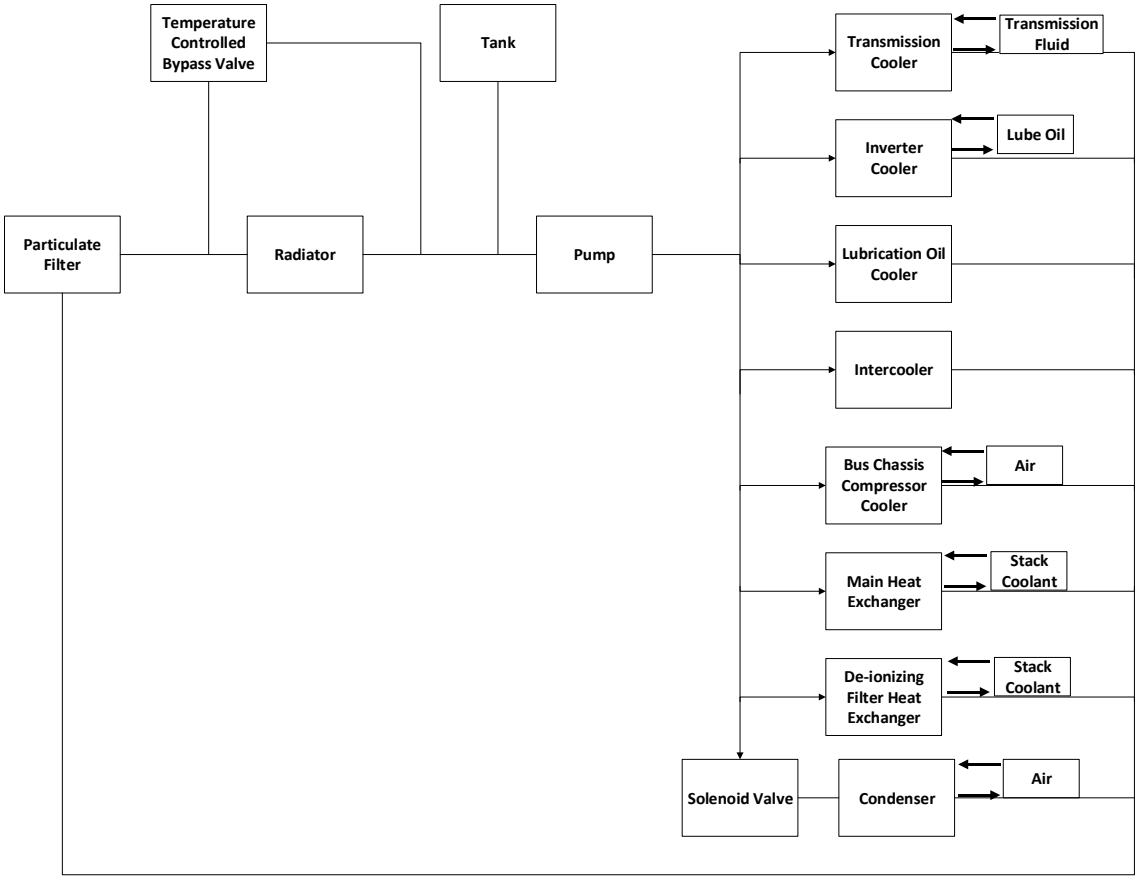

Fig. 6.35 Bus Cooling System (adapted from [81])

Rather than circulating coolant throughout the system, a bus cooling system can be utilized. The bus cooling system absorbs the heat from the various system components and releases the heat into the environment.

Also, given that the reaction rate is temperature-dependent, methods of temperature regulation should also be considered. A simple electrical heating system that uses metal coils, is sufficient. However, it is important for heat to be provided outside of the reaction vessel, rather than inside. This is due to NaOH being a main component of the reaction, and it will react readily if it comes in contact with the metal coils.

CHAPTER 7: CONCLUSIONS AND RECOMMENDATIONS

After the design, development, and testing of the hydrogen production and water recovery experimental setup, the respective system was successfully studied and analyzed. The new system was evaluated based on its hydrogen conversion efficiency or yield, hydrogen production rate, standard efficiency, and overall system efficiency.

7.1 Conclusions

As the world shifts more towards renewable and sustainable energy options, hydrogen as a potential fuel source and energy carrier is still not being utilized to its maximum potential. As previously stated, hydrogen as a fuel source and potential energy carrier has tremendous potential as it is able to release 141.9 MJ/ kg of energy during the combustion process while having water as it is the only by-product. Presently the majority of hydrogen is produced via coal reformation, as it is considered to be the most efficient method of hydrogen production; however, this method is counter-intuitive. The primary benefit of utilizing hydrogen as a fuel source is its zero greenhouse gas emissions; this method of hydrogen production would be creating emissions.

This thesis presents a novel method to produce hydrogen gas without the presence of any fossil fuel, while also harnessing of abundant resources primarily. The resources used to produce hydrogen in this thesis was water and aluminum. Water covers most of the earth's surface, and aluminum is one of the cheapest and most abundant metals on earth.

The major contribution to the natural and applied science field is the experimental setup utilized to produce hydrogen gas. Never before has a distillation system been integrated within an experimental setup, targeting hydrogen production through an aluminum water reaction. The proposed distillation system can capture the wastewater produced during the reaction so that it can be recycled for later use. The recycling of wastewater back into the system to produce additional hydrogen should have a positive effect on the system's overall efficiency due to less material being wasted. Furthermore, the data acquisition station used within the experimental setup can provide real-time updates to monitor the system performance in terms of temperature, pressure, volumetric flow, mass flow, and the concentration of hydrogen passing through the experimental setup. The data acquisition station provides a more detailed and intensive look at the hydrogen, rather than simply

using a conventional bubbler system. Lastly, an exergy analysis has never been conducted to this level of detail, about hydrogen production, using aluminum and water. The exergy analysis included the calculation of various efficiencies, the system exergy destruction, entropy generated, and the sustainability index.

The major and significant findings from this research project were identified by conducting 3 types of tests. The three tests included variations in the water temperature, water medium, and the amount of NaOH added to the reaction process.

The major and significant findings from this project are as follows:

- Seawater is a viable and abundant option for hydrogen production in this particular experimental setup, although there is still room for improvement. This is evident in its conversion efficiency at a conversion efficiency of 58.8%.
- The 50% increase in sodium hydroxide gave a relatively high conversion efficiency of 97.15 % and 95.44 % for the 3g and 6g sample, respectively. However, it should be noted that the increase in sodium hydroxide negatively affected the molecular efficiency of the process.
- During the varying water temperature test, the hydrogen production rate and conversion efficiency were at its highest at 70^{o}C. This indicated that higher temperatures within experiments best facilitate a reaction taking place.

7.2 Recommendations

After completion and analysis of the testing of the physical system, researchers identified several areas in which the study can be improved upon or potential opportunities to expand on the research previously conducted. Areas of improvement are as follows:

- The implemented system uses a batch process in which the starting reactants must be replenished manually at the end of each trial, and the water that was recovered from the process can only be collected by disconnecting the parts of the experimental setup. Presently the issue with implementing a continuous cycle is backflow and cross-contamination. However, in the future, the researcher can investigate ways to make the cycle continuous without compromising the functionality and effectiveness of the system.

- Upscaling the system for commercial use was briefly investigated within Aspen Plus software. The thesis project conducted can serve as a potential starting point, or prototype to test, to identify if the system can still operate effectively under varying operating conditions. Creating a commercialized model for the system would encourage the researcher to use more industrialized materials, rather than equipment geared specifically towards scientific testing, such as glass flasks.
- In this thesis, one size aluminum powder was used, with high purity. For future tests, researchers can try to introduce a novel aluminum powder that has been ball milled or prepared differently, then investigate how it operates within the designed system. After this, the alloy's performance within the system the alloys. Presently many pieces of literature utilize lithium, gallium, and indium within aluminum alloys to increase the hydrogen yield. Therefore, these more commonly used alloys can be used as a benchmark to gauge the collected result.

REFERENCES

[1] H. Lund, "Renewable energy strategies for sustainable development," *Energy*, vol. 32, no. 6, pp. 912–919, 2007.

[2] E. Holden, K. Linnerud, and D. Banister, "The Imperatives of Sustainable Development," *Sustain. Dev.*, vol. 25, no. 3, pp. 213–226, 2017.

[3] Government of Canada, "Government of Canada sets ambitious GHG reduction targers for federal operations," 2017. [Online]. Available: https://www.canada.ca/en/treasury-board-secretariat/news/2017/12/government_of_canadasetsambitiousghgreductiontargetsforfederalop.html.

[4] JWP, "Renewable Energy In Canada," August 2017, pp. 18–20, 2017.

[5] Sunita Satyapal, "U . S . Department of Energy Hydrogen and Fuel Cell Overview," *U.S. Dep. Energy EERE*, 2016.

[6] US DOE (Fuel Cell Technologies Office), "Hydrogen Production," *Energies*, 2018.

[7] US DOE, "Reaction of aluminum with water to produce hydrogen," *US DOE Rep.*, pp. 1–26, 2008.

[8] US DOE, "DOE Technical Targets for Hydrogen Production from Electrolysis." [Online]. Available: https://www.energy.gov/eere/fuelcells/doe-technical-targets-hydrogen-production-electrolysis.

[9] M. Conte, "ENERGY | Hydrogen Economy," *Encycl. Electrochem. Power Sources*, pp. 232–254, 2009.

[10] DOE, "DOE Hydrogen and Fuel Cells Program: Hydrogen Storage," *U.S Dep. Energy*, vol. 25, p. 6, 2009.

[11] K. W. A. Guy, "The hydrogen economy," *Process Saf. Environ. Prot.*, vol. 78, no. 4, pp. 324–327, 2000.

[12] T. N. Vezirolu and F. Barbir, "Hydrogen: the wonder fuel," *Int. J. Hydrogen Energy*, vol. 17, no. 6, pp. 391–404, 1992.

[13] P. Nikolaidis and A. Poullikkas, "A comparative overview of hydrogen production processes," *Renew. Sustain. Energy Rev.*, vol. 67, no. January, pp. 597–611, 2017.

[14] C. Acar and I. Dincer, "Hydrogen Energy," *Compr. Energy Syst.*, vol. 1–5, no. 1853, pp. 568–605, 2018.

[15] M. Y. Azwar, M. A. Hussain, and A. K. Abdul-Wahab, "Development of biohydrogen production by photobiological, fermentation and electrochemical processes: A review," *Renew. Sustain. Energy Rev.*, vol. 31, pp. 158–173, 2014.

[16] R. Łukajtis *et al.*, "Hydrogen production from biomass using dark fermentation," *Renew. Sustain. Energy Rev.*, vol. 91, no. March, pp. 665–694, 2018.

[17] M. L. Chong, V. Sabaratnam, Y. Shirai, and M. A. Hassan, “Biohydrogen production from biomass and industrial wastes by dark fermentation,” *Int. J. Hydrogen Energy*, vol. 34, no. 8, pp. 3277–3287, 2009.

[18] S. Ghosh, U. K. Dairkee, R. Chowdhury, and P. Bhattacharya, “Hydrogen from food processing wastes via photofermentation using Purple Non-sulfur Bacteria (PNSB) – A review,” *Energy Convers. Manag.*, vol. 141, pp. 299–314, 2017.

[19] S. Papari and K. Hawboldt, “A review on condensing system for biomass pyrolysis process,” *Fuel Process. Technol.*, vol. 180, no. June, pp. 1–13, 2018.

[20] I. Hannula, *VTT WORKING PAPERS 131 Hydrogen production via thermal gasification of biomass in near-to-medium term Hydrogen production via thermal gasification of biomass in near-to-medium term*. 2009.

[21] M. Aasadnia and M. Mehrpooya, “Large-scale liquid hydrogen production methods and approaches: A review,” *Appl. Energy*, vol. 212, no. March 2019, pp. 57–83, 2018.

[22] “Hydrogen Production: Electolysis,” *Office of Energy Production & Renewable Energy*. [Online]. Available : https://www.energy.gov/eere/fuelcells/hydrogen-production-electrolysis

[23] “An Overall Assessment Of Hydorgen Production By Solar Water Thermolysis Equilibrium relations :,” vol. 14, no. 12, pp. 881–891, 1989.

[24] X. Gu, S. Yuan, M. Ma, and J. Zhu, “Nanoenhanced Materials for Photolytic Hydrogen Production,” *Nanotechnol. Energy Sustain.*, pp. 629–648, 2017.

[25] “Hydrogen Production: Natural Gas Reforming,” *Office of Energy Efficiency & Renewable Energy*. [Online]. Available: https://www.energy.gov/eere/fuelcells/hydrogen-production-natural-gas-reforming.

[26] F. Gallucci, “The water-gas shift reaction : from conventional catalytic systems to Pd-based membrane reactors – a review INTRODUCTION : HISTORICAL BACKGROUND,” *Encylopedia Membr.*, no. December 2015, pp. 111–137, 2015.

[27] A. Kerkhof, “Towards a hydrogen economy,” *Public Transp. Int.*, vol. 52, no. 5, p. 53, 2003.

[28] U.S.G.S., “How Much Water is There on Earth?” [Online]. Available: https://www.usgs.gov/special-topic/water-science-school/science/how-much-water-there-earth?qt-science_center_objects=0#qt-science_center_objects.

[29] B. E. Sawe, “The Most Abundant Elements In The Earth’s Crust.” [Online]. Available: https://www.worldatlas.com/articles/the-most-abundant-elements-in-the-earth-s-crust.html.

[30] C. Exley, “The toxicity of aluminium in humans,” *Morphologie*, vol. 100, no. 329, pp. 51–55, 2016.

[31] P. Vashishta *et al.*, “Rapid hydrogen production from water using aluminum nanoclusters: A quantum molecular dynamics simulation study,” *Solid State Ionics*, vol. 262, pp. 908–910, 2014.

[32] F. Shimojo, S. Ohmura, R. K. Kalia, A. Nakano, and P. Vashishta, “Molecular dynamics simulations of rapid hydrogen production from water using aluminum clusters as catalyzers,” *Phys. Rev. Lett.*, vol. 104, no. 12, pp. 1–4, 2010.

[33] S. S. Razavi-Tousi and J. A. Szpunar, “Effect of ball size on steady state of aluminum powder and efficiency of impacts during milling,” vol. 284, pp. 149–158, 2015.

[34] Y. Yavor, S. Goroshin, J. M. Bergthorson, D. L. Frost, R. Stowe, and S. Ringuette, “Enhanced hydrogen generation from aluminum-water reactions,” *Int. J. Hydrogen Energy*, vol. 38, no. 35, pp. 14992–15002, 2013.

[35] S. Gorjian and B. Ghobadian, “Erratum: Solar desalination: A sustainable solution to water crisis in Iran (Renew. Sustain. Energy Rev. (2015) 48 (571-584)),” *Renew. Sustain. Energy Rev.*, vol. 49, no. October 2018, p. 1323, 2015.

[36] V. Rosenband and A. Gany, “Application of activated aluminum powder for generation of hydrogen from water,” *Int. J. Hydrogen Energy*, vol. 35, no. 20, pp. 10898–10904, 2010.

[37] J. Lu, W. Yu, S. Tan, L. Wang, X. Yang, and J. Liu, “Controlled hydrogen generation using interaction of artificial seawater with aluminum plates activated by liquid Ga-In alloy,” *RSC Adv.*, vol. 7, no. 49, pp. 30839–30844, 2017.

[38] M. Pudukudy, Z. Yaakob, B. Narayanan, R. Ramakrishnan, and S. Viswanathan, “Hydrogen production from sea water using waste aluminium and calcium oxide,” *Int. J. Hydrogen Energy*, vol. 37, no. 9, pp. 7451–7456, 2012.

[39] A. V. Ilyukhina, O. V. Kravchenko, and B. M. Bulychev, “Studies on microstructure of activated aluminum and its hydrogen generation properties in aluminum/water reaction,” *J. Alloys Compd.*, vol. 690, pp. 321–329, 2017.

[40] M. Q. Fan, D. S. Mei, D. Chen, C. J. Lv, and K. Y. Shu, “Portable hydrogen generation from activated Al-Li-Bi alloys in water,” *Renew. Energy*, vol. 36, no. 11, pp. 3061–3067, 2011.

[41] M. Q. Fan, F. Xu, and L. X. Sun, “Hydrogen generation by hydrolysis reaction of ball-milled Al-Bi alloys,” *Energy and Fuels*, vol. 21, no. 4, pp. 2294–2298, 2007.

[42] C. Wang *et al.*, “A novel self-assembling al-based composite powder with high hydrogen generation efficiency,” *Sci. Rep.*, vol. 5, pp. 1–6, 2015.

[43] P. Dupiano, D. Stamatis, and E. L. Dreizin, “Hydrogen production by reacting water with mechanically milled composite aluminum-metal oxide powders,” *Int. J. Hydrogen Energy*, vol. 36, no. 8, pp. 4781–4791, 2011.

[44] P. Li *et al.*, “Hydrogen generation performance of novel Al-LiH-metal oxides,” *Inorg. Chem. Front.*, vol. 5, no. 7, pp. 1700–1706, 2018.

[45] S. S. Martínez, W. L. Benítes, A. A. Á. Gallegos, and P. J. Sebastián, “Recycling of aluminum to produce green energy,” *Sol. Energy Mater. Sol. Cells*, vol. 88, no. 2, pp. 237–243, 2005.

[46] A. K. Narayana Swamy and E. Shafirovich, “Conversion of aluminum foil to powders that react and burn with water,” *Combust. Flame*, vol. 161, no. 1, pp. 322–331, 2014.

[47] T. Hiraki, M. Takeuchi, M. Hisa, and T. Akiyama, “Hydrogen Production from Waste Aluminum at Different Temperatures, with LCA,” *Mater. Trans.*, vol. 46, no. 5, pp. 1052–1057, 2005.

[48] C. Y. Ho and C. H. Huang, “Enhancement of hydrogen generation using waste aluminum cans hydrolysis in low alkaline de-ionized water,” *Int. J. Hydrogen Energy*, vol. 41, no. 6, pp. 3741–3747, 2016.

[49] S. Elitzur, V. Rosenband, and A. Gany, “Urine and aluminum as a source for hydrogen and clean energy,” *Int. J. Hydrogen Energy*, vol. 41, no. 28, pp. 11909–11913, 2016.

[50] D. Putnam, “Composition and Concentrative Administration,” *NASA Contractor Report*, July, 1971.

[51] L. Soler, J. Macanás, M. Muñoz, and J. Casado, “Aluminum and aluminum alloys as sources of hydrogen for fuel cell applications,” *J. Power Sources*, vol. 169, no. 1, pp. 144–149, 2007.

[52] A. Chaklader and D. Chandra, “Hydrogen generation from water split reaction,” Canada Patent WO 02/14213 A2, Feb. 21, 2002.

[53] Z. Y. Deng, J. M. F. Ferreira, Y. Tanaka, and J. Ye, “Physicochemical mechanism for the continuous reaction of γ-Al 2O3-modified aluminum powder with water,” *J. Am. Ceram. Soc.*, vol. 90, no. 5, pp. 1521–1526, 2007.

[54] T. Troczynski, “Compositions and Methods of Generating Hydrogen From Water," US 0131113 A1, Oct. 20, 2005.

[55] A. Irankhah, S. M. Seyed Fattahi, and M. Salem, “Hydrogen generation using activated aluminum/water reaction,” *Int. J. Hydrogen Energy*, vol. 43, no. 33, pp. 15739–15748, 2018.

[56] J. K. Anand, “ Method and Composition For Production of Hydrogen " US 0177543, Jun. 26, 2008.

[57] H. Wang, J. Lu, S. J. Dong, Y. Chang, Y. G. Fu, and P. Luo, “Preparation and hydrolysis of aluminum based composites for hydrogen production in pure water,” *Mater. Trans.*, vol. 55, no. 6, pp. 892–898, 2014.

[58] X. Jiang, R. Saito, and P. Classification, “A1 generated on the Surface when Al fine particles are room temperature ,” US 0034756, 2006.

[59] S. J. O. White and J. P. Shine, “Exposure Potential and Health Impacts of Indium

and Gallium, Metals Critical to Emerging Electronics and Energy Technologies," *Curr. Environ. Heal. reports*, vol. 3, no. 4, pp. 459–467, 2016.

[60] M. Klanchar and T. G. Hughes, "United States patent," 1985.

[61] J. M. Woodall, J. Ziebarth, and C. R. Allen, "The science and technology of Al-Ga alloys as a material for energy storage, transport and splitting water," *Proc. 2nd Energy Nanotechnol. Int. Conf. ENIC2007*, vol. 3, no. 1, pp. 15–17, 2007.

[62] J. J. Cuomo and J. M. Woodall, "United States Patent (19) 54).," 1982.

[63] V. Shmelev, H. Yang, and C. Yim, "Hydrogen generation by reaction of molten aluminum with water steam," *Int. J. Hydrogen Energy*, vol. 41, no. 33, pp. 14562–14572, 2016.

[64] Alicat-Scientific, "M-Series Operating manual," *TLS - Times Lit. Suppl.*, no. Opeating Manual, p. 90, 2016.

[65] Neodym, "Catalytic Hydrogen Gas Monitor Specifications," p. 1, 2006.

[66] Mastercraft, "Instruction Manual Temperature Reader With Digital Display And Laser Pointer." pp. 1–15.

[67] Boading Longer Precision Pump.Ltd, "BT100-1L Longer Peristaltic Pump Operating Manual."

[68] Mettler Toledo, "Operating instructions Mettler Toledo B-L line of balances," p. 34, 2003.

[69] Fisher-Scientific, "Isotemp Hotplates, Stirrers and Stirring Hotplates Operation Manual and Parts List," no. Operation Manual And Parts List, pp. 1–11.

[70] R. J. Charlson, "The Atmosphere," *Int. Geophys.*, vol. 50, no. C, pp. 213–238, 1992.

[71] LibreTets, "6 . 15 : Periodic Trends : Atomic Radius," in *LibreTexts*, pp. 1–2.

[72] Y. Cengel and M. Boles, *Thermodynamics An Engineering Approach 8th ed.* McGraw-Hill Education, 2014.

[73] Newton South High School, "Standard Enthalpy of Formation for Various Compounds," *Nshs-Science.Net*, pp. 7–8, 2015.

[74] W. P. S. Szargut, J., Egzergia. Poradnik obliczania I stosowania, "Appendix: Standard Chemical Exergy," *Thermodyn. Destr. Resour.*, pp. 489–494, 2011.

[75] L. P. H. Jeurgens, W. G. Sloof, F. D. Tichelaar, and E. J. Mittemeijer, "Growth kinetics and mechanisms of aluminum-oxide films formed by thermal oxidation of aluminum," *J. Appl. Phys.*, vol. 92, no. 3, pp. 1649–1656, 2002.

[76] Health Canada, "Guidelines for Canadian Drinking Water Quality Summary Table Prepared by the Federal-Provincial-Territorial Committee on Drinking Water of the Federal-Provincial-Territorial Committee on Health and the Environment March 2006," *Environments*, no. October 2014, pp. 1–16, 2012.

[77] City of Toronto, “Drinking Water Analysis Summary,” pp. 8–9, 2016.

[78] C. Pretet, S. Reynaud, C. Ferrier-Pagès, J. P. Gattuso, B. S. Kamber, and E. Samankassou, “Effect of salinity on the skeletal chemistry of cultured scleractinian zooxanthellate corals: Cd/Ca ratio as a potential proxy for salinity reconstruction,” *Coral Reefs*, vol. 33, no. 1, pp. 169–180, 2014.

[79] G. L. Ma, H. Bin Dai, D. W. Zhuang, H. J. Xia, and P. Wang, “Controlled hydrogen generation by reaction of aluminum/sodium hydroxide/sodium stannate solid mixture with water,” *Int. J. Hydrogen Energy*, vol. 37, no. 7, pp. 5811–5816, 2012.

[80] C. B. Porciúncula, N. R. Marcilio, I. C. Tessaro, and M. Gerchmann, “Production of hydrogen in the reaction between aluminum and water in the presence of NaOH and KOH,” *Brazilian J. Chem. Eng.*, vol. 29, no. 2, pp. 337–348, 2012.

[81] DOE, “Module 5: Fuel Cell Systems,” *Modul. 5 Fuel Cell Syst.*, 2001.